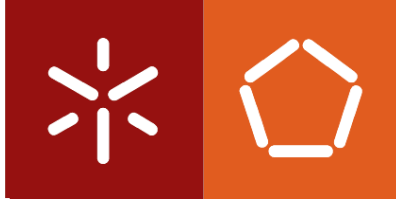**Universidade do Minho**
Escola de Engenharia

Luís Pedro Bidarra Fernandes

An integrated model for simulation of construction phasing of arch concrete dams

Universidade do Minho
Escola de Engenharia

Luís Pedro Bidarra Fernandes

An integrated model for simulation of construction phasing of arch concrete dams

Msc Dissertation
Integrated Master in Civil Engineering

Supervised by:
Professor Miguel Azenha
and
Professor João Pedro Couto

dezembro 2015

DECLARAÇÃO

Nome

Luís Pedro Bidarra Fernandes

Endereço electrónico: a61866@alumni.uminho.pt

Número do Bilhete de Identidade: 14090100

Título dissertação

An integrated model for simulation of construction phasing of arch concrete dams

Orientador(es):

Professor Miguel Azenha

Professor João Pedro Couto

Ano de conclusão: 2015

Designação do Mestrado:

Mestrado Integrado em Engenharia Civil

1. DE ACORDO COM A LEGISLAÇÃO EM VIGOR, NÃO É PERMITIDA A REPRODUÇÃO DE QUALQUER PARTE DESTA DISSERTAÇÃO

Universidade do Minho, ___/___/_____

Assinatura: _____

ACKNOWLEDGEMENTS

Although a dissertation is, by its academic purpose, an individual work, there are contributions of diverse nature that cannot and should not be forgotten to be highlighted.

Thereby, I want to express my deepest gratitude to my scientific supervisor Prof. Miguel Azenha. Thanks for believing in me, the wise advices, the motivation, patience, interest, guidance, tireless availability, the dispended time, and above all, for the trust placed in me and consequent opportunities presented which allow me to grow in a professional and personal level. His remarkable knowledge of the concrete thermal problem, of BIM and dams constructive phasing revealed to be imperative for the delivery of this thesis. I also acknowledge the importance of Prof. João Pedro Couto for all the monitoring throughout the entire process.

To my family, especially my Mother, my Grandmother, my aunt São, my uncle Nelo, my Father, my goddaughter Ana Sofia and my cousin Rui Miguel a huge thank you by your affection, by always believing in me and your selflessness with regards to me. To my departed grandfather Quim for all the love and courage conveyed throughout my life, to who I dedicate this work.

Also a word of appreciation to all my close friends I made during the academic path, I keep with much esteem the friendship here created and developed, a thank you all for the strength and will, who passed me and without which we often feel I should be lost.

ABSTRACT

The construction of dams and their constructive phasing are extremely complex activities, which lead to very high costs and thus require optimization. However, this type of optimization is only assessed by the constructor trying to evaluate alternative scenarios compared to reference scenarios proposed by the designer himself. In this sense it must be increasingly an attempt to approach the integrated project delivery (IPD) approaches advocated by BIM philosophies. The developed framework intends to integrate several valences in an automated way and supported in software tools combine various capacities both in terms of modeling BIM models, but also of thermal calculations and also defining construction phasing. It is precisely in this line that is intended this dissertation.

Therefore, in this study the main objective was the establishment of an integrated framework that would connect the modeling, the thermal calculation and dams constructive phasing according to an IPD. The developed framework will allow that an engineer in the design phase can already take into account a consequence weighted of alternatives and reference scenarios that are quickly investigated and let quickly combine the enormous impact that exists on decisions taken in very preliminary stages of the project.

In the dissertation are presented the three developed computational tools related to the dam's modelling, the thermal calculation and the constructive phasing.

The dam was modelled through visual programming resorting to Dynamo, that in turn is interoperable with the others developed tools. The thermal analysis preconized by 2D finite difference with a non-linear heat generation and division between layers was implemented in MATLAB. The developed tool for the constructive phasing, equally implemented in MATLAB, is based in a cellular automata algorithm. Finally, is presented a proposed integrated framework containing all of these aspects and where are demonstrated its feasibility and utility.

KEYWORDS: Dams; Visual Programming; Thermal calculations; Constructive phasing; Integrated framework.

RESUMO

A construção de barragens e o seu faseamento construtivo são atividades extremamente complexas, que acarretam custos muito elevados e que assim requerem otimização. No entanto este tipo de otimização só é avaliado por parte do construtor que tenta estudar cenários alternativos em relação a cenários de referência propostos pelo próprio projetista. Nesse sentido impõe-se cada vez mais uma tentativa de aproximação às abordagens de Integrated Project Delivery (IPD) preconizadas pelas filosofias BIM, nomeadamente através da integração entre várias valências de uma forma automática e com suporte a ferramentas informáticas combinar várias capacidades, quer ao nível da modelação para obter modelos BIM, como também dos cálculos térmicos e da definição dos faseamentos construtivos. Tendo por base estes princípios foi elaborada esta dissertação.

Assim sendo, o principal objetivo deste trabalho consistiu no estabelecimento de um framework integrado que permite a ligação entre a modelação, o cálculo térmico e o faseamento construtivo de barragens, permitindo assim que um engenheiro na fase de conceção já consiga ter em conta uma consequência ponderada de alternativas e de cenários de referência que são rapidamente estudados e que permitem aliar o impacto sobre decisões que possam existir em fases muito preliminares do projeto.

Na dissertação são apresentadas três principais ferramentas desenvolvidas referentes à modelação da barragem, ao cálculo térmico e ao faseamento construtivo.

A barragem foi modelada através de programação visual com recurso ao Dynamo, que por sua vez é interoperável com as restantes ferramentas desenvolvidas. O cálculo térmico preconizado por diferenças finitas 2D com processo não linear de geração de calor e divisão entre camadas foi implementado no MATLAB. A ferramenta desenvolvida para o faseamento construtivo, igualmente implementada no MATLAB, é baseada num algoritmo de automação celular. No final apresenta-se uma proposta de um framework integrador contendo todos estes aspetos e onde é demonstrada a sua viabilidade e a sua utilização.

Palavras-Chave: Barragens; Programação Visual; Cálculo térmico; Faseamento construtivo; Framework integradora.

CONTENTS

INDEX OF FIGURES

INDEX OF TABLES

CHAPTER 1

1 INTRODUCTION

1.1 Scope and motivation

The analysis of the behavior of the concrete during the first ages is covered of an great importance in multiples dominium's, among which it could be referred which aims to avoid the cracking related to the thermal problem due to the heat of hydration of the concrete (Azenha, 2004).

The study of the concrete temperature of hydration is especially important at the concreting of the concrete pieces of large dimensions or too thick, or in concretes with considerable percentage of cement, from which the differential of the temperature due by the heat of hydration it's the fact prepondering to the premature cracking of concrete.

By the motive enunciated above it became needed to dispose of methodologies of analysis of the evolution of the temperature of the concrete along the time that requires the mobilization of calculus processes.

Due to the problem complexities, especially in mass-concrete works as dams, a common practical between the projectors is the search to control the cracking risk impounding maximum concrete layers height or establishing minimum waiting times between concreting successive layers. This measures are taken aiming a more speed-up dissipation of the generated heat, in order to avoid a very sharp elevation of the temperature of the concrete element. However, once the cracking risk depends on a large set of factors beyond the geometrical conditions (concrete mix, ambient temperature, initial temperature of the concrete, boundaries conditions), it is understood that the commonly established rules in the contract documents turn out to be conservative, translating accumulated experience or prescriptions that normally lead to positive results.

So, it's relevant, in addition to the thermal-mechanical calculation of the concrete element, the utilization of methodology that allows the constructive phasing of dams. In this context it's pertinent the development of methodologies that permit an optimization of this processes that leads to an improvement of the planned construction schedule and associated costs.

The aforementioned problematics are related to mass-concrete works, as the dams' construction, which are large structures with complex shapes, whose modelling is a very difficult process through traditional modeling tools, thereby, it's interesting the use of advanced modeling tool, as the visual programing in order to obtain a parametric model that could assist and improve the design procedures of arch dams from early stages of development.

The dam's modelling, the thermic problem and the constructive phasing could be integrated in a framework based in the Integrated Project Delivery approaches advocated by BIM philosophies. Integrated Project Delivery (IPD) is a project delivery approach that integrates practices into a collaborative process to optimize project results and maximize efficiency through all phases of design and construction. (Aia, 2007)

The IPD based framework intends to anticipate the design efforts and by this way, making the design decisions earlier when opportunity to influence positive outcomes is maximized and the cost of changes minimized. The IPD is supported on the "MacLeamy Curve" presented in Figure 1-1, where is noticeable the gains in using the IPD.
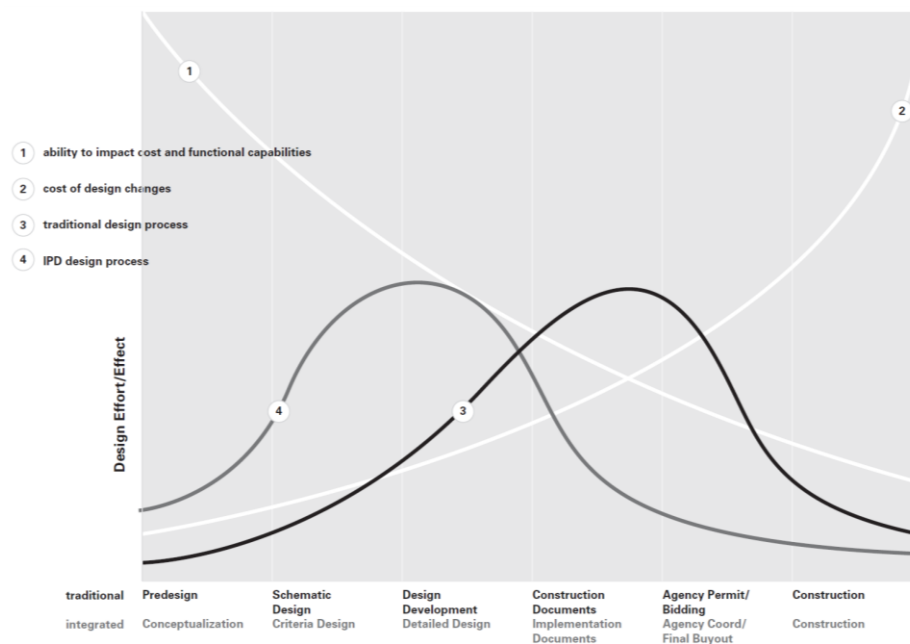
Figure 1-1 - MacLeamy curve.

Hence, it's important to develop a framework the helps the dam design in their early stages of the project and thus allows the choice for the best construction scenario through the study of multiple construction scenarios alternative scenarios.

1.2 Objectives

The aim of this work is to address the challenges and opportunities that are posed to the early stages of design of the dam's projects: (i) the availability of software capable of modelling complex geometries, (ii) perform fast pre-design thermal calculations and (iii) easily study alternative construction scenarios.

In what regards to the modelling of complex structures the main objective is model an arch dam complex double curvature shape and the minor objectives are centered in the modeling some of the dam's details, as for example the intersection with the underling terrain and the dam's galleries. Another important aspect to explore are the interoperability of the created BIM model with another BIM platforms and with the developed computational tools.

In what refers to the thermal analysis the major objective is the development of a computational tool that allows the performing of the need thermal calculation to pre-design stage of a dam project. In a more specific way, the achievement of the aforementioned objective is pursued by a set of partial objectives which includes the derivation of heat conducting equations that support the thermal calculations, simulation of the layered construction phasing, the heat conduction inside the concrete, the heat convection with the surrounding environment, with due consideration of the effects of formwork and their withdrawal and the non-linear heat generation of concrete. The developed computational tool must also be capable of automatically generating temperature maps and plots of temperature evolution for selected relevant instants over time.

Relatively to the study of the dam's constructive scenarios the objective is the development of a computational tool that allows quick study of different construction scenarios. To achieve the above-mentioned objective a set of partial objectives were defined, which consist find a set of rules that materialize the usual dam's planning, implement a decision-taking algorithm capable of perform the desired planning.

Lastly, it is intended to propose an integration of the modelling of the dam and the developed computational tools in a framework increasing the efficiency of use of developed works. The proposed framework will allow to compare different construction scenarios and will allow the best decision-making for the economical and fastest one.

1.3 Outline of the thesis

This dissertation is organized in seven chapters, the first of which consists of this introduction.

In chapter 2 is presented the literature review about the themes addressed in this dissertation. The first addressed theme was the complex shape of arch dam, the challenges and opportunities that advanced modelling methodologies as the visual programming and parametric modelling present to these hydraulic structures. The following was addressed the thermal problem in mass concrete structures, passing by the processes of transfer and heat generation, as well as the adverse effects that may arise, such as the premature thermal cracking of the concrete and the measures to prevent these risks either on site or by numerical simulations. The last theme addressed was the typical methods of dam's construction and planning.

In chapter 3 were made the modelling of the dam following the line of visual programming using Dynamo. This way was made the modeling of the dam's body, their intersection with the underlying terrain and its galleries. Finally, were made yet, the division of dam's body by horizontal and vertical joints.

Chapter 4 is related to the thermal analysis on dam's. Along this chapter are derivated the finite difference equations that support the development of a computational tool and its implementation. Are also presented multiple program validations.

In chapter 5 were proposed a method to generate construction dam schedules, following a pre-established set of rules, by the implementation of a cellular automata algorithm. Along this chapter the developed computational tool was used to test multiple construction scenarios.

Chapter 6 propose a framework that integrates the proceedings developed in the previous three chapters.

To conclude, chapter 7 provides a summary of the main conclusions and some suggestions for possible extensions of the conducted work.

CHAPTER 2

2 DESIGN, PLANNING AND CONSTRUCTION OF DAMS: CLASSICAL APPROACH AND NEW CHALLENGES

2.1 Arch dam geometry

According to (USDI, 1977) an arch dam is a solid concrete dam, curved upstream in plan. A large part of the stability results by transmitting the the water pressure and other loads by arch action into the canyon walls additionally to resisting part of the pressure of the reservoir by its own weight.

A good structural behavior of an arch dam in face of actions requires a monolithic structure, and special care in the construction to guarantee that no structural discontinuities, as open joints or cracks, occur when the structure dam assumes its water load.

The complete design of a concrete arch dam includes not only the determination of the most efficient and economical proportions for the water impounding structure, but also the determination of the most suitable appurtenant structures for the control and release of the impounded water consistent with the purpose or function of the project.

Arch dams are commonly classified as thin, medium-thick, or thick arch dams. This relation is obtained with a *b/h* ratio, where *b* is the base thickness of the crown cantilever and *h* is the structural height of the dam. So a thin arch is defined as an arch dam with a *b/h* of 0.2 or less, a medium-thick arch dam is defined as an arch dam with *b/h* ratio between 0.2 and 0.3 and a thick arch dam is an arch dam with a *b/h* ratio of 0.3 or greater.

The type of arch dams is essential defined as two category of sections, commonly arch section and cantilever section (U.S. Army Corps of Engineers, 1994), as presented in Figure 2-1. Therefore, the faces of the cantilever units are referred as upstream and downstream and the matching arch faces are Extrados and Intrados, as appropriate.
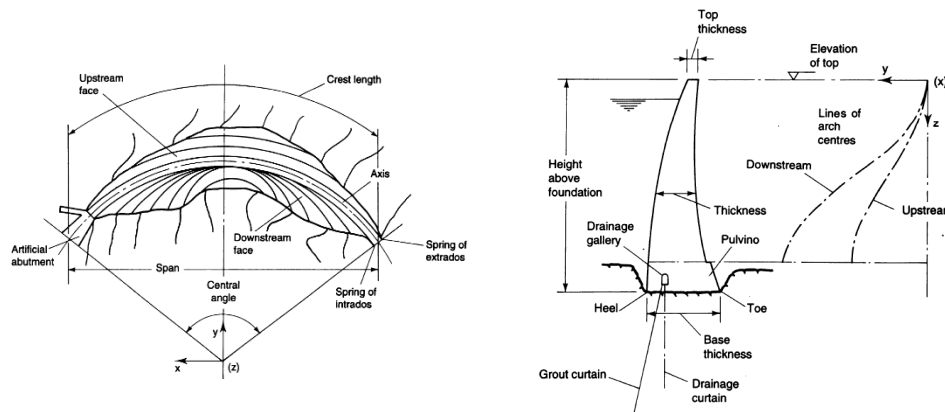
Figure 2-1 - Arch dam terminology: a) Plan view; b) Central Cantilever. Adapted from (Pedro, 1999).

The canyon walls could have schematic profiles of various dam sites, formed in "V" or "U". A Narrow-V site is related to canyon walls generally straight, with few undulations, and converge to a narrow streambed. This type of site is favored for arch dams since the applied load will be transferred to the rock predominantly by arch action. Another "V" form is a Wide-V, being the principal difference for the previous "V" is that the arch would be thicker. In wide-V the canyon walls will have more pronounced undulations but will be generally straight after excavation, converging to a less pronounced v-notch below the streambed.

According to (Pedro, 1999; U.S. Army Corps of Engineers, 1994), an arch dam may be classified as single curvature or double curvature in plan.

Single curvature arch dams are curved in plan only, as shown in Figure 2-2. Vertical sections, or cantilevers, have vertical or straight sloped faces, or may also be curved with the limitation that no concrete overhangs the concrete below. Overhang refers to the concrete on the downstream face where the upper portion overhangs the lower portion. Overhang is most at the crown cantilever, gradually diminishing toward the abutments. The single curvature is normally use in arch gravity dams with thick vaults.

Double curvature arch dams means the dam is curved in plan and elevation as shown in Figure 2-2. This type of dam utilizes the concrete weight to greater advantage than single-curvature arch dams. Consequently, less concrete is needed resulting in a thinner, more efficient dam.

The double curvature dams are used to arch dams with thin shells or domes, with a vertical and horizontal curvature as shown in the Figure 2-2.
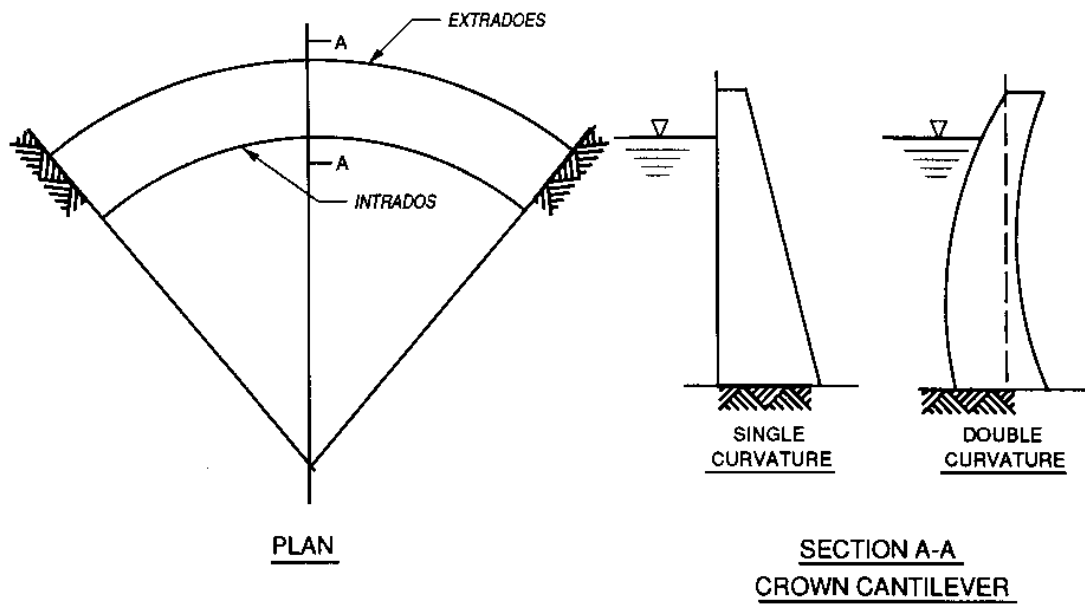
Figure 2-2 - Example of single and double-curvature dams. (U.S. Army Corps of Engineers, 1994).

The main loads to be considered in dams are: the reservoir and tailwater, the temperature, the internal hydrostatic pressures, the dead load and the earthquake. (USDI, 1977).

In the scope of the present work will be addressed the temperature loads that are imposed on a concrete dam when the concrete undergoes a temperature change and volumetric change is restrained. The magnitude of the temperature load is related to the closure temperature, to the thermal coefficient of expansion of the concrete, and to the temperature difference between the closure temperature and the operating temperatures. (Townsend, 1965).

2.2 Visual programming of dam body

2.2.1 History and definition of visual programming

Visual programing, among other things, it's mainly utilized for the generation of geometry through parametric modeling.

Modeling frequently involves establishing visual, systemic, or geometric relationships between the parts of a model. Many times, these relationships are developed by workflows ranging from

concept to result by way of rules. When modeling, without knowing, the user is working algorithmically - defining a step-by-step set of actions that follow a basic logic of input, processing, and output. Programming allows to continue to work this way but by formalizing algorithms. Algorithms can generate any kind of complex geometries.

The process is essentially the same for both Programming and Visual Programming. They utilize the same framework of formalization. However, in visual programming we define the instructions and relationships of our program through a graphical (or "Visual") user interface. Instead of typing text bound by syntax, we connect pre-packaged nodes together. Then is presented a comparison of the same algorithm - "draw a circle through a point" - programmed with nodes versus python programming language code:

Visual Program:
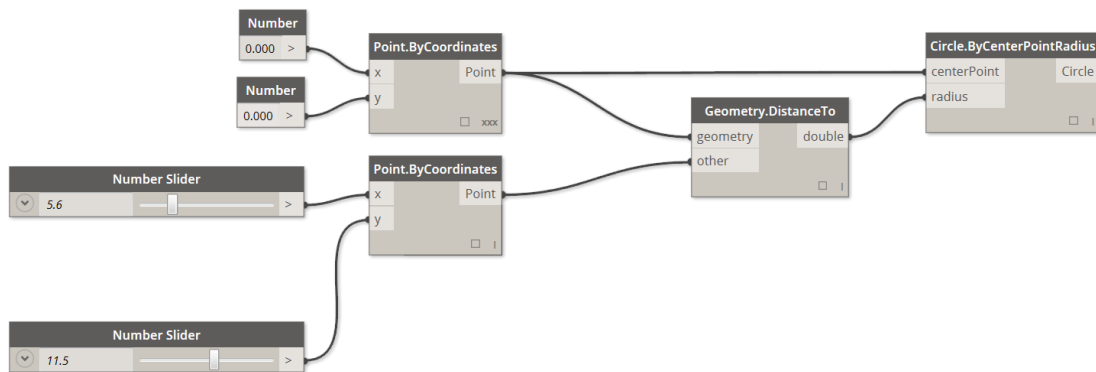
Figure 2-3 - Draw a circle through a point using visual programming.

Textual Program:

```
myPoint = Point.ByCoordinates(0.0,0.0,0.0);
x = 5.6;
y = 11.5;
attractorPoint = Point.ByCoordinates(x,y,0.0);
dist = myPoint.DistanceTo(attractorPoint);
myCircle = Circle.ByCenterPointRadius(myPoint,dist);
```

Visual programing, among other things, it's mainly utilized for the generation of geometry through parametric modeling.

Parametric modeling is a modeling methodology that become especially relevant in early nineties with the creation of the first commercial successful parametric software, Pro/ENGINEER which producer said at the time: *"The goal is to create a system that would be flexible enough to encourage the engineer to easily consider a variety of designs. And the cost*

of making design changes ought to be as close to zero as possible" (Geisberg quoted in: (Teresko, 1993)).

Geisberg highlights two points. The first is that parametric modelling should enable designers to explore a variety of designs (Teresko, 1993) and the second point is that parametric models allow choices to be made later in the design process.

Since nineteen ninety parametric modeling was used by mechanical and aerospace engineers. This methodology of modeling is based upon the creation of algorithms capable of generating models fully controlled by a reduced number of parameters. (Azenha, Lino, & Caires, 2015)

Through use of this modeling methodology, the user is able to create any kind of complex geometry easily and recognize the influence of each parameter in the model. Thus, it is easier and intuitive to make changes to the parameters to the final model in order to achieve the desired result.

The exploitation of this methodology is interesting to the modelling of complex structures as concrete arch dams, due to their double curvature shape.

2.2.2 Dynamo: a visual programming tool for parametric geometry modelling

Dynamo falls in the Visual Programming paradigm, although the textual programming is possible in the application as well. Dynamo is a visual programming tool that aims to be accessible to both non-programmers and programmers alike. It gives users the ability to visually script behavior, define custom pieces of logic, and script using various textual programming languages.

Dynamo will enable the user to work within a Visual Programming process wherein he connects elements together to define the relationships and the sequences of actions that compose custom algorithms. The user can use their algorithms for a wide array of applications - from processing data to generating geometry - all in real-time and without writing any code.
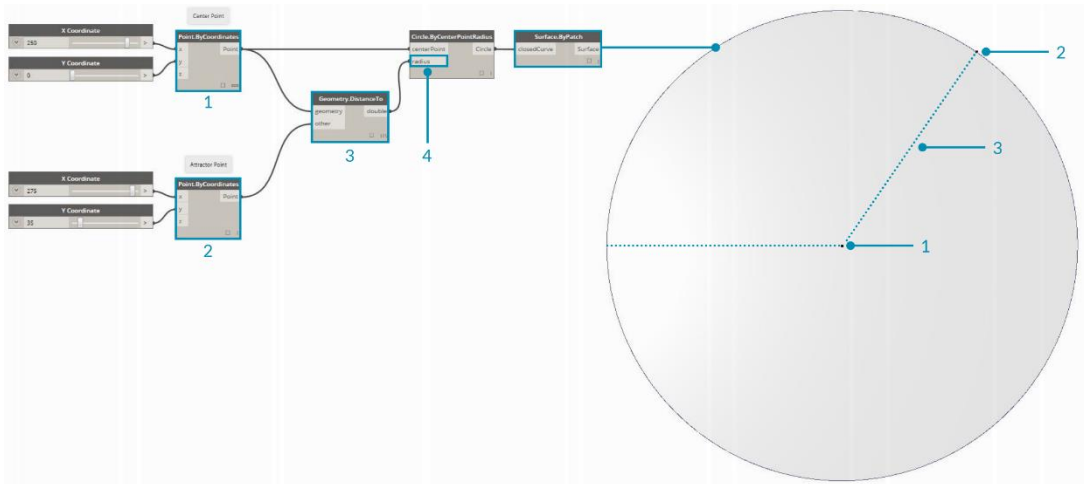
Figure 2-4 - The dynamo code and their results. ("Dynamo Primer," 2015)

2.2.2.1 Simple example of visual programming

To better understand how to use dynamo and its visual programming language, one detailed example will be given of how to create a parametric surface model.

The first step to creating a parametric surface model, is the creation of points which will be the surface's vertices. Using a node for creating a point, three inputs are needed, corresponding to the x-coordinate, the y-coordinate and the z-coordinate, similar to presented in Figure 2-5. In this case the inputs may be any real number and can be introduced by using a slider node. The slider node allows the creation of any number in a range defined by the user, for example, integers ranging from 0 to 10. The sliders can be connected to the point node's inputs thus outputting a three-dimensional point in dynamo with the desired coordinates as presented in Figure 2-6.
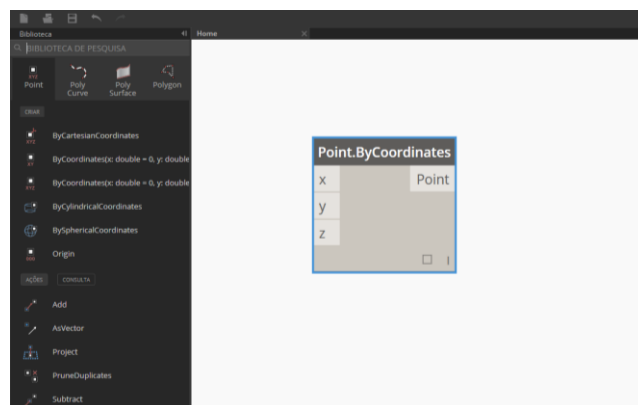
Figure 2-5 - Point dragged into dynamo workspace
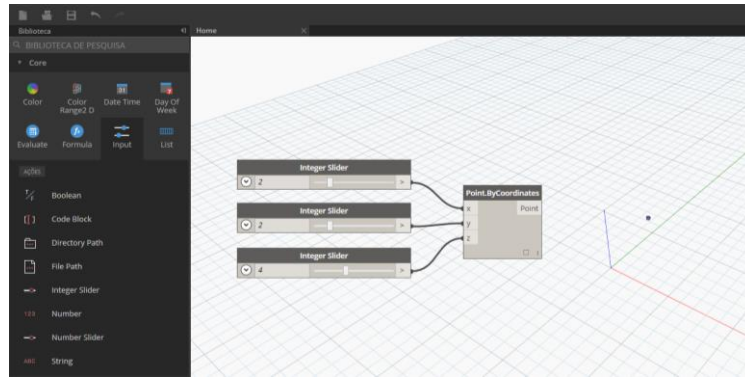
Figure 2-6 - Slider components and geometry preview

These nodes can be copied in order to create the three additional vertices of the surface. The surface's vertices will be connected by lines which will form the surface's edges.
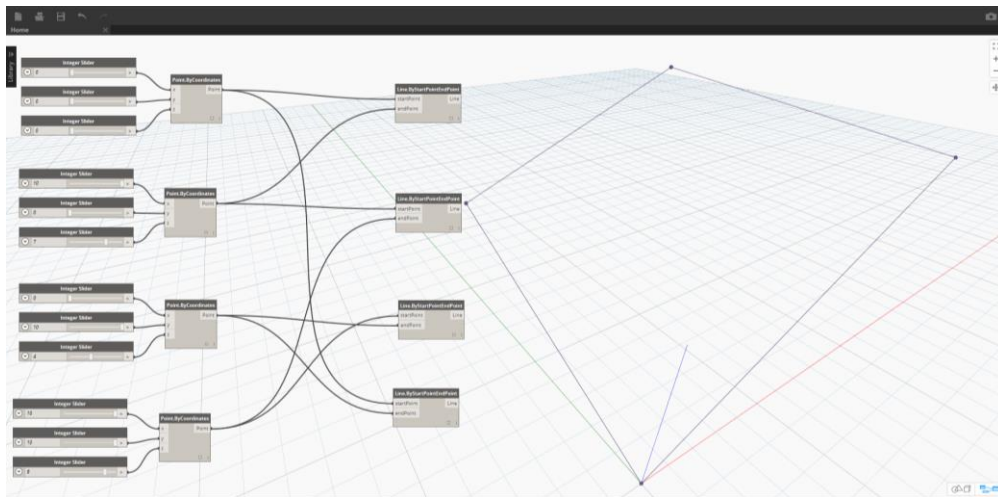
Figure 2-7 - Surface's vertices and edges.

Any adjustment in the values of the point's coordinates will automatically be reflected onto the geometry as presented on Figure 2-8.
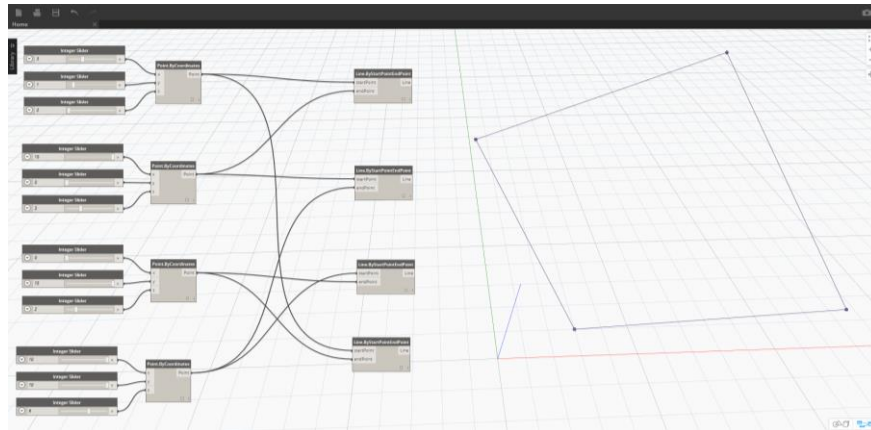
Figure 2-8 - Alteration on surface's vertices coordinates

After the creation of surfaces, vertices and edges, the surface can be created using the create surface by patch node that create a surface between closed curves as seen on Figure 2-9.
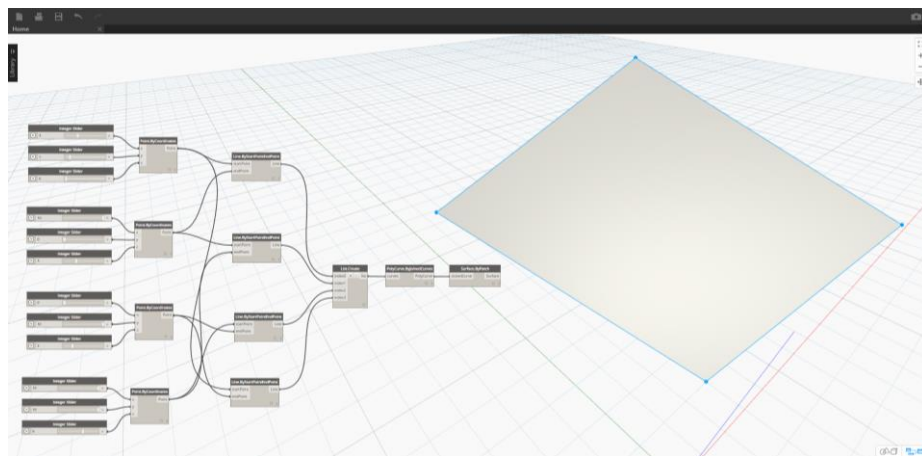
Figure 2-9 - Creation of parametric surface on dynamo

2.3 Thermal control of concrete

2.3.1 Thermal cracking risk and thermal control in dams

Mass concrete structures produce significant temperature differentials between the interior and the outside surface of the structures. Mass concrete is defined by American Concrete Institute Committee 207 as "any volume of concrete with dimensions large enough to require that measures be taken to cope with the generation of heat from hydration of cement and the respective volume change to minimize cracking.".

The proper design and construction of mass concrete dams can help prevent disasters due to the thermal cracking of concrete. To ensure safety and durability, mass concrete have attracted increasing attention in the structural design and construction. (Kim, 2010)

The main difference between mass concrete dam construction and other typical concrete structure types is its thermal behavior. Cracking in mass concrete structures is undesirable because it affects the water tightness, internal stresses, durability, and the appearance of these structures. Cracking will occur when the developed tensile stresses exceed the concrete tensile strength. These tensile stresses may occur because of imposed loads on the structure, but more often occur because of restraint against volumetric change. The largest volumetric change in mass concrete results from change in temperature. (USDI, 1977)

The cracking tendencies occur with high thermal gradient between the center and the surface, when the thermal stress in concrete exceeds its tensile strength. The cracking can be reduced to acceptable levels, in most instances, by the use of appropriate design and construction procedures.

Thus, temperature control measures are employed in mass concrete dams to facilitate construction of the structure, minimize and/or control the size and spacing of cracks in the concrete, and permit completion of the structure during the construction period, because minimizing volumetric changes makes also possible the use of larger construction blocks, thereby resulting in a more rapid and economical construction.

The thermal control could be made through numerical simulation of the temperatures inside the concrete, obtaining temperature maps as presented in Figure 2-10. The important factor to prevent cracking is the thermal stresses inside concrete and not the temperatures, because the thermal stresses are not only related with the temperatures, but with the restraints of the concrete element. Traditionally only the temperature is considered in the early stages of development of the project, because the temperature gradients are a good indicator of the thermal stresses generated inside the concrete for that stage of development of the project.
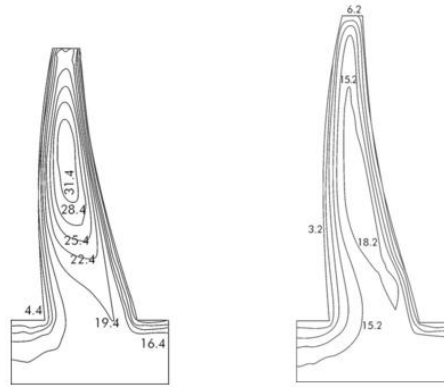
Figure 2-10 - Example of interior temperature distribution [ºC]. Adapted from (Li, Ren, Wu, & Zhao, 2008).

The most common methods of temperature control, are the precooling that is the most effective temperature control, which reduces the placing temperature of the concrete.

Methods of reducing the placing temperature range from restricting concrete placement during the hotter part of the day or the hotter months of the year, to a full treatment of refrigerating the various parts of the concrete mix to obtain a predetermined, maximum concrete placing temperature.

The refrigeration of the concrete mix includes the cooling of the water in the concrete mix, the cooling of the aggregates and addition of ice to the concrete mix. (Bofang, 2014)
Another method of minimizing the concrete temperatures are the reduction of the amount and type of cement or adding pozzolan materials to reduce the heat hydration reaction of cement. (Spanish Commitee on Large Dams, 1990)

2.3.2 Thermal problem of the concrete

The analysis of the behavior of concrete in the first ages requires the knowing of his origin. (Azenha, 2004)

The water addition in concrete starts the hydration reaction that is responsible for the development of the mechanical properties of the concrete. The chemical reactions related to the concrete hydration are exothermic, with great heat generation.

The heat generation causes a temperature rise in concrete, which becomes higher than the surrounding environmental temperature. Thereby, heat transfer between concrete and the surrounding environment starts through the mechanism of convection. During the period while the amount of heat generated is greater than the amount of heat transferred between the concrete and the environment, the temperature in the concrete element keeps rising, with the core of the element standing hotter than the external surfaces. At some point in time, the heat generated by the chemical reaction equals the heat transferred to the surrounding environment. From this instant the concrete element starts cooling until it attains thermal equilibrium with the environment, which represents the end of the thermal problem related to the heat of hydration of cement. This thermal equilibrium rely on element size, shape, the concrete composition, the initial concrete temperature and environmental temperature, (Bofang, 2014).

This temperatures differentials in the concrete generate a volumetric expansion, when the temperatures are rising, followed by and contraction, when the temperatures are dropping, that in presence of external or internal restrictions could cause cracking of the concrete.

2.3.3 Heat transfer

Before proceed, it's important the identification of the phenomena and the parameters involved in the characterization of a mass thermal behavior.

The heat transfer consists in the movement of thermal energy due to temperature differentials. Thus, when occur temperature differentials there are conditions for heat transfer.

In the thermal study of concrete in the first ages, the heat transfer could occur from different natures: conduction, convection or radiation (Figure 2-11), (Azenha, 2004; Kim, 2010). The temperatures distribution in a mass is, indeed, controlled by the combination of those three mechanisms, it's not possible isolate completely one mechanism from their interactions with

the remaining. However it's usual the separation of the heat transfer mechanisms, which does not involve significant errors (M. N. Ozisik, 1985) and simplifies the analysis.
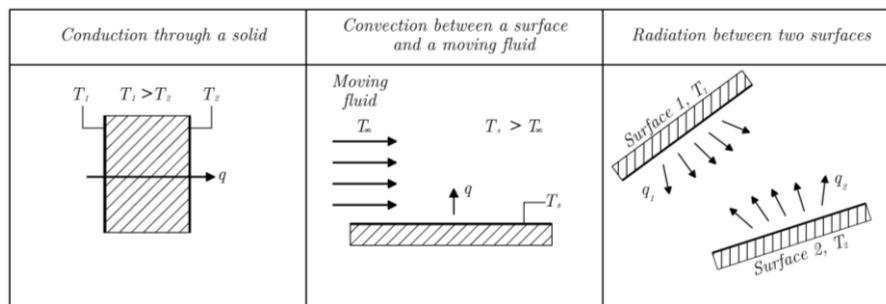
Figure 2-11 - Heat transfer mechanisms (Azenha, 2004).

The three heat transfer mechanisms aforementioned are described next.

Internal heat transfer by conduction

Conduction is the process of heat transfer wherein the exchange in thermal energy is made by the random movement of molecules or by the movement of free electrons. It is the typical process of heat transfer inside a solid (Azenha, 2004, 2009; Kim, 2010). One example of heat transfer by conduction is the case of concreting of a concrete piece adjacent the other previously existing. The heat generated by the reactions of hydration of a newly concreted piece will be transmitted by conduction to the existing piece through their physical boundaries.

The heat conduction in a solid could occur in steady-state regime (when the temperature in any point don't changes along the time), or in variable regime (with the temperature variations in the time).

- Conduction on steady-state regime

The empirical equation of heat conduction is based in experimental observations and its governed by Fourrier's law, that for the one-dimensional case on steady-state conditions is:

$$q''_x = \frac{q_x}{A} = -k\frac{\partial T}{\partial x}$$

[2.1]

Where:

q_x'' – heat flow through a surface by area unity (W/m^2)

q_x – heat flow (W);

A – area crossed by the heat flow (m^2);

k – thermal conductivity (W/m K);

T – temperature (K);

x – coordinate (m).

The signal (-) in the equation is related to the fact of the flow occur towards decreasing temperatures.

According to equation [2.1], the heat flow direction will always be perpendicular to the isothermal surface.

Taking in account that a solid is constituted by free electrons and atoms connected according a periodic arrangement (atomic mesh), the transmission of thermal energy by conduction occurs in two ways: by movement of free electrons and by vibrating waves propagating through the atomic mesh. These effects are additive, and k is the result of the sum of the electric and the mesh components. In nonmetallic solids (like the constituents of fresh concrete) the value of k its conditioned mainly by the mesh component, which depends on the frequency of the interaction between the constituents. The regularity of the mesh arrangement affects the thermal conductibility by the following way: crystalline materials (well-ordered meshes) have bigger values of k than amorphous materials like the glass (Incropera & DeWitt, 2001).

For utilization in multidimensional means the Fourrier's law generalizes by the vectorial representation

$$q_x'' = -k\nabla T = -k\left(i\frac{\partial T}{\partial x} + j\frac{\partial T}{\partial y} + k\frac{\partial T}{\partial z} \right) \qquad [2.2]$$

where:

x, y, z – coordinates in the reference axis system;

i, j, k – inverters of the reference axis system.

It's implicit in the equation [2.2] that the heat flow is always perpendicular to isothermal surfaces.

- Conduction in variable regime

The Fourrier's law is applicable to the conduction of heat in variable regime, for which the temperature distribution evolves along time until the equilibrium point is reached. It is important, before anything else, to retain some remarks about the heat conduction to better understand the heat conduction phenomes in variable regime: the specific heat, the specific volumetric heat and the thermal diffusibility (Azenha, 2004).

The specific heat c is the quantity of heat necessary to rise a unity of mass of a body by one unity of temperature; it's expressed in J / (Kg K).

The specific volumetric heat ρc results from the product of the specific heat by specific mass of the material (ρ), it's usually utilized to represent the material capacity to store energy; the unities in which it is expressed are J/(m^3 K).

The relation between the thermal conductibility and the specific volumetric heat it's called thermal diffusibility α_T (m^2/s)

$$\alpha_T = \frac{k}{\rho c} \qquad [2.3]$$

witch represents a measure of the capacity of a material to conduct thermal energy in relation to their ability to store it. Materials with elevate α_T respond quickly to thermal changes in the surrounding environment, taking less time until the attain point is established.

The main objective of a conduction analysis is determinate the temperatures inside an element, as result of boundary conditions and heat generation due cement hydration. For that purpose, is

used the Fourrier's equation that is based on the Fourrier's law. For aiding the following deduction let's consider the representative elementary volume (REV) presented in Figure 2-12.
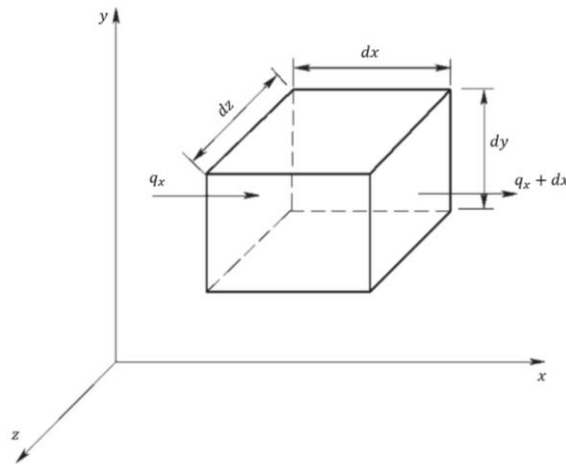
Figure 2-12 – Elementary concrete element – adapted from (Bofang, 2014).

In the presence of temperature differentials between the REV surface and the REV core it will be heat convection through faces of the REV, in perpendicular directions to the correspondent surfaces. In three faces of the element with different directions the heat fluxes could be identified by q_x, q_y and q_z. In the opposite faces, the heat fluxes can be represented in Taylor's series expansion by:

$$q_{x+\partial x} = q_x + \frac{\partial q_x}{\partial x} dx \qquad [2.4]$$

$$q_{y+\partial y} = q_y + \frac{\partial q_y}{\partial y} dy \qquad [2.5]$$

$$q_{z+\partial z} = q_z + \frac{\partial q_z}{\partial z} dz \qquad [2.6]$$

According to the First Law of Thermodynamics in a closed system we have:

$$\dot{E}_{in} + \dot{E}_g - \dot{E}_{out} = \dot{E}_{st} \qquad [2.7]$$

$$\dot{E}_g = \dot{Q} \, dx \, dy \, dz \qquad [2.8]$$

$$\dot{E}_{st} = \rho c \frac{\partial T}{\partial t} dx \, dy \, dz$$

[2.9]

Where:

$\dot{E}_{in}$ – is the entrance energy rate (W);

$\dot{E}_{out}$ – is the exit energy rate (W);

$\dot{E}_g$ – is the generation energy rate (W);

$\dot{E}_{st}$ – is the storing energy rate (W);

$\dot{Q}$ – is the energy generation rate by volume unit (W/m³);

t – is the time (s);

Thus, considering the heat fluxes in concrete element faces that are represented by $\dot{E}_{in}$ and $\dot{E}_{out}$, and substituting in the equations [2.7] and [2.8] in [2.9]:

$$q_x + q_y + q_z + \dot{Q} \, dx \, dy \, dz - q_{x+\partial x} - q_{y+\partial y} - q_{z+\partial z} = \rho c \frac{\partial T}{\partial t} dx \, dy \, dz \qquad [2.10]$$

Substituting [2.4], [2.5] and [2.6] in [2.10]:

$$-\frac{\partial q_x}{\partial x} dx - \frac{\partial q_y}{\partial y} dy - \frac{\partial q_z}{\partial z} dz + \dot{Q} \, dx \, dy \, dz$$

$$= \rho c \frac{\partial T}{\partial t} dx \, dy \, dz \qquad [2.11]$$

The heat fluxes in the elementary element faces can be obtained by the multiplication of the components [2.2] by the respective areas,

$$q_x = -k \, dy \, dz \frac{\partial T}{\partial x} \qquad [2.12]$$

$$q_y = -k \, dx \, dz \frac{\partial T}{\partial y} \qquad [2.13]$$

$$q_z = -k \, dy \, dx \frac{\partial T}{\partial z} \qquad [2.14]$$

substituting [2.12], [2.13] and [2.14] in [2.11]:

$$\frac{\partial}{\partial x}\left(k\frac{\partial T}{\partial x}\right) + \frac{\partial}{\partial y}\left(k\frac{\partial T}{\partial y}\right) + \frac{\partial}{\partial z}\left(k\frac{\partial T}{\partial z}\right) + \dot{Q} = \rho c \frac{\partial T}{\partial t} \qquad [2.15]$$

This expression is the general form of Fourrier's equation, from which could be obtained the temperature distribution $T(x, y, z, t)$.

Finally, for the cases in which thermal conductivity is spatially constant during the period of analysis, it is usual to represent the equation [2.16] as

$$\frac{\partial^2 T}{\partial x^2} + \frac{\partial^2 T}{\partial y^2} + \frac{\partial^2 T}{\partial z^2} + \frac{\dot{Q}}{k} = \frac{1}{\alpha_T}\frac{\partial T}{\partial t} \qquad [2.16]$$

The variable $\dot{Q}$ is the energy generation rate of by unit of volume and represents the internal heat generation in concrete due to the exothermic nature of the hydration reaction of concrete. Hence, the $\dot{Q}$ it's very important for the thermal analysis of concrete, and thus it's very important to proceed to a careful characterization of the heat generation potential of the concrete mix in study.

External heat transfers through boundaries

The heat transfers between a solid and the surrounding environment occur in two ways:

- Convection – the heat exchange is caused by temperature differentials between the bulk of air and the air neighboring the solid (whose temperature is directly influenced by the solid which is in contact). In consequence, densities of the two air masses changes and the cycled air movement is enforced indefinitely while the temperatures of the solid and the bulk of air are different. The air movement over the solid could be enforced by an external condition like the wind and heat exchange are strongly intensified once the air near the solid is renovated at a higher rate.

- Radiation – Thermal energy transmission due to radiation is related to energy emission of a body because of its temperature. According to Maxwell's Classic theory, this energy is emitted in the form of electromagnetic waves. While convection heat transfer requires a transmission medium such as air, radiation transmission can happen in vacuum conditions. Generally speaking, any solid is constantly emitting and receiving radiation from its surroundings.

2.3.4 Heat generation

The heat generation rate $\dot{Q}$, which reflects the thermal activated nature of the hydration of cement is usually expressed through the Arrhenius Law:

$$\dot{Q} = f(\alpha_T) A_T e^{\frac{-E_a}{RT}}$$

where:

$f(\alpha_T)$ – is the normalized heat generation rate;

A_T – is a rate constant;

E_a – is the apparent activation energy (J/mol);

R – is the ideal gas constant (8.314 J/mol/K);

T – is the reaction temperature (K).

However, the concrete's heat generation experimental characterization is not object of study in this thesis, but, even so, it's important to retain some of the variables involved to better understand the further numerical implementation.

The degree of heat development, represented by α_T as the thermal diffusibility, is the ratio between $Q(t)$, the accumulated heat generated until a certain instant t and Q_{total}, the total heat generated by the concrete and it represents the amount of reaction developed yet:

$$\alpha_T = \frac{Q(t)}{Q_{total}}$$

The normalized heat generation rate $f(\alpha_T)$, defined as the ratio between $\dot{Q}(\alpha_T)$ and $\dot{Q}_{peak}$, and was created in order to obtain a heat generation rate independent from temperature (Figure 2-13).

The apparent activation energy E_a represents the energy that a molecule in the initial state of the process must acquire before it can take part in a reaction.
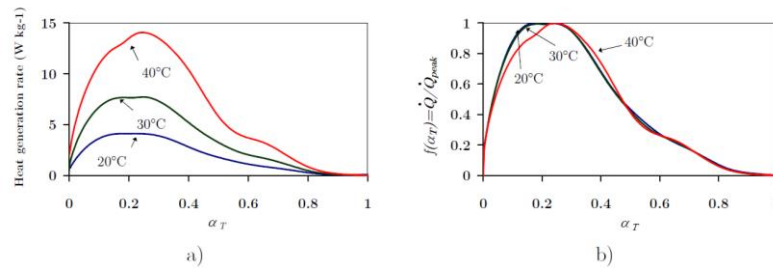
Figure 2-13 a) Heat generation rate as a function of α_T; b) normalized heat generation rate f(α_T) - (Azenha, 2009).

The aforementioned variables can be consulted in the following table, resultant from a research conducted with the purpose of creating a wide collection of data pertaining to the heat development characteristics of a representative group of cements commercially available in Portugal (Azenha, 2009). In this study the two main Portuguese cement selling companies, named here as Company A and Company B, were selected for the sake of representativeness, with the selection of five cements from each.

Table 2-1 - Adopted heat parameters (per Kg of cement) (Azenha, 2009).

	CA CEM I 42.5R	CA CEM I 52.5R	CA CEM II A L 42.5R	CA CEM II B L 32.5N	CA CEM IV 32.5N	CB CEM I 42.5R	CB CEM I 52.5R	CB CEM II AL 42.5R	CB CEM II B L 32.5N	CB CEM II B L 32.5R White
A_T	2.150E+08	1.607E+09	3.553E+09	4.096E+09	7.807E+07	3.522E+08	1.374E+09	7.683E+07	5.128E+07	3.423E+07
E_A	43.83	48.19	51.02	52.10	41.84	44.38	47.40	41.30	40.66	40.59
Q_∞	355.2	386.3	327.4	296.2	279.5	370.3	414.0	343.1	315.8	261.6
α_T	$f(\alpha_T)$	$f(\alpha_T)$	$f(\alpha_T)$	$f(\alpha_T)$	$f(\alpha_T)$	$f(\alpha_T)$	$f(\alpha_T)$	$f(\alpha_T)$	$f(\alpha_T)$	$f(\alpha_T)$
0.00	0.00	0.00	0.00	0.00	0.00	0.00	0.00	0.00	0.00	0.00
0.05	0.65	0.62	0.75	0.83	0.62	0.58	0.53	0.68	0.74	0.68
0.10	0.91	0.88	0.95	0.99	0.85	0.85	0.83	0.92	0.96	0.91
0.15	1.00	0.99	1.00	0.99	0.98	0.98	0.99	1.00	1.00	0.99
0.20	0.98	1.00	0.97	0.95	0.99	1.00	0.98	0.98	0.96	0.99
0.25	0.94	1.00	0.96	0.87	0.92	1.00	0.89	0.91	0.88	0.92
0.30	0.86	0.95	0.90	0.83	0.82	0.94	0.76	0.82	0.82	0.82
0.35	0.75	0.85	0.78	0.77	0.72	0.83	0.57	0.74	0.76	0.77
0.40	0.63	0.70	0.66	0.68	0.58	0.69	0.39	0.64	0.66	0.67
0.45	0.51	0.56	0.56	0.59	0.41	0.55	0.24	0.52	0.55	0.56
0.50	0.41	0.45	0.46	0.51	0.27	0.41	0.17	0.41	0.45	0.47
0.55	0.32	0.36	0.34	0.42	0.19	0.30	0.16	0.31	0.36	0.38
0.60	0.24	0.28	0.25	0.30	0.15	0.22	0.14	0.24	0.29	0.31
0.65	0.18	0.23	0.20	0.21	0.12	0.17	0.11	0.18	0.22	0.23
0.70	0.13	0.18	0.16	0.16	0.10	0.13	0.08	0.14	0.16	0.16
0.75	0.09	0.13	0.12	0.12	0.08	0.10	0.06	0.10	0.12	0.11
0.80	0.06	0.08	0.08	0.08	0.05	0.07	0.04	0.07	0.08	0.07
0.85	0.04	0.04	0.04	0.04	0.03	0.04	0.03	0.04	0.04	0.05
0.90	0.02	0.02	0.02	0.02	0.02	0.02	0.02	0.02	0.02	0.03
0.95	0.01	0.01	0.01	0.01	0.01	0.01	0.01	0.01	0.01	0.01
1.00	0.00	0.00	0.00	0.00	0.00	0.00	0.00	0.00	0.00	0.00

2.3.5 Numerical Simulations

The numeric modelling of behavior of concrete during fist ages, implies the consideration of the exothermic and thermal activated reaction of the hydration phenomena. Hence, it should be

used a numerical model that is capable to assess the thermic field of the concrete during the hydration process and further cooling.

Nowadays, with the existing computational power, it's possible to take into account the dependency of the hydration reaction relating to the real conditions on site, conducting a nonlinear analysis, because the heat liberated in the reaction depends on the surrounding temperature on the same instant.

Numerical methods are useful for solving fluid dynamics, heat and mass transfer problems, and other partial differential equations of mathematical physics when such problems cannot be handled by the exact analysis techniques because of nonlinearities, complex geometries and complicated boundary conditions.

Presently, the finite difference method (FDM) and the finite element method (FEM) are widely used for the solution of partial differential equations of heat. Each method has its advantages depending on the nature of the physical problem to be solved, but there is no best method for all problems. Finite difference methods are simple to formulate and can readily be extended to two or three-dimensional problems and require less computational work than the FEMs. Furthermore, FDM is very easy to learn and apply for the solution of partial differential equations encountered in the modelling of engineering problems for simple geometries. For problems involving irregular geometries in the solution domain, the FEM may have the flexibility, since the region near the boundary can readily be divided in sub regions. A major drawback of FDM appears to be in its inability to handle effectively the solution of problems over arbitrarily shaped complex geometries because of interpolation difficulties between the boundaries and the interior points in order to develop finite difference expressions for nodes next to the boundaries. Hence, the main difference between both methods is their capacity to handle the mesh in complex shaped geometries and the accuracy of both is mostly the same. (N. Ozisik, 1994)

2.4 Planning and construction of dams

2.4.1 General remarks

The choice of an arch structure as a suitable design solution for a dam project may be affected by different factors, particularly by geotechnics, topography, hydrology and climate.

Hence, methods and timing of construction should be considered at all times during the design of the dam and its appurtenant structures. The early consideration problems can result in significance savings in the cost of construction. By developing an anticipated construction schedule, potential problems in the timing of construction of the various parts can be identified. If practicable, revisions in the design can be made to eliminate or minimize the effect of the potential problems. (U.S. Army Corps of Engineers, 1994)

In general, a tighter schedule results in a lower cost. The selection of an adequate schedule should reflect a balance between cost and the certainty of meeting deadlines, and, as in almost engineering problems, the correct decision will depend on a weighted assessment of costs and risks.

A proper application of scheduling techniques, updating when necessary and sensible usage of the calculations and automatic drawings are indispensable for planning resources, improving costs and execution times and minimizing risks. (Spanish Commitee on Large Dams, 1990).

As examples are presented in Figure 2-15 and Figure 2-16 the concreting schedule and the concreting works for Almendra dam in Spain (Figure 2-14).
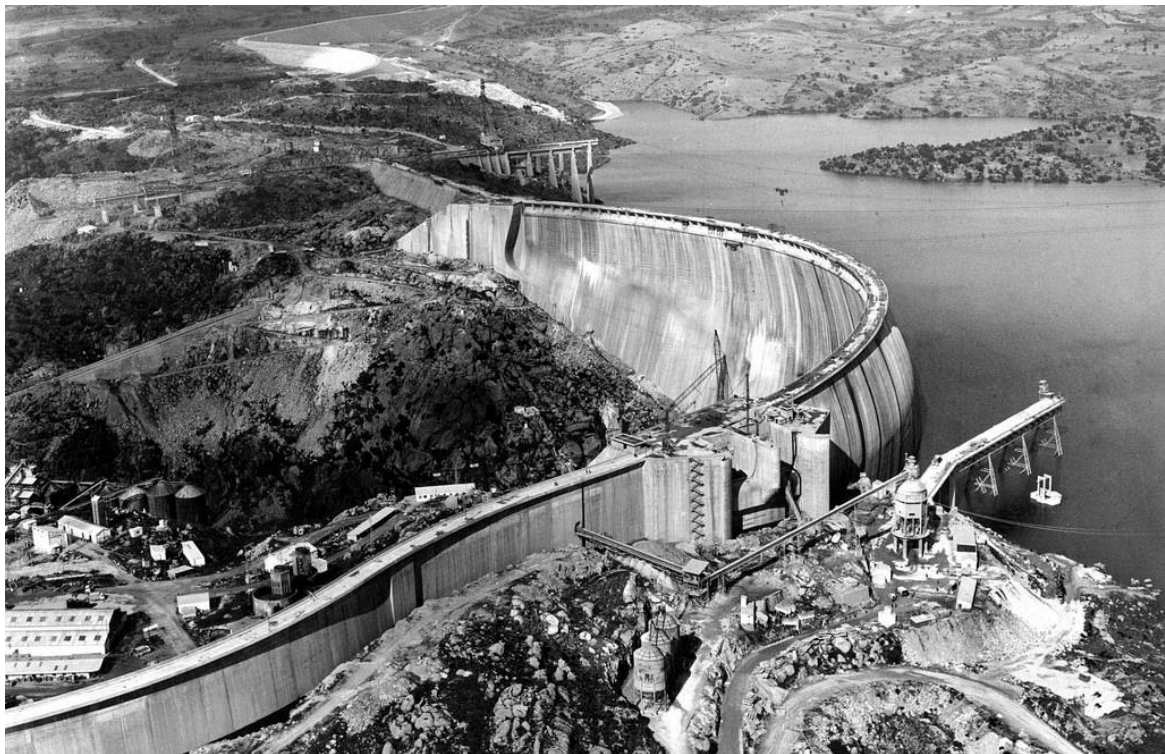
Figure 2-14 - Construction of Almendra Dam in Spain. (Iberdrola, 2014)

(1) Right bank.
(2) Left bank.
(3) Symmetry axis.
(4) First year.
(5) Second year.
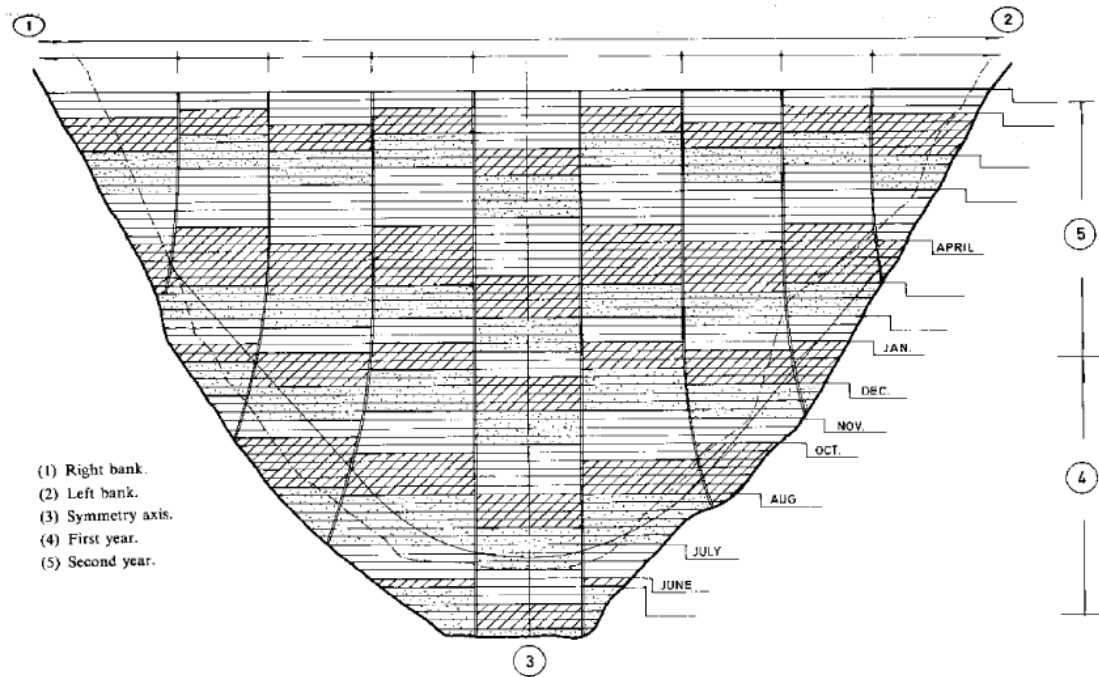
Figure 2-15 - Concreting schedule of an arch dam (developed downstream view). Adapted from (Spanish Commitee on Large Dams, 1990)

(1) Accumulated volume (m³)
(2) Monthly volume (m³).
(3) Months.
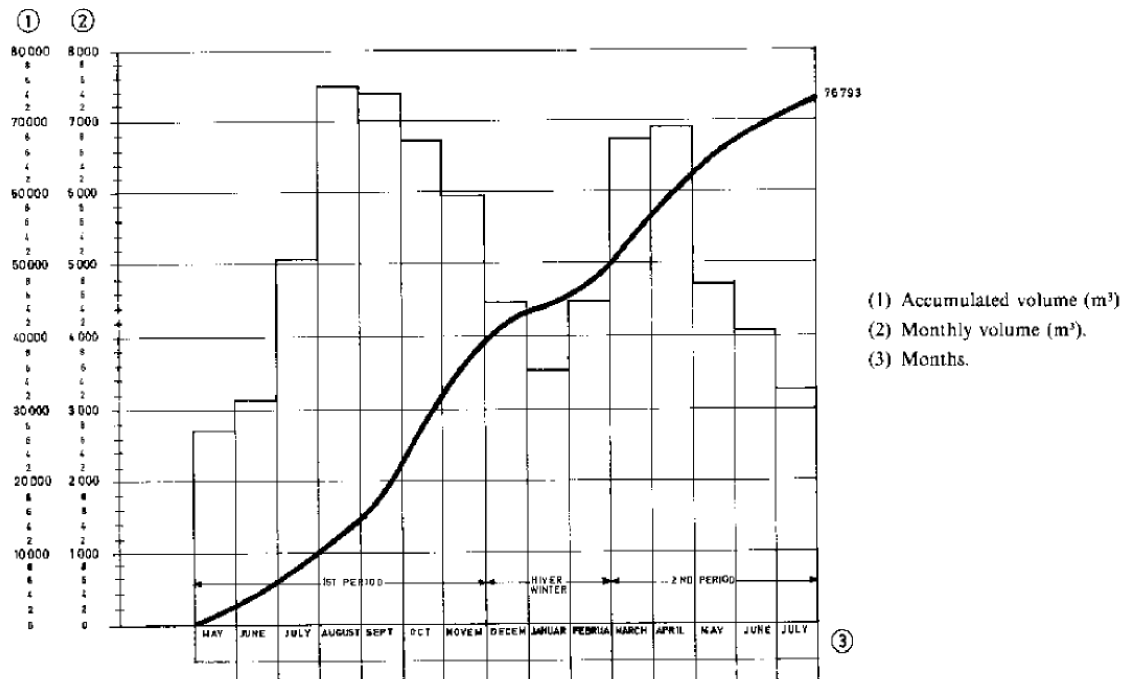
Figure 2-16 - Concreting works. Adapted from (Spanish Commitee on Large Dams, 1990)

2.4.2 Typical dam construction strategies

The arch dams are traditionally constructed by means of individual blocks, because if it's constructed by one continuous shape between banks, will be verified the cracking occurrence perpendicular to the foundation, due to the rigidity of the foundation (Spanish Commitee on Large Dams, 1990). By this reason the arch dams are traditionally constructed through individual blocks divided by joints, as shown in Figure 2-17 and Figure 2-18.

a)   b)
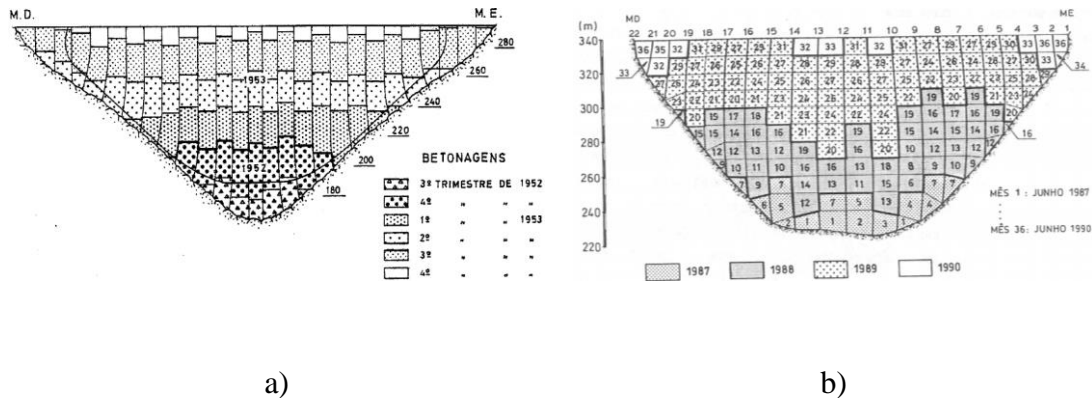
Figure 2-17 – Constructive phasing: a)Cabril; b)Alto Lindoso. (Batista, 1998; Teles, 1985)
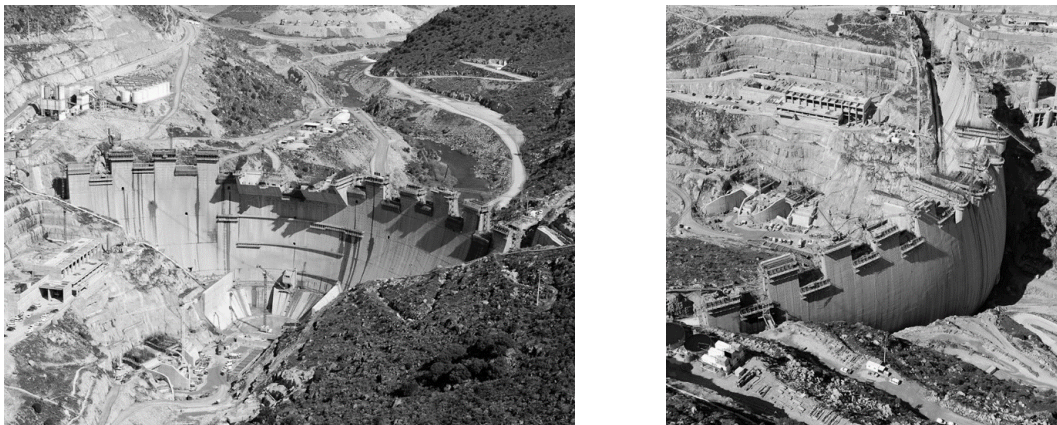
Figure 2-18 - Construction of Baixo Sabor Dam (August 2012).

In concrete dam's, cracking is undesirable because it conducts to the early deterioration of concrete, which leads to the destruction on the structural monolithism. Consequently, the joints are cracks, carefully projected, with the aim of minimizing the adverse effects.

The joints prevent the stresses appearance (thermal or mechanical), enabling the construction of the dam, or result from the unpredictable stops of the concrete works. In a general way the

joints are classified in five types: contraction joints, expansion joints, foundation joints, construction joints and cold joints. (Spanish Commitee on Large Dams, 1990)

The contraction joints minimize uncontrolled cracking caused by the thermal contraction of the concrete, mainly due to dissipation of the cement heat of hydration and drying shrinkage in the early age of the concrete. This joints are located vertically from the bottom to the top of the dam, as presented in Figure 2-19.
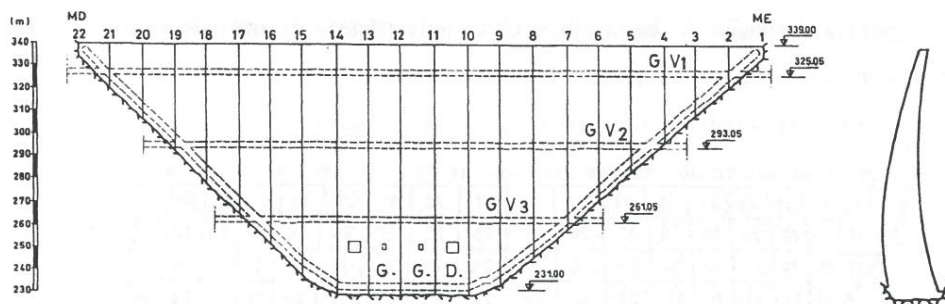
Figure 2-19 - Alto Lindoso dam contraction joints. (Farinha, 2003)

The expansion joints maintain a certain opening to limit face-to-face contact. The initial opening must be sufficient wide to absorb the increased dimensions of structural elements separated by the joint, arising from thermal expansion due to temperatures rise.

The foundations joints have as objective separate adjacent parts of a concrete structure, normally in a vertical plane, in order to confine movement to the specific part in which this occurs, generally due to differential settlement of the foundation

The construction joints divide part of the structural element that should theoretically be monolithic, due to construction factors. Construction joints are connections between dam layers or other vertical elements that, given their height, cannot or must not be concreted in a single operation.

The cold joints are separation surfaces caused by a connection defect between two consecutive vibration layers in the same placement layer of any type of concrete work. These occur when compaction of the upper layer takes place once the bottom layer has already set. Cold joints nearly always occur due to concrete placement faults, either in programming, method or execution.

The dams' construction planning is controlled essentially by the concreting schedule. The concreting schedule for successive concreting layers is conditioned by the ambient temperature, layer thickness, heat of hydration per Kg of cement, if the project has foreseen artificial cooling or not. These conditions limit concreting frequency for successive layers. The minimum time between concreting successive layers is fixed at 72 hours.

On the other hand, a limit must be placed on the time lapsing between concreting successive layers, in order to avoid detachment or cracking on the upper layer due to the advanced stage of hardening completely contracted state of the below layer. It is not advisable to leave more than two weeks between concreting successive layers.

Another important factor to the dam schedule definition is the minimum level difference between adjacent blocks. It is determined by the free height required for formwork, generally, two or three lifts. In arch dams' where the downstream face is out of plumb, specifications may limit the maximum level difference between all blocks to ensure the structure works as an arch above a certain height, and thus avoid possible tensile stresses in the upstream face, caused by blocks out of plumb working as independent cantilevers.

Taking into account the above principals it's possible to define the concrete scheduling. Nowadays only a few construction scenarios are studied due to the complex and time-consuming nature of this process that nowadays is handmade, merely assisted with simple computational tools as *Microsoft Excel* or *Microoft Project*.

On the bibliographic search was not found any methodology of computational tool for automatic generation of dam's construction schedules so is relevant the exploitation of these automations in the scope of the study of multiple dam constructive phasing.

CHAPTER 3

3 VISUAL PROGRAMMING AND MODELLING OF AN ARCH DAM

3.1 Introduction

The use of software that has the capability of creating complex geometries presents a set of challenges and opportunities to the modelling of complex constructions such as hydraulic structures. This chapter is focused in some examples of such challenges and opportunities applied to a case study of the main body of an arch dam. The case study, which will also be focused in the next two chapters, further intends to show that the concepts of parametric modelling and interoperability can be used together to assist and improve the design procedures of arch dams from early stages of development.

The main focus of the present chapter is to describe the procedures that were adopted to model the arch dam with support of visual programming through Dynamo for REVIT. The main requirements and objectives for such modelling are:

1. Creation of a full 3D model (solid objects/bodies) compliant with relevant equations for a dam, in including its intersection with the underlying terrain;
2. The model should be fully parametric, thus allowing easy alternative geometrical studies;
3. The model should be capable of self-dividing the entire dam according to its several horizontal and vertical construction joints, as to support the studies of construction phasing/scheduling;
4. The internal galleries of the dam should be automatically included in the model regardless of their potential intersection with the construction joints;
5. The resulting model should be exportable to a BIM platform, where it is recognized as solid object with geometrical and non-geometrical information. The model should also be exportable to the IFC format;
6. The programming of the model should allow direct interoperability of information with third party tools such as Excel or Matlab as to support data analysis (e.g. thermal analysis in the scope of Chapter 4; scheduling analysis with cellular automata in the scope of Chapter 5).

3.2 Case study of an arch dam

The case study of this dissertation is a double curvature arch dam, which poses relevant modelling challenges due to its complex geometry.

The selected dam is schematically represented through a plan, cross-section and elevation in Figure 3-1, where the reference axis x, y and z are also represented (origin located in the medium sheet on the dam's crest). It has 98 meters height, 300 meters of crest length and its shape is defined by the following functions presented in Figure 3-1. The mathematical description of the shape of the dam is performed according to standard procedures in arch dams. y(x,z) corresponds to the axis of the parabolic arches (equation [3.1]), whereas e(x,z) is the arch thickness (equation [3.2]). In order to define both y and e, it is necessary to know p(z) that corresponds curvature radius of the parabolic arches axis at the crown cantilever (equation [3.3]), a(z) which is the crown cantilever axis (equation [3.4]), e_0(z) that stands for the crown cantilever thickness (equation [3.5]) and A(z), which is related to the increasing evolution of the arches thickness to the abutments (equation [3.6]).
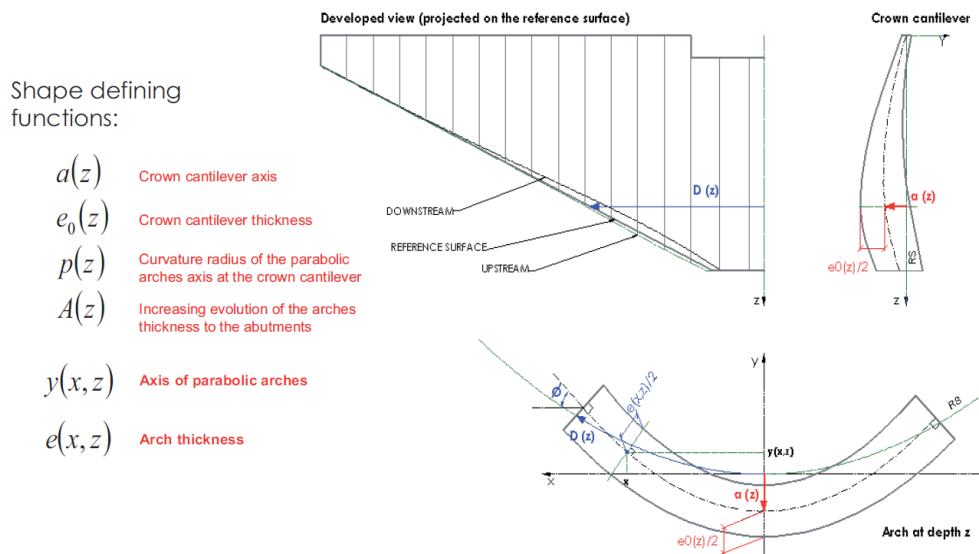
Figure 3-1 - Shape defining functions.

Equation of the axis parabolic arches y:

$$y(x,z) = \frac{x^2}{2 \times p(z)} - a(z)$$

[3.1]

Equation of the arch thickness e:

$$e(x, z) = e_0(z) \times (1 + A(z) \times x^2) \tag{3.2}$$

Equation of the curvature radius of the parabolic arches axis at the crown cantilever p:

$$
\begin{aligned}
p(z) = {} & 1.2 \times 10^2 - 2.769025 \times 10^{-1} \times z - 4.851959 \times 10^{-2} \times z^2 + 2.177441 \\
& \times 10^{-3} \times z^3 - 5.768579 \times 10^{-5} \times z^4 + 8.424111 \times 10^{-7} \times z^5 \\
& - 6.214043 \times 10^{-9} \times z^6 + 1.840075 \times 10^{-11} \times z^7
\end{aligned} \tag{3.3}
$$

Equation of the crown cantilever axis a:

$$
\begin{aligned}
a(z) = {} & 3.033612 \times 10^{-1} \times z - 3.525621 \times 10^{-3} \times z^2 + 3.98983 \times 10^{-5} \times z^3 \\
& - 3.395747 \times 10^{-7} \times z^4
\end{aligned} \tag{3.4}
$$

Equation of the crown cantilever thickness e_0:

$$
\begin{aligned}
e_0(z) = {} & 5 + 1.696654 \times 10^{-1} \times z + 6.206034 \times 10^{-4} \times z^2 - 4.299792 \times 10^{-6} \\
& \times z^3 - 3.838551 \times 10^{-8} \times z^4
\end{aligned} \tag{3.5}
$$

Equation of the increasing evolution of the arches thickness to the abutments A:

$$
\begin{aligned}
A(z) = {} & -1.588312 \times 10^{-6} \times z + 7.975187 \times 10^{-7} \times z^2 - 1.709577 \times 10^{-8} \times z^3 \\
& + 1.859955 \times 10^{-10} \times z^4 - 5.79229 \times 10^{-13} \times z^5
\end{aligned} \tag{3.6}
$$

This dam has four galleries whose basis is located at 10.1, 22.2, 45.6 and 69 meters depth (Figure 3-2 – a)), according to the coordinate system defined in Figure 3-1, with the following dimensions (Figure 3-2 – b).
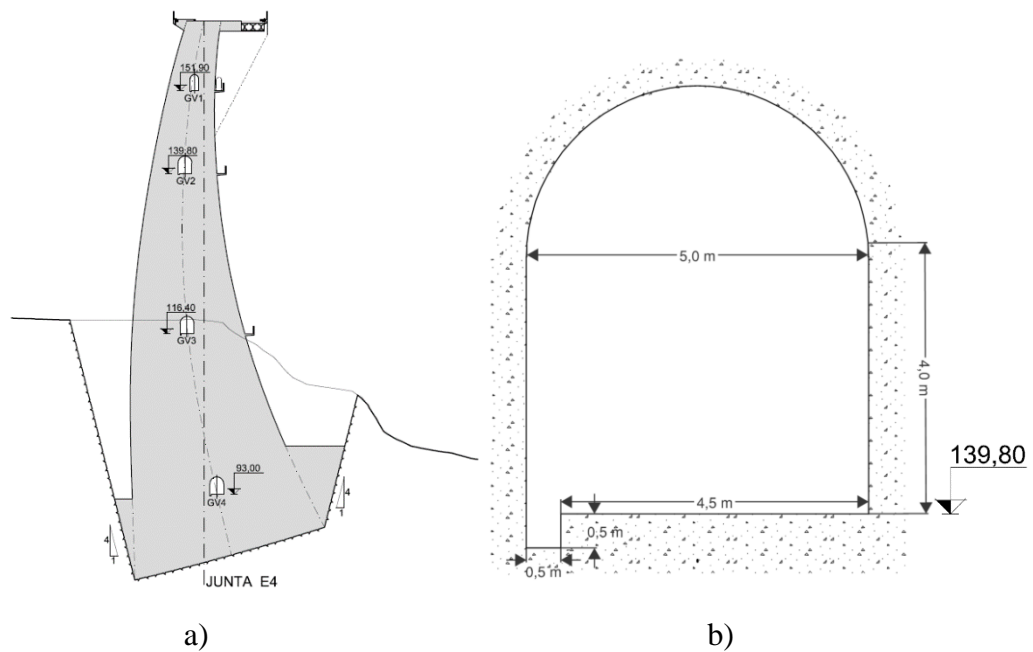
Figure 3-2 - Dam's galleries: a) Galleries location; b) Galleries dimensions.

In *Figure* 3-3 is presented the dam's vertical construction joints configuration, the terrain profile and the dam's intersection with the underlying terrain.
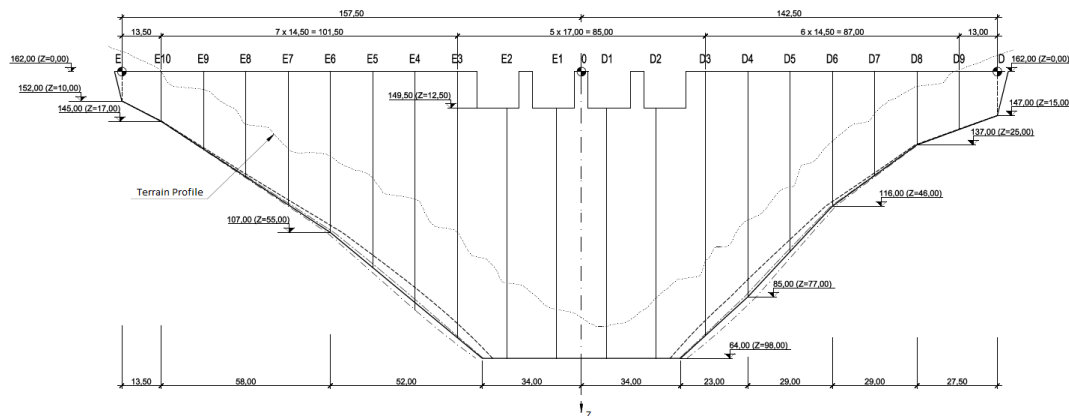
Figure 3-3 - Dam's vertical joint configuration.

3.3 Visual programming applied to the case study

In order to create the parametric model of the dam under study, the workflow depicted in Figure 3-4 was implemented. At first the dam's medium sheet surface was modelled (chapter 3.3.1.1) followed by attributing thickness to the modelled surface (chapter 3.3.1.2). Afterwards, care

was taken in modelling the intersection between the dam and the underlying terrain (chapter 3.3.2). Then, all the galleries were modelled (chapter 3.3.3) and finally the dam's body was cut by vertical and horizontal planes according to the dam's construction joints and the concreting layers height (chapter 3.3.4).
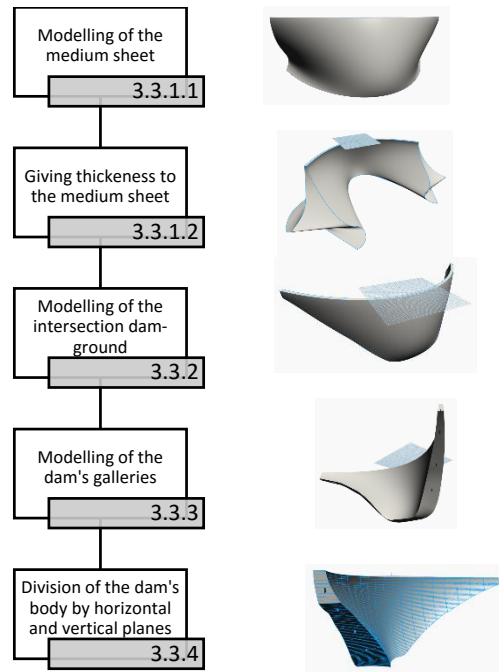
Figure 3-4 - Overall workflow towards modelling the case study dam.

As a principle, the descriptions of this sub-chapter pertain to the operations themselves and not to the visual programming code that was created. However, for the readers interested in specific aspects of the visual programming, Annex I contains the full program, with details on each of the described operation. In the text of the thesis, the reference to stretches of code of visual programming that pertain to a specific operation will be referred in brackets with the 'VizPro' acronym in the following fashion: [VizPro_2:3] refers to the stretch of Visual programming number 3, present in Section 2.

3.3.1 Arch dam body

3.3.1.1 Modelling of the medium sheet

The first step for modelling the medium sheet was the implementation of the shape defining equation system (Figure 3-1 and equations [3.1], [3.3] and [3.4]) of the arch medium sheet.

The system of equations was solved for a mesh of points created with sixty horizontal points in each row and rows spaced by five meters along the z axis defined in Figure 3-1 (Figure 3-5) [VizPro_1:1].
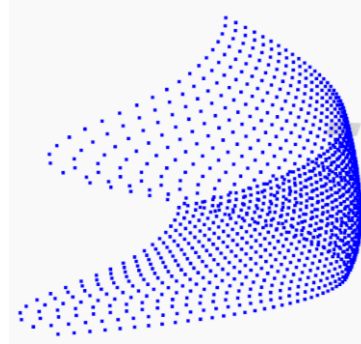
Figure 3-5 - Mesh Grid created for the medium sheet of the dam.

Afterwards NURBS[1] were created curves to connect the horizontal mesh points (Figure 3-6) [VizPro_1:1].
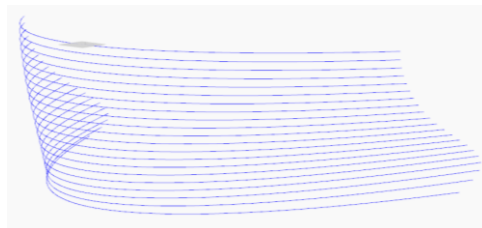
Figure 3-6 - NURBS curves.

Then were created a surface by a LOFT[2] between the created curves (Figure 3-7) [VizPro_1:2].
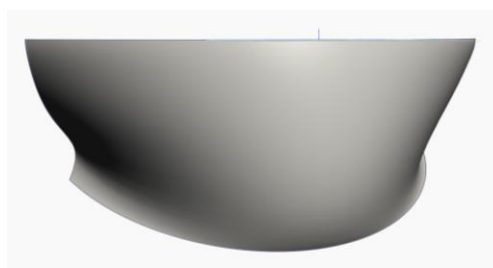
Figure 3-7 - Medium sheet of the arch dam.

---

[1] Non-Uniform Rational B-Splines.

[2] A solid or surface between two given cross sections.

The accuracy of the geometry that was obtained with the above-mentioned strategy was tested through the evaluation of the *y* coordinate of ten points of the medium sheet, with a given set of randomly selected *x* and *z* coordinates (which were more or less evenly distributed along the dam). A comparison was made between the solution obtained with Dynamo (that incorporates interpolations due to the use of NURBS and loft operations), and the analytical solution (equations [3.1], [3.3] and [3.4]), as shown in Table 3-1.

Table 3-1 - Comparison between dynamo and analytical solution coordinates for the used mesh.

	Given Coordinates [m]		Dynamo [m]	Analytical Solution [m]			Error
	X	*Z*	*Y*	*p(z)*	*a(z)*	*y(x,z)*	
Point 1	0	55	-9,493	72,387	9,551	-9,551	0,058
Point 2	12,5	72,5	-7,906	59,626	9,285	-7,974	0,068
Point 3	80	3	26,106	118,787	0,879	26,060	0,046
Point 4	-7	77	-8,237	57,633	8,733	-8,308	0,071
Point 5	123	19	66,379	106,451	4,721	66,341	0,038
Point 6	36	36	-0,453	90,704	7,643	-0,499	0,046
Point 7	-45	17	5,089	108,204	4,306	5,051	0,038
Point 8	-63	52	17,096	75,143	9,369	17,041	0,055
Point 9	117	90	115,197	56,718	5,551	115,124	0,073
Point 10	-99	81,5	79,098	56,357	7,923	79,032	0,066

Through the analysis of the Table 3-1 it can be concluded that the error is rather high, in the order of 7.5 centimetres. This error could have been minimized through introducing more points in the mesh grid (Figure 3-5), although it will affect the model calculation time in dynamo. Thus, a study was made in order to know how many points are necessary to obtain a lower error, under 0.5 centimetres, (Table 3-2) and was verified that with a mesh of points equally spaced by one meter in horizontal and vertical directions that error can be accomplished.

Table 3-2 - Comparison between dynamo and analytical solution coordinates for a mesh of points spaced by 1 meter.

	Given Coordinates [m]		Dynamo [m]	Analytical Solution [m]			Error
	X	Z	Y	p(z)	a(z)	y(x,z)	
Point 1	0	55	-9,549	72,387	9,551	-9,551	0,002
Point 2	12,5	72,5	-7,972	59,626	9,285	-7,974	0,002
Point 3	80	3	26,061	118,787	0,879	26,060	0,001
Point 4	-7	77	-8,306	57,633	8,733	-8,308	0,002
Point 5	123	19	66,342	106,451	4,721	66,341	0,001
Point 6	36	36	-0,497	90,704	7,643	-0,499	0,002
Point 7	-45	17	5,053	108,204	4,306	5,051	0,002
Point 8	-63	52	17,043	75,143	9,369	17,041	0,002
Point 9	117	90	115,12	56,718	5,551	115,124	0,004
Point 10	-99	81,5	79,035	56,357	7,923	79,032	0,003

Although the mesh of points equally spaced by one meter conducts to a more accurate medium sheet shape it wasn't used due to the higher computational calculation time needed by dynamo.

3.3.1.2 Attributing thickness to the modelled surface (dam's medium sheet)

The thickness of the dam is expressed by equations [3.5] - [3.6]. The dam's thickness was modelled through a similar methodology to the one that had already been used in the scope of the medium sheet. At first, a mesh of points was created, which was parallel to the medium sheet, and distanced $\frac{e_0(z)}{2}$ from the medium sheet (Figure 3-1) according to a vector perpendicular to the surface. Afterward, NURBS curves were created to connect the previously created points and then a LOFT operation was made to assemble this curve into a surface. This process was the same for both upstream and downstream surfaces of the dam.

Certain operations involved in the process demanded capacities that were not directly embedded in Dynamo's library of commands. Therefore, it was necessary to write some code in Python - within a custom Dynamo 'node' - to conduct such operations. An example of a created node

used Python programming language is presented in Figure 3-8. The node has two inputs named as IN[0] and IN[1]. If IN[0] is positive, it will be added to IN[1] to produce the desirable output. If not, it will be subtracted from [1]. This specific program was prepared to obtain the points that were used to model the downstream and upstream surfaces. [VizPro_1:2]

Figure 3-8 - Created Dynamo node using Python.

With the availability of the upstream and downstream surfaces of the dam's body, and bearing in mind the intent of generating a solid body from them, it was necessary to create the left and right bank surfaces, as well as the top and bottom surfaces. These surfaces were created through LOFT's between the perimeter curves of the downstream and upstream surfaces. With the six faces of the solid could be created (see Figure 3-9). [VizPro_1:2 and VizPro_1:3]
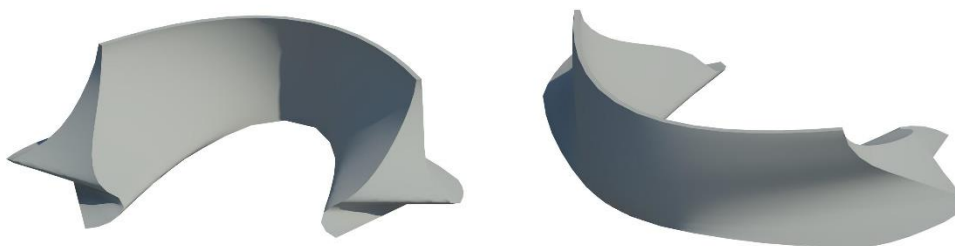
Figure 3-9 - a) View of the upstream face of the dam's body; b) View of the downstream face of the dam's body.

3.3.2 Modeling of the intersection of dam/ground

In order to model the intersection between the dam and the underlying terrain, the input data consisted in a set of base lines as defined in the dam's drawings (see Figure 3-10) for a group of cross-sectional representations that coincide with the vertical construction joints.
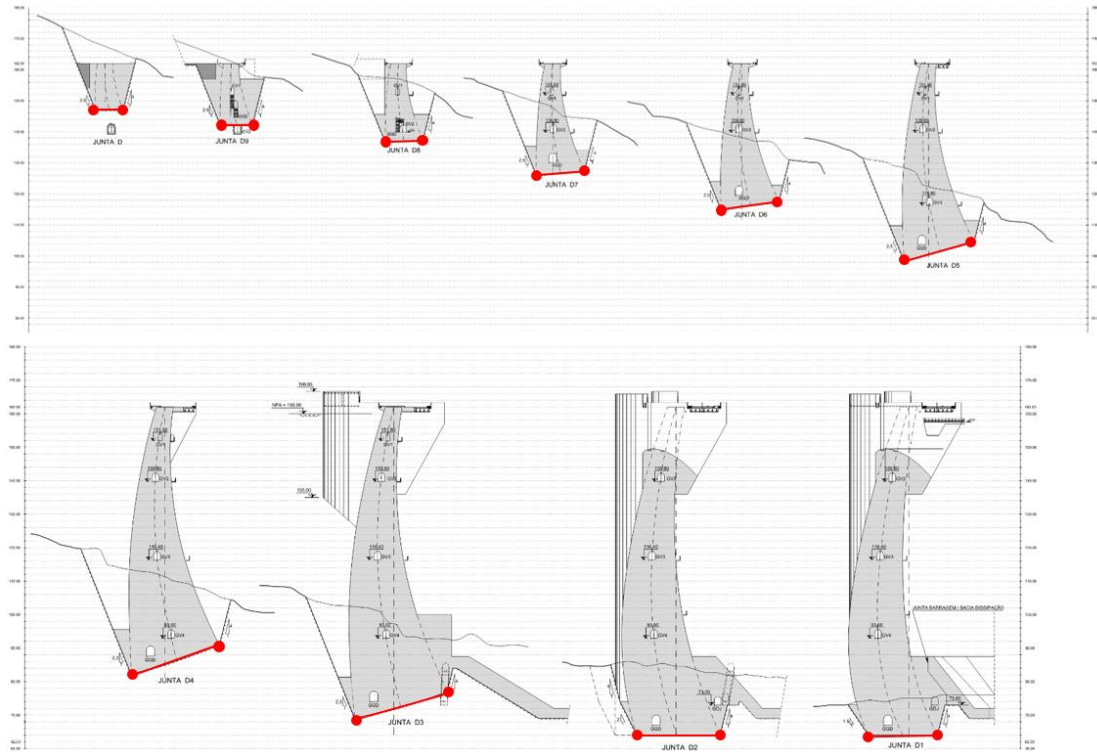
Figure 3-10 - Points and lines picked from the dam's structural project.

The methodology to determine the above points in the model is described in Figure 3-11. At first, was intersected the vertical plane defined by the construction vertical joint (perpendicular to the dam's body) and the horizontal plane determined by the depth of the points (Figure 3-10) witch result in a straight line. The intersection of that straight line with the downstream or upstream surfaces gives the desired points (red points in Figure 3-10). After the drawn of the all the points they were connected by lines (Figure 3-12).
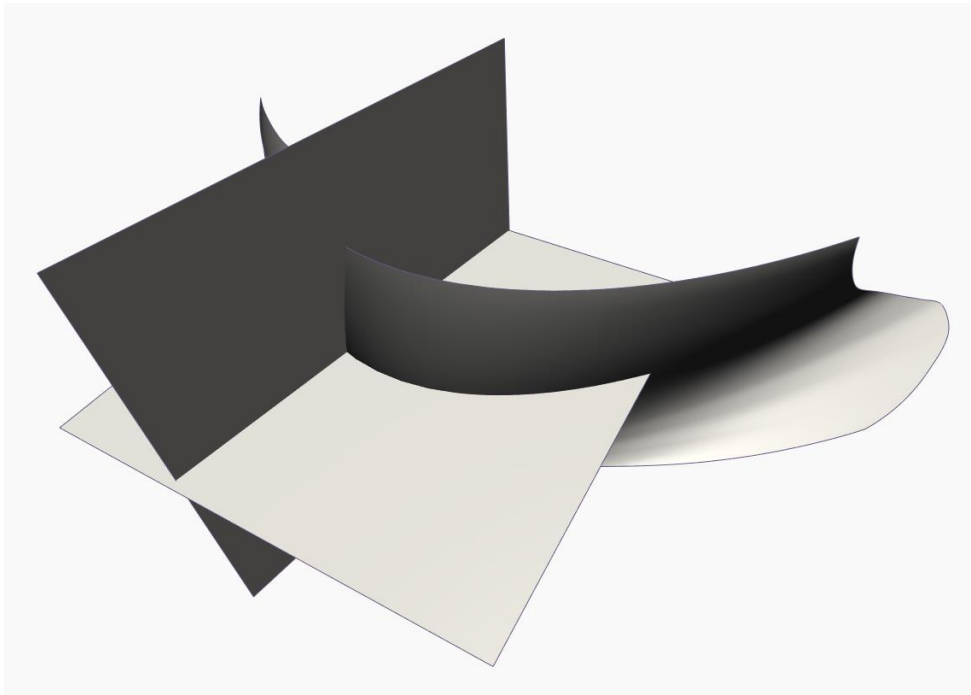
Figure 3-11 - Planes intersection with the downstream and upstream surfaces of the dam.
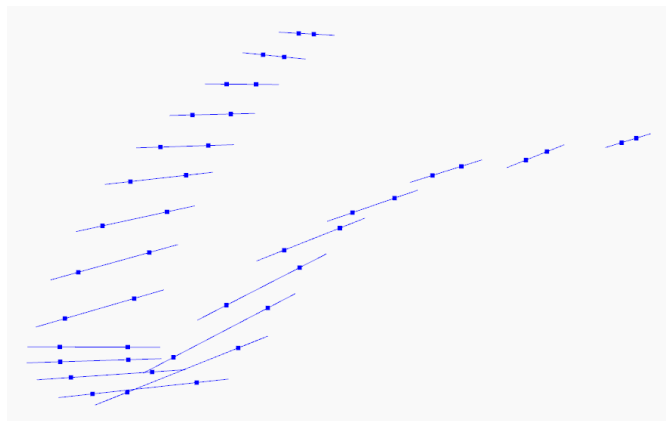
Figure 3-12 - Modelling of the points and lines withdrawn from structural project.

Afterwards, a LOFT operation was made between the previously created lines in order to obtain the surface of intersection of the dam's body with the ground – see Figure 3-13.
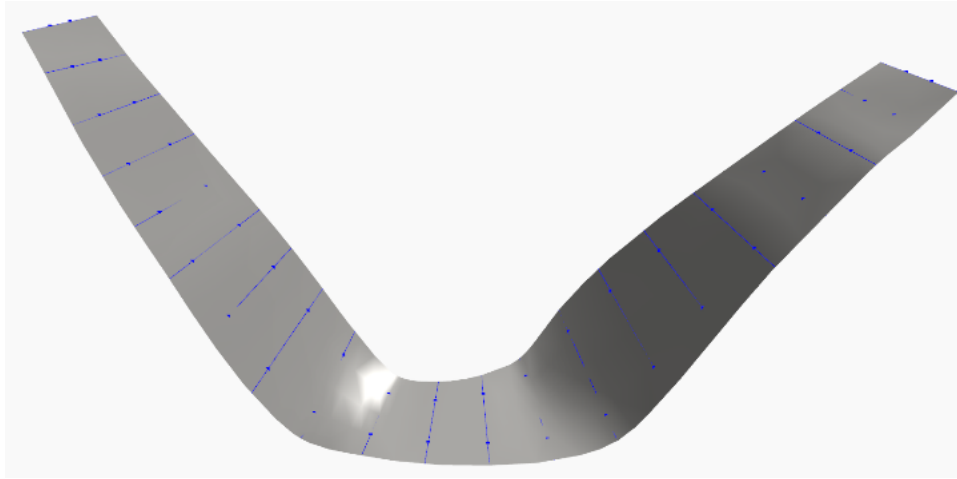
Figure 3-13 - Surface of intersection of the dam's body and the ground.

After that the dam's body was sliced by the previously created surface (see Figure 3-13) and the resulting dam's body is present in Figure 3-14.

a)

b)
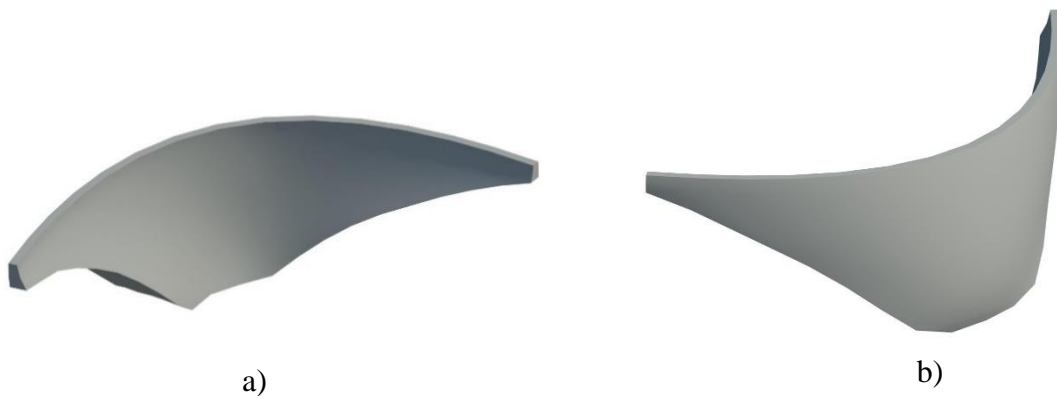
Figure 3-14 - Dam's views: a) Upstream; b) Downstream.

3.3.3 Modelling of the dam's galleries

The dam's galleries are located along the dam's medium sheet with the dimension's and depth's presented in Figure 3-2. In order to model the dam's galleries, the dam's medium sheet was cut by a horizontal plane at the dam's gallery depth to obtain the green line in Figure 3-15. Then were drawn lines parallel to those who passes at the red and blue points (Figure 3-15), according to the dimension's presented in Figure 3-2-b), was shown in Figure 3-16.
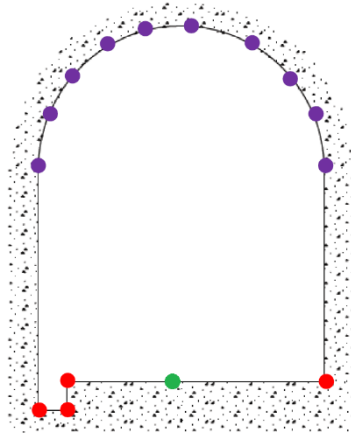
Figure 3-15 - Points used to model the dam's galleries.
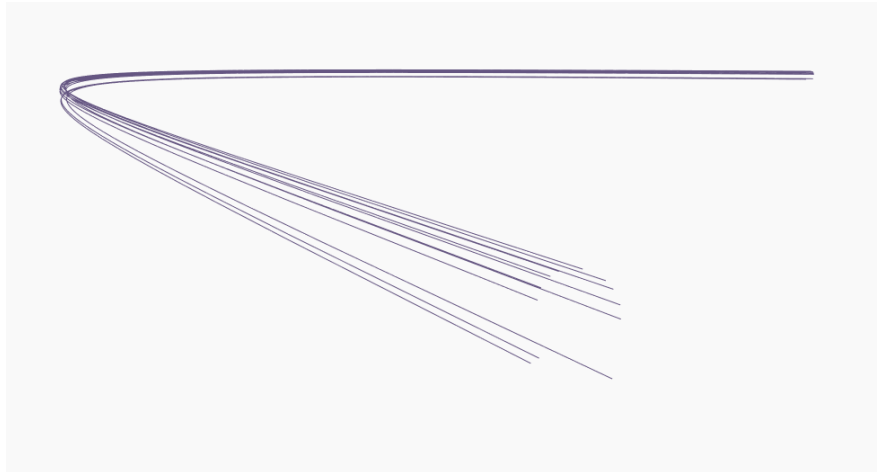
Figure 3-16 – Curves used to model the dam's galleries.

After that, surfaces were made connecting the lines that pass through the red points in Figure 3-15. Then, an extrusion of these surfaces was made with an adopted height (much higher than the actual height of the gallery), creating a solid with the cross-sectional aspect shown in Figure 3-17 – a). A LOFT of the lines passing at the blue points in Figure 3-15 was made creating a surface, and the dam's galleries modelling was made through the cut of the previously created solid and surface (Figure 3-17 – b)), as presented in Figure 3-17 – c).

a)   b)   c)
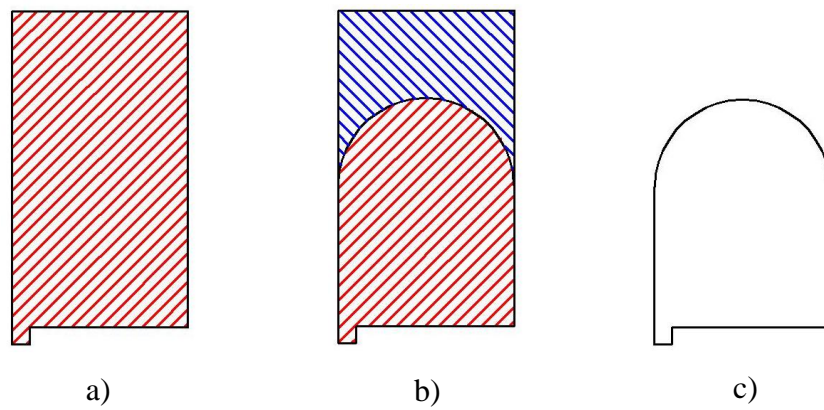
Figure 3-17 - Adopted modelling phases in order to model the dam's galleries.

The resulting shape of the dam's galleries is presented in Figure 3-18 and the boolean difference between the dam's body (Figure 3-14) and the modelled galleries (Figure 3-18) is presented in Figure 3-19 and in Figure 3-20.

Figure 3-18 - Views of dam's galleries.

a)   b)

Figure 3-19 - a) Dam's view from left bank; b) Dam's view from right bank.
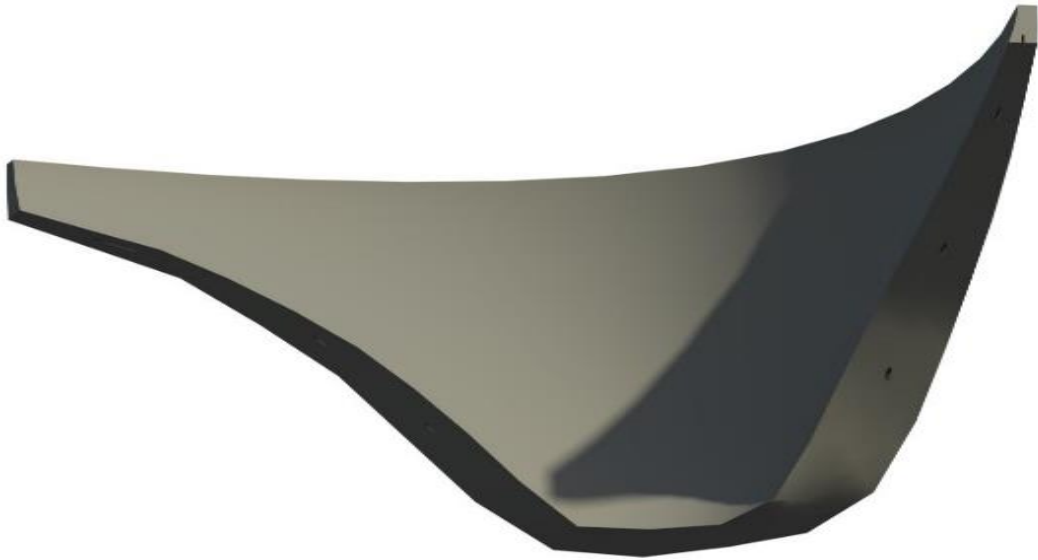
Figure 3-20 – Dam with the galleries modelled.

3.3.4 Division of dam's body by horizontal and vertical joints

The dam was cut by horizontal and vertical planes according to the dam's construction joints and the height of the concrete layers. The number of vertical and horizontal divisions of the model is totally parametric, so it can be easily changed in order to study different construction scenarios.

To all the resulting solids of the vertical cuts of the dam's body by the construction vertical joints, applies the following cut methodology in order to slice that solids by horizontal planes according to the concrete layers' height.

Due to an impossibility of dynamo to cut a solid by more than one plane at a time, was necessary to create an algorithm that successively cuts the solid by one plane, resulting one part of the solid with the intended height and the another part of the solid that will be cut in next cycle of the algorithm till the solid resulting of the cut process has a height lower or equal to the concrete layers' height.

Taking into account the cutting methodology explained above a custom node was created in dynamo (Figure 3-21), where the inputs are the cutting planes and the dam's body solid and the outputs are the solid sliced by the input planes. [VizPro_4:5]
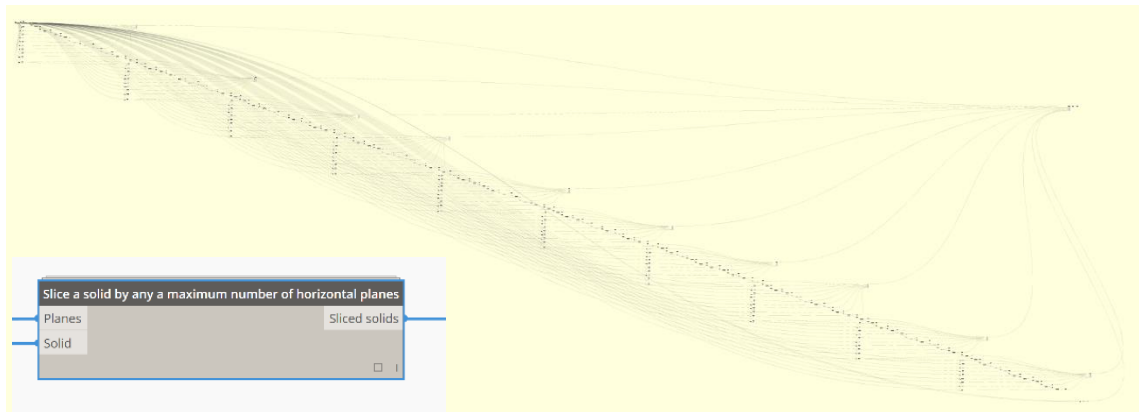
Figure 3-21 - Custom node created to cut the dam's body by horizontal planes.

The dam body sliced by horizontal and vertical planes is presented in Figure 3-22.

a)   b)
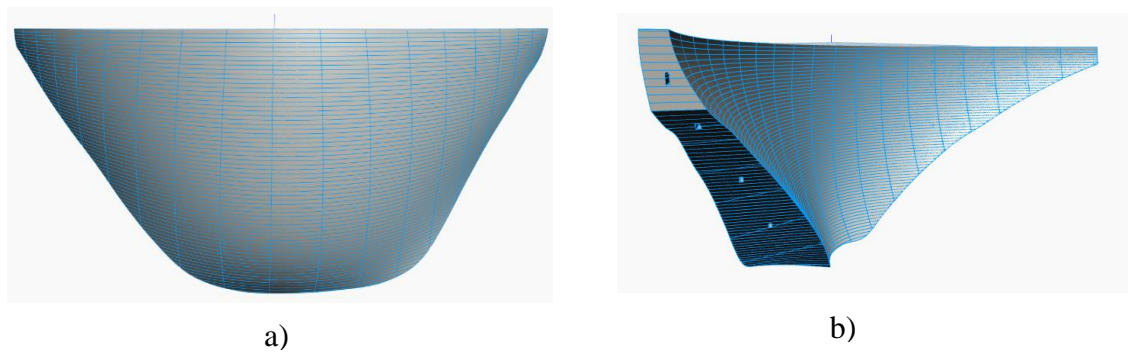
Figure 3-22 - Views of the dam: a) sliced downstream view; b) sliced right bank view.

3.4 Interoperability

Chapters 4 and 5 present computer programs created in order to conduct thermal analyses and construction phasing studies of dams through interoperability with the modelling software adopted in the present chapter.

The interoperability was made through the creation of CSV (comma separated values) files by the Dynamo that are read by subsequent programs. This was a simplified interoperability framework that can easily be transformed into an automatic procedure of direct exchange between Dynamo/Excel or Dynamo/Matlab, materialized through API (application programmable interface) programming or similar procedure.

The interoperability between Dynamo and REVIT is direct, because Dynamo is a REVIT plugin. So the challenge to the interoperability of the created model is the creation of an IFC file that turns the created model interoperable with the all the BIM platforms and allow to embed non-geometrical information related to the identification of the concrete layers as well as the possibility of extraction of quantities within the IFC file for each concrete layer.

The identification of layers was made through their vertical profile ID as presented in Figure 3-23 and with the casting order of the concrete layers of each vertical profile.
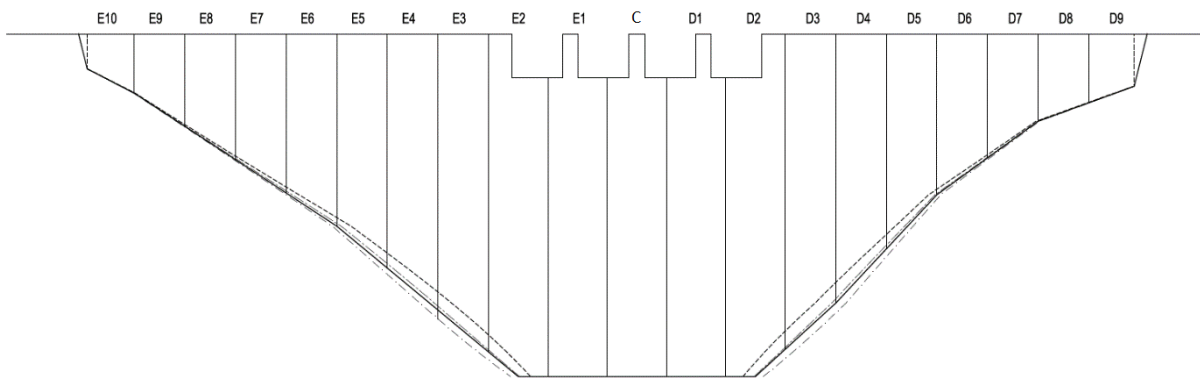
Figure 3-23 - Dam elevation and vertical profiles.

In order to achieve the aforementioned objective two project parameters were created in REVIT to be handled in Dynamo.

After the creation of the project parameters some code in dynamo was made to handle introduction of the non-geometrical information to each concrete layer. The developed visual programming code is presented in VizPro_4:6.

In REVIT the model was exported to IFC format using the REVIT IFC Exporter Alternative User Interface ("IFC Exporter 2016," n.d.) due to a larger number of available options that allow a better configuration of the exported IFC file. This Alternative UI was used to allow the exportation of the Revit and IFC common property sets as well as the base quantities.

The created IFC file was opened in multiple BIM platforms as Solibri Model Checker and TEKLA BIMsight in order to verify if the created parameters were indeed embedded in the model and the extraction of the volumes of each layer was possible. Figure 3-24 presents the created IFC file in Solibri Model Checker and in TEKLA BIMsight was made a similar experience.
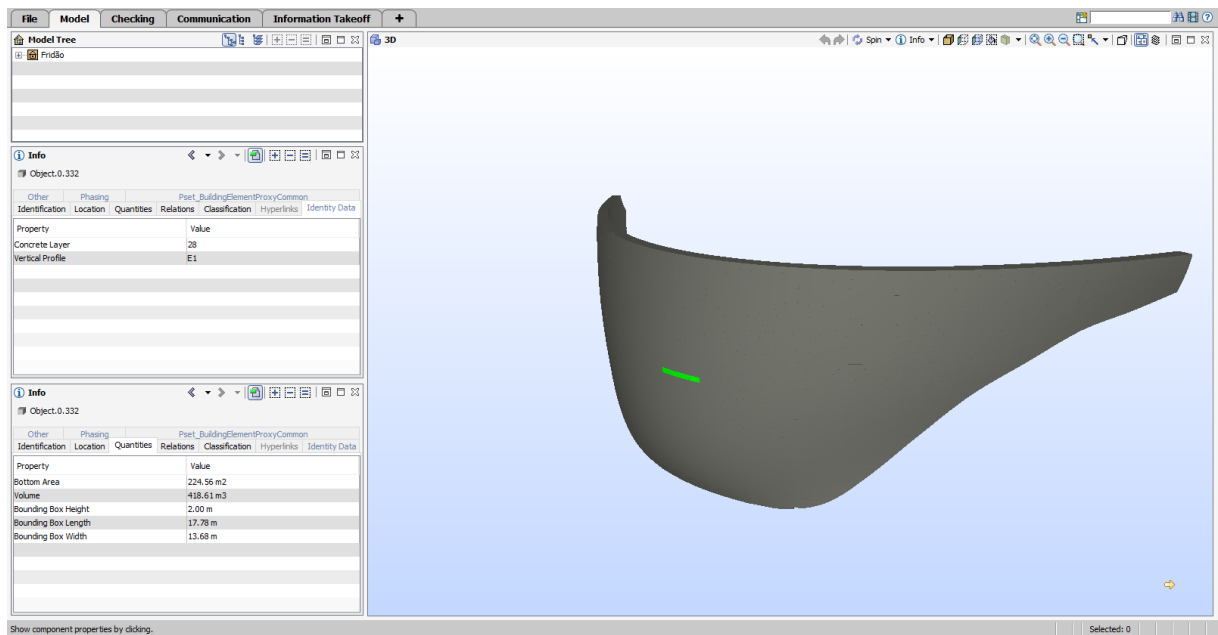
Figure 3-24 - IFC file open on Solibri Model Checker.

Thereby, the interoperability of the created model was achieved, allowing the utilization of the created model in different BIM platforms to perform multiple analysis, as structural calculations or construction planning.

3.5 Final considerations

The final geometry outcome exalts the fact, that at this point there are no complex geometries to visual programing and parametric modeling, being this type of tools indispensable to modeling of complex shape structures.

The created full 3D served as support to the developed computational tools of chapter 4 and chapter 5, through the created interoperability through the creation of files that were written by Dynamo and read by the computational tool to use.

CHAPTER 4

4 THERMAL ANALYSIS: IMPLEMENTATION OF A FINITE DIFFERENCE TOOL

4.1 Introduction

Taking into account the intent to create an integrated framework for modelling and analysis of the construction phasing of dam bodies, one of the fundamental aspects is the creation of a simulation tool that allows quick decisions to be made in regard to the impact of construction strategy decisions on the temperature development in the dam body. In fact, a choice of increase of the thickness of concreting layers can accelerate the completion of the construction, but may induce unacceptably high cracking risks. On the other hand, very conservative choices on casting layer thicknesses (i.e. very slim layers) can induce significant delays and added costs due to the global duration of the construction. The availability of an expedite yet reasonably accurate tool to estimate the temperature fields that result from each studied scenario can be an important asset at the early stages of design of dams. That is precisely the objective of the tool developed in the scope of this chapter, which is intended to be quick for assisting the study of several alternative scenarios.

In the numeric derivation that supports the development of the computational tool was used the finite difference method due to their ease to implement and their relatively fast calculation time. The adopted software for programming the developed tool was MATLAB due to their capacities in matrix manipulation and calculus with matrixes and vectors.

The requirements and objectives to for the developed computational tool are:

1. Be capable of interoperability with the BIM modelling framework outlined in the previous chapter (Dynamo/REVIT);
2. Simulate the heat conduction inside the concrete and the heat convection with the surrounding environment, with due consideration of the effects of formwork and their withdrawal;
3. Simulate the layered construction phasing;

4. Simulate the non-linear heat generation of concrete containing with the basis on a preloaded database of the most common cements in the Portuguese market (easily expandable database, though);

5. Being capable of automatically generating temperature maps and plots of temperature evolution for selected relevant instants over time.

4.2 Intended inputs/outputs and operation of the developed tool

The classical finite differences have some limitations in the definition of the boundary conditions that limits the definition of the curved shape of the dam's body. Therefore, a simplification the dam's shape needed to be made. The adopted simplification, on interoperability with the modeling tool used in chapter 3 – Dynamo, was the creation of an alternative dam with the same concrete layers and total height and the maximum width of the real dam's body.

Hence, the geometrical information that are transferred from Dynamo to MATLAB are the number of concrete layers, the layers' height and the medium width of the dam's body. This information is interoperable through a CSV (comma separated values) file that dynamo writes in the file path of the developed computational tool and MATLAB reads.

a)   b)
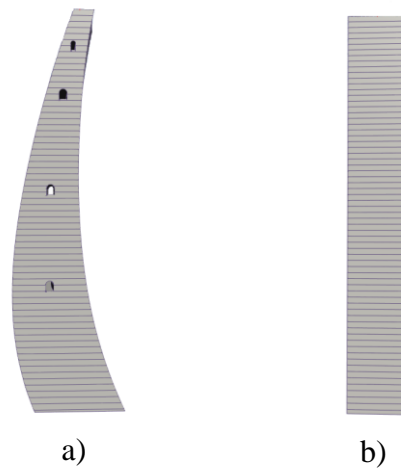
Figure 4-1 - Simplification introduced in the developed program: a) Real dam's shape;
b) Adopted dam's shape.

Another important definition is the boundaries of the computed model, as presented below in Figure 4-2 for three different concrete phases. Boundaries are labelled B1 to B3, according to the following:

- B1 represents the limit of the modelled ground. It is considered that no heat is transmitted through this boundary during the whole analysis, so this boundary is adiabatic;
- B2 represents the lateral boundaries of the multiple concreting layers. These boundaries have different convective coefficients before and after the formwork withdrawal;
- B3 represents the upper boundary of the multiple concreting layers until the concreting of the following layer. This boundary has the same convective coefficient than the lateral boundaries without formwork.
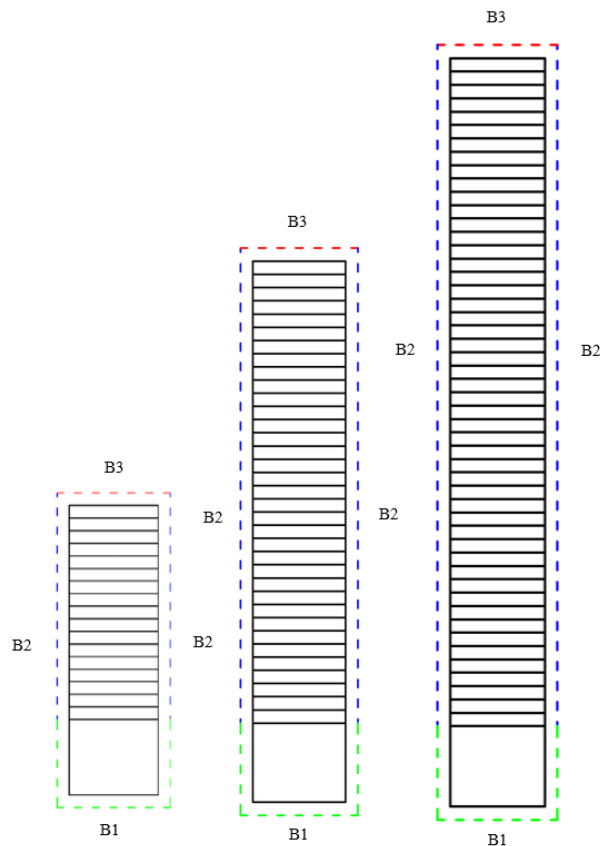
Figure 4-2 - Boundaries of the computed model for three different phases.

The height of the ground beneath the dam has to be such as the heat exchanges between the dam and its foundation do not affect the first dam's concrete layer temperature.

The basic principle of analysis of this phased model is to carry the results of a previous phase (temperatures, grade of hydration) as initial conditions for the subsequent phase. The input of a new phase of analysis also includes the additional geometry, as well as information about the previously existing geometry or boundaries that remain active.

Other than these input specificities, and result superimposition, the procedures for each phase of the analysis are the same of a regular non-phased analysis model.

So, the program should be capable of generating temperature maps, as presented in Figure 4-3 and plots of temperature evolution for selected relevant instants over time as shown in Figure 4-4.
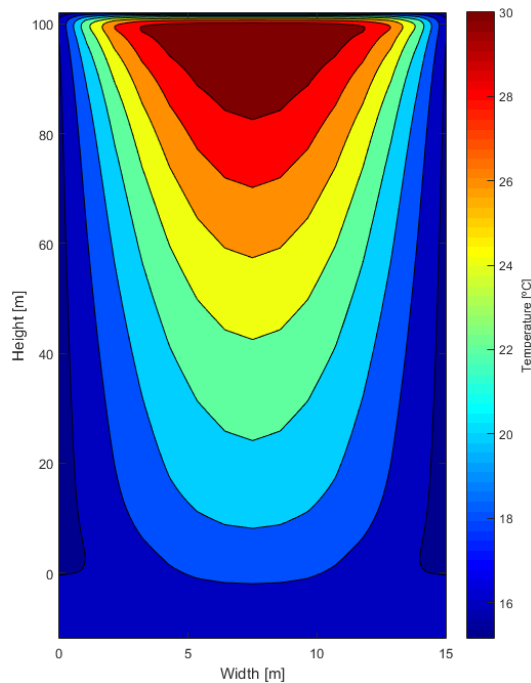
Figure 4-3 - Expected temperature map for an instant.
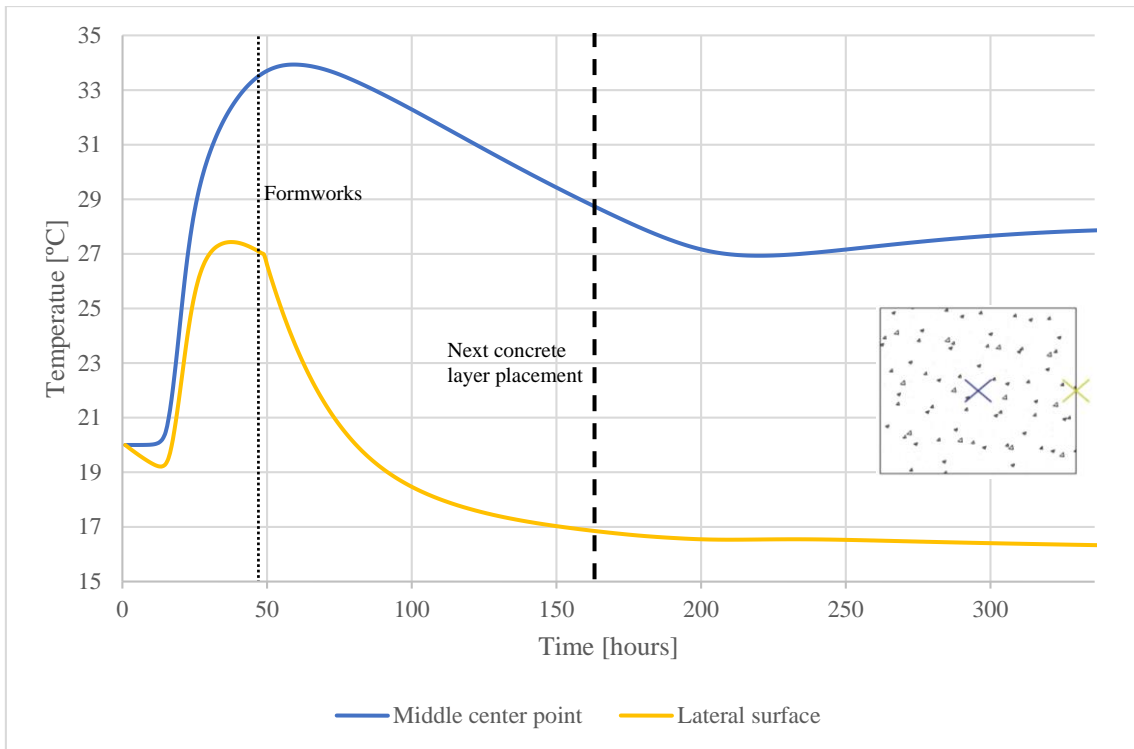
Figure 4-4 - Expected temperature plot over time for a concrete layer for an instant.

The zero time of the graphic presented in Figure 4-4 is the concrete placing time for a certain concrete layer. Along time can be verified the heating and cooling phases of the middle center point and the middle point on a surface.

4.3 Discretization through the finite difference method

The discretization to 2D finite difference method was made according to the Fourier equation presented in chapter 2.2 and the following schema (Figure 4-5).
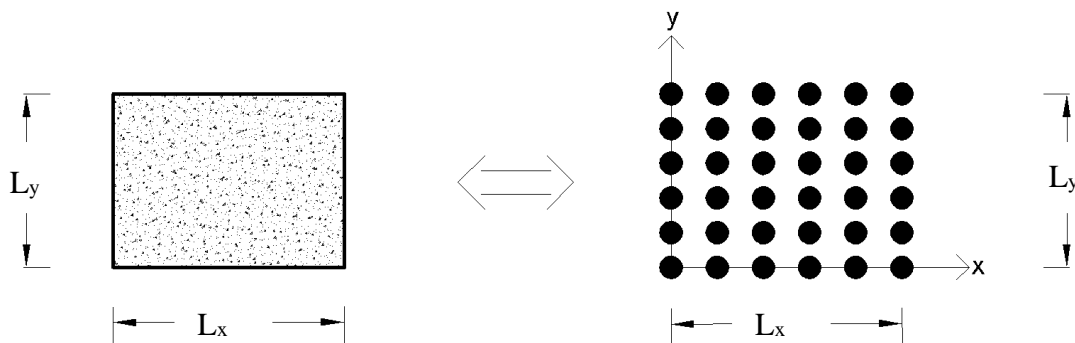
Figure 4-5 - Schema adopted for the 2D algorithm.

Hence, using the finite difference method to the spatial and temporal discretization and applying to the case study:

$$\alpha_T \frac{\partial^2 T}{\partial x^2}\bigg|_{n+1} + \alpha_T \frac{\partial^2 T}{\partial y^2}\bigg|_{n+1} + \frac{\alpha_T}{k}\dot{Q}\big|_{n+1} = \frac{\partial T}{\partial t}\bigg|_{n+1} \qquad (0 < x < L_x ; 0 < y < L_y ; t > 0) \qquad [4.1]$$

being the following boundary conditions:

$$\begin{cases} \dfrac{dT}{dx} = 0 & \text{for } x = 0 \\[2mm] k\dfrac{dT}{dx} + h_L T = h_L T_\infty & \text{for } x = L_x \\[2mm] k\dfrac{dT}{dy} + h_L T = h_L T_\infty & \text{for } y = L_y \end{cases} \qquad [4.2]$$

Following are presented the three different type of nodes for two different construction phases: internal nodes (blue in Figure 4-6), lateral nodes (green in Figure 4-6) and corner nodes (red in Figure 4-6).
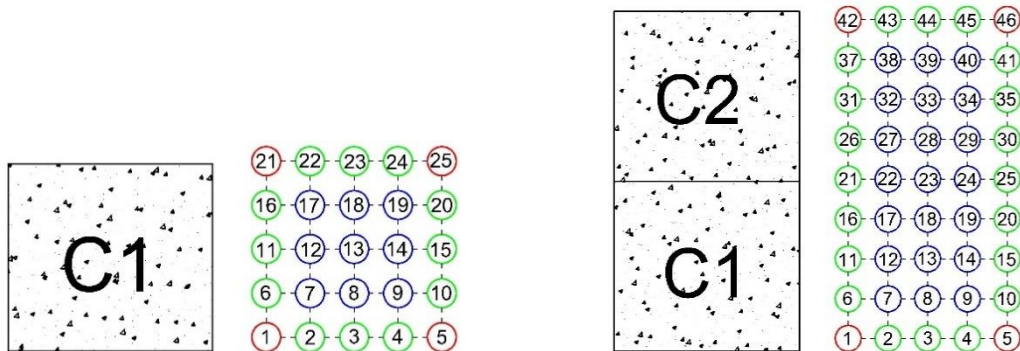
Figure 4-6 - Types of nodes on a finite difference mesh.

4.3.1 General nodes

In the following derivation will be used a local coordinate system for each point of the mesh that by simplification is represented by the point in study (Point) and its cardinal points (North, East, South and West).
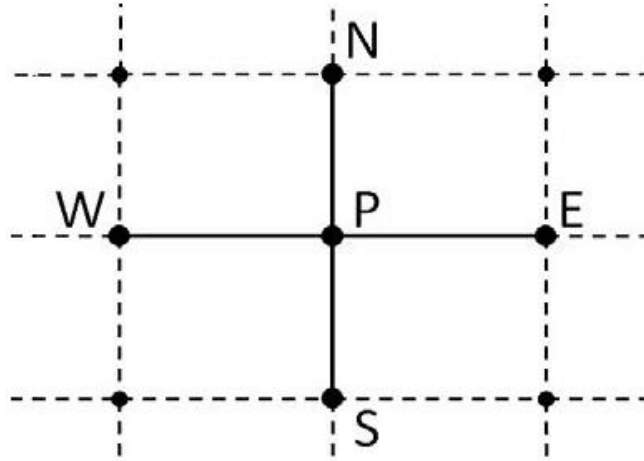
Figure 4-7 - Local coordinate system used for the internal points.

Afterward are presented the derivation of the internal nodes of the finite different mesh.

Using the notation T_n^i to designate the temperature in the instant *n* relative to the node *i*, and applying the finite differences to the expression [4.1] applied to an interior node:

$$\frac{T_{n+1}^P - T_n^P}{\Delta t} = \alpha_T \times \frac{T_{n+1}^W - 2T_{n+1}^P + T_{n+1}^E}{\Delta x^2} + \alpha_T \times \frac{T_{n+1}^S - 2T_{n+1}^P + T_{n+1}^N}{\Delta y^2}$$
$$+ \frac{\alpha_T}{k}\dot{Q}_{n+1} \qquad [4.3]$$

Solving in order to T_n^P:

$$T_{n+1}^P - T_n^P = \frac{\alpha_T \times \Delta t}{\Delta x^2} \times (T_{n+1}^W - 2T_{n+1}^P + T_{n+1}^E) + \frac{\alpha_T \times \Delta t}{\Delta y^2}$$
$$\times (T_{n+1}^S - 2T_{n+1}^P + T_{n+1}^N) + \frac{\alpha_T \times \Delta t}{k}\dot{Q}_{n+1} \qquad [4.4]$$

Being $x = \frac{\alpha_T \times \Delta t}{\Delta x^2}$ and $y = \frac{\alpha_T \times \Delta t}{\Delta y^2}$:

$$-T_n^P = -T_{n+1}^P + x \times (T_{n+1}^W - 2T_{n+1}^P + T_{n+1}^E) + y$$
$$\times (T_{n+1}^S - 2T_{n+1}^P + T_{n+1}^N) + \frac{\alpha_T \times \Delta t}{k} \dot{Q}_{n+1} \qquad [4.5]$$

$$T_n^P = T_{n+1}^P - T_{n+1}^W \times x + 2T_{n+1}^P \times x - T_{n+1}^E \times x - T_{n+1}^S \times y + 2T_{n+1}^P \times y$$
$$- T_{n+1}^N \times y - \frac{\alpha_T \times \Delta t}{k} \dot{Q}_{n+1} \qquad [4.6]$$

Equation to the heat conduction for the internal nodes of the finite difference mesh are:

$$T_n^P = (2x + 2y + 1) \times T_{n+1}^P - T_{n+1}^W \times x - T_{n+1}^E \times x - T_{n+1}^S \times y - T_{n+1}^N$$
$$\times y - \frac{\alpha_T \times \Delta t}{k} \dot{Q}_{n+1} \qquad [4.7]$$

4.3.2 Definition of the boundary conditions

The nodes near the boundaries beyond the conduction are affected by convection from the block external borders.

The nodes in the lateral of the concrete blocks have the following boundary conditions:

$$\begin{cases} k\frac{dT}{dx} + h_l T = h_l T_\infty \quad \text{for the east and west boundaries} \\ \\ k\frac{dT}{dy} + h_l T = h_l T_\infty \quad \text{for the north and south boundaries} \end{cases} \qquad [4.8]$$

According to equation the boundary condition can be expressed:

$$k\frac{T_{n+1}^{external\ point} - T_{n+1}^{internal\ point}}{2 \times (\Delta x\ or\ \Delta y)} = h_l(T_\infty - T_{n+1}^P) \qquad [4.9]$$

By example will be derived the expressions to the east and north nodes to hereafter derivate the expression to the northeast corner.

East nodes

For the east nodes will be used the following local coordinate system:
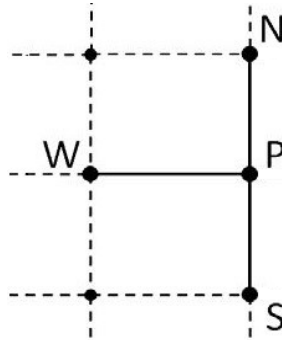
Figure 4-8 - Coordinate system for the east points.

According to [4.8] and [4.9] the boundary condition can be expressed:

$$k \frac{T_{n+1}^E - T_{n+1}^W}{2 \times \Delta x} = h_l(T_\infty - T_{n+1}^P) \qquad [4.10]$$

$$T_{n+1}^E - T_{n+1}^W = 2 \frac{\Delta x \times h_l}{k} T_\infty - 2 \frac{\Delta x \times h_l}{k} T_{n+1}^P \qquad [4.11]$$

Being $\gamma = \frac{h_l}{k} T_\infty$:

$$T_{n+1}^E = T_{n+1}^W + 2 \times \Delta x \times \gamma - 2 \frac{\Delta x \times h_l}{k} T_{n+1}^P \qquad [4.12]$$

Substituting in the equation to the heat conduction for the internal nodes [4.7]:

$$T_n^P = (2x + 2y + 1) \times T_{n+1}^P - T_{n+1}^W \times x$$
$$- \left(T_{n+1}^W + 2 \times \Delta x \times \gamma - 2 \frac{\Delta x \times h_l}{k} T_{n+1}^P \right) \times x - T_{n+1}^S \times y$$
$$- T_{n+1}^N \times y - \frac{\alpha_T \times \Delta t}{k} \dot{Q}_{n+1} \qquad [4.13]$$

Being $\mu = 2x + 2y + 2\frac{\Delta x \times h_l}{k} x$:

$$T_n^P = (1 + \mu) \times T_{n+1}^P - 2T_{n+1}^W \times x - T_{n+1}^S \times y - T_{n+1}^N \times y - 2 \times \Delta x \times \gamma$$
$$\times x - \frac{\alpha_T \times \Delta t}{k} \dot{Q}_{n+1} \qquad [4.14]$$

The above expression is the heat equation for the east nodes of the finite difference mesh.

North nodes

For the north nodes will be used the following local coordinate system:
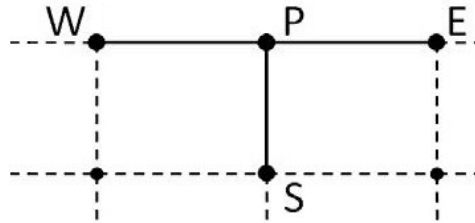
Figure 4-9 - Local coordinate system used for the north nodes.

According to [4.8] and [4.9] the boundary condition can be expressed:

$$k \frac{T_{n+1}^N - T_{n+1}^S}{2 \times \Delta y} = h_l(T_\infty - T_{n+1}^P) \qquad [4.15]$$

$$T_{n+1}^N - T_{n+1}^S = 2 \frac{\Delta y \times h_l}{k} T_\infty - 2 \frac{\Delta y \times h_l}{k} T_{n+1}^P \qquad [4.16]$$

Being $\gamma = \frac{h_l}{k} T_\infty$:

$$T_{n+1}^N = T_{n+1}^S + 2 \times \Delta y \times \gamma - 2 \frac{\Delta y \times h_l}{k} T_{n+1}^P \qquad [4.17]$$

Substituting in the equation to the heat conduction for the internal nodes [4.7]:

$$
\begin{aligned}
T_n^P = (2x + 2y + 1) \times T_{n+1}^P &- T_{n+1}^W \times x - T_{n+1}^E \times x - T_{n+1}^S \times y \\
&- \left(T_{n+1}^S + 2 \times \Delta y \times \gamma - 2 \frac{\Delta y \times h_l}{k} T_{n+1}^P \right) \times y \\
&- \frac{\alpha_T \times \Delta t}{k} \dot{Q}_{n+1}
\end{aligned}
\qquad [4.18]
$$

Being $\theta = 2x + 2y + 2 \frac{\Delta y \times h_l}{k} y$:

$$
\begin{aligned}
T_n^P = (1 + \theta) \times T_{n+1}^P &- T_{n+1}^W \times x - T_{n+1}^E \times x - 2T_{n+1}^S \times y - 2 \times \Delta y \times \gamma \\
&\times y - \frac{\alpha_T \times \Delta t}{k} \dot{Q}_{n+1}
\end{aligned}
\qquad [4.19]
$$

The above expression is the heat equation for the north nodes of the finite difference mesh.

Northwest corner node

For the northwest nodes the local coordinate system used was:
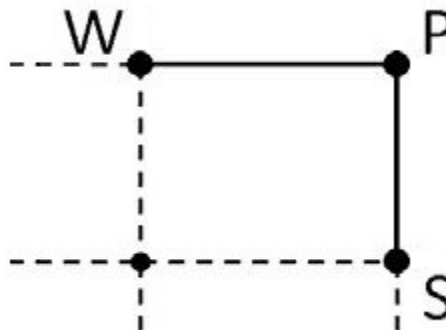
Figure 4-10 - Local coordinate system used for the northwest corner node.

Substituting [4.12] and [4.17] in [4.7]:

$$T_n^P = (2x + 2y + 1) \times T_{n+1}^P - T_{n+1}^W \times x - \left(T_{n+1}^W + 2 \times \Delta x \times \gamma - 2\frac{\Delta x \times h_l}{k}T_{n+1}^P\right) \times x - T_{n+1}^S \times y$$
$$- \left(T_{n+1}^S + 2 \times \Delta y \times \gamma - 2\frac{\Delta y \times h_l}{k}T_{n+1}^P\right) \times y - \frac{\alpha_T \times \Delta t}{k}\dot{Q}_{n+1}$$

[4.20]

Being $\beta = 2x + 2y + 2\frac{h_l}{k}(\Delta x \times x + \Delta y \times y)$:

$$T_n^P = (1 + \beta) \times T_{n+1}^P - 2T_{n+1}^W \times x - 2T_{n+1}^S \times y - 2\gamma$$
$$\times (\Delta x \times x + \Delta y \times y) - \frac{\alpha_T \times \Delta t}{k}\dot{Q}_{n+1}$$

[4.21]

The above expression is the heat equation for the northwest node of the finite difference mesh.

Hence, the resulting matrix to a 3x3 finite difference mesh is presented in Figure 4-11:

Figure 4-11 - Three point square mesh for one concrete layer.

$$
\begin{bmatrix}
(1+\beta) & -2x & 0 & -2y & 0 & 0 & 0 & 0 & 0 \\
-x & (1+\theta) & -x & 0 & -2y & 0 & 0 & 0 & 0 \\
0 & -2x & (1+\beta) & 0 & 0 & -2y & 0 & 0 & 0 \\
-y & 0 & 0 & (1+\mu) & -2x & 0 & -y & 0 & 0 \\
0 & -y & 0 & -x & (2x+2y+1) & -x & 0 & -y & 0 \\
0 & 0 & -y & 0 & -2x & (1+\mu) & 0 & 0 & -y \\
0 & 0 & 0 & -2y & 0 & 0 & (1+\beta) & -2x & 0 \\
0 & 0 & 0 & 0 & -2y & 0 & -x & (1+\theta) & -x \\
0 & 0 & 0 & 0 & 0 & -2y & 0 & -2x & (1+\beta)
\end{bmatrix}
\times
\begin{bmatrix}
T_{n+1}^1 \\
T_{n+1}^2 \\
T_{n+1}^3 \\
T_{n+1}^4 \\
T_{n+1}^5 \\
T_{n+1}^6 \\
T_{n+1}^7 \\
T_{n+1}^8 \\
T_{n+1}^9
\end{bmatrix}
$$

$$
=
\begin{bmatrix}
T_n^1 + 2\gamma \times (\Delta x \times x + \Delta y \times y) + \dfrac{\alpha_T \cdot \Delta t}{k}\dot{Q}_{n+1}^1 \\[2mm]
T_n^2 + 2 \times \Delta y \times \gamma \times y + \dfrac{\alpha_T \cdot \Delta t}{k}\dot{Q}_{n+1}^2 \\[2mm]
T_n^3 + 2\gamma \times (\Delta x \times x + \Delta y \times y) + \dfrac{\alpha_T \cdot \Delta t}{k}\dot{Q}_{n+1}^3 \\[2mm]
T_n^4 + 2 \times \Delta x \times \gamma \times x + \dfrac{\alpha_T \cdot \Delta t}{k}\dot{Q}_{n+1}^4 \\[2mm]
T_n^5 + \dfrac{\alpha_T \cdot \Delta t}{k}\dot{Q}_{n+1}^5 \\[2mm]
T_n^6 + 2 \times \Delta x \times \gamma \times x + \dfrac{\alpha_T \cdot \Delta t}{k}\dot{Q}_{n+1}^6 \\[2mm]
T_n^7 + 2\gamma \times (\Delta x \times x + \Delta y \times y) + \dfrac{\alpha_T \cdot \Delta t}{k}\dot{Q}_{n+1}^7 \\[2mm]
T_n^8 + 2 \times \Delta y \times \gamma \times y + \dfrac{\alpha_T \cdot \Delta t}{k}\dot{Q}_{n+1}^8 \\[2mm]
T_n^9 + 2\gamma \times (\Delta x \times x + \Delta y \times y) + \dfrac{\alpha_T \cdot \Delta t}{k}\dot{Q}_{n+1}^9
\end{bmatrix}
\qquad [4.22]
$$

The case study model is evolutionary along the time, it grows at the placement of a new concreting layer, therefore the derivated equation above [4.22] has to be evolutionary too.

To make the equation [4.22] evolutionary, some changes to the boundary nodes between the two consecutive layers needed to be made.

Each time a new concrete layer is placed is required to made a standardization with the previous concreted layer. In order to made that standardization, that grants the correct heat conduction between the consecutive concrete layers, the nodes in the mesh (nodes 7 to 9 in Figure 4-13) that are common to both the layers need to be changed.

The changes scheme is the presented below (Figure 4-12). The green zones in Figure 4-12 are related to the previously concreted layer, the blue zones are related to the new concreted layer and the red zones represent the set of points in the mesh that needed to change in order to the model conduct heat from one concrete layer to another. The changed points in the mesh in Figure 4-13 are presented in equation [4.23].
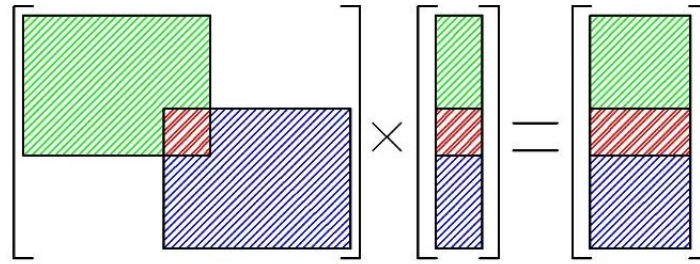
Figure 4-12 - Changes scheme to make the equation evolutionary.
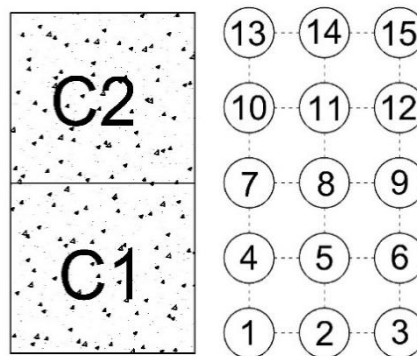
Figure 4-13 - Three point square mesh for two concrete layers.

$$\begin{bmatrix} (1+\beta) & -2x & 0 & -2y & 0 & 0 & 0 & 0 & 0 & 0 & 0 & 0 & 0 & 0 & 0 & 0 & 0 \\ \ddots & \ddots & \ddots & \ddots & \ddots & \ddots & \ddots & & \ddots & \ddots & \ddots & \ddots & \ddots & \ddots & \ddots & \ddots & \ddots \\ 0 & 0 & 0 & -y & 0 & 0 & (1+\mu) & -2x & 0 & -y & 0 & 0 & 0 & 0 & 0 & 0 & 0 \\ 0 & 0 & 0 & 0 & -y & 0 & -x & (2x+2y+1) & -x & 0 & -y & 0 & 0 & 0 & 0 & 0 & 0 \\ 0 & 0 & 0 & 0 & 0 & -y & 0 & -2x & (1+\mu) & 0 & 0 & -y & 0 & 0 & 0 & 0 & 0 \\ \ddots & \ddots & \ddo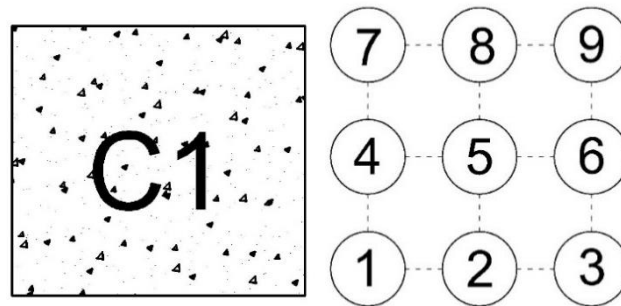ts & \ddots & \ddots & \ddots & \ddots & & \ddots & \ddots & \ddots & \ddots & \ddots & \ddots & \ddots & \ddots & \ddots \\ 0 & 0 & 0 & 0 & 0 & 0 & 0 & 0 & 0 & 0 & 0 & 0 & 0 & 0 & -2y & 0 & -2x & (1+\beta) \end{bmatrix} \times \begin{bmatrix} T_{n+1}^1 \\ \vdots \\ T_{n+1}^7 \\ T_{n+1}^8 \\ T_{n+1}^9 \\ \vdots \\ T_{n+1}^{15} \end{bmatrix}$$

$$= \begin{bmatrix} T_n^1 + 2\gamma \times (\Delta x \times x + \Delta y \times y) + \dfrac{\alpha_T \cdot \Delta t}{k} \dot{Q}_{n+1}^1 \\ \vdots \\ T_n^7 + 2 \times \Delta x \times \gamma \times x + \dfrac{\alpha_T \cdot \Delta t}{k} \dot{Q}_{n+1}^7 \\ T_n^8 + \dfrac{\alpha_T \cdot \Delta t}{k} \dot{Q}_{n+1}^8 \\ T_n^9 + 2 \times \Delta x \times \gamma \times x + \dfrac{\alpha_T \cdot \Delta t}{k} \dot{Q}_{n+1}^9 \\ \vdots \\ T_n^{15} + 2\gamma \times (\Delta x \times x + \Delta y \times y) + \dfrac{\alpha_T \cdot \Delta t}{k} \dot{Q}_{n+1}^{15} \end{bmatrix}$$

[4.23]

4.4 Implementation of the computational tool

4.4.1 Explanation of the produced algorithm

The developed computational tool uses the finite difference equations above derivated (expressions [4.22] and [4.23]). A brief outline of the overall procedure for the thermal analysis will be presented next.

The inputs of the program inserted by the user are divided in multiple categories, as explained below:

Table 4-1 - Developed program inputs

	User Inputs	Interoperability inputs
Material related	Kind of cement; Amount of cement in the concrete mix; Thermal conductivity of the concrete; volumetric specific heat	
Environmental related	waiting time between consecutive concreting layers;	
Time related	Time step; waiting time between consecutive concreting layers; Time between placing and withdrawal of the formwork	
Numerical simulation related	number of elements by concrete layer in the finite difference mesh	
Dam's configuration related		concrete layers height, the dimensions and the number of layers of the element in study

A brief outline of the overall operation of the created computational program will be presented next.

Box 1 - Outline of the created program to the thermal calculations.

For each concrete layer:

1. Regenerates de expression [4.22], (as shown in Figure 4-12 and expression [4.23]) with the new size of the mesh and the convective coefficients of the formwork;
2. Performs the thermal calculation until the instant of withdrawal of the formwork;

3. Regenerates de expression [4.22] with the convective coefficients of the concrete;

4. Performs the thermal calculation until the instant of placement of a new concrete layer.

The heat generation implemented in the program is based in the algorithm box created by (Azenha, 2009).

The heat parameters adopted in numerical modelling were characterized by (Azenha, 2009) for the most common used cements of in Portugal, as shown in Table 2-1.

The outputs of the developed computational tool are the temperatures in all the points and all time steps of the finite difference mesh that can be presented in temperature maps and temperature graphics.

4.5 Validation and demonstration of the developed tool

4.5.1 Validation

The created program was validated by a finite element commercial software called DIANA. This software uses the finite difference method, which is best for the validation because it is supposed the validation to achieve similar results through the utilization of different numerical methods.

For this purpose were validated two different situations for the same element with 10 vertical divisions and two horizontal divisions (Figure 4-14).

In the first situation, to test the heat generation in the developed tool, were simulated the model with all boundaries adiabatic (without heat transfer) and the temperature of the element of 20ºC.

In the second situation were tested the heat transfer with the surrounding environment. This simulation has the lateral and bottom boundaries adiabatic, the top boundary with a heat transfer coefficient of 5.208 and the temperature of the element and the environment of 20ºC.
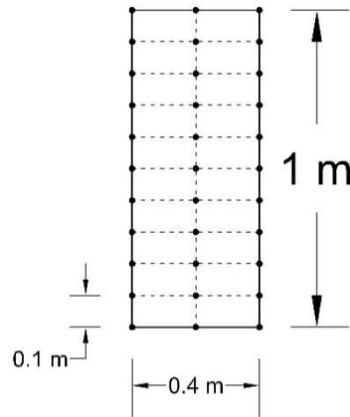
Figure 4-14 - Element used for validation.

The properties of the material used for the validations are:

- Volumetric specific heat: $\rho c = 2.4 \times 10^6$ [J/m^3·K];

- Concrete thermal conductivity: $k = 2.6$ [W·m^{-1}·K^{-1}];

- Potential heat generation: $Q_\infty = 164.746$ [kJ/Kg];

- Rate constant: $A_T = 5.18287 \times 10^{11}$;

- Arrhenius constant: $\frac{E_a}{R} = 5.71497 \times 10^3$ [K^{-1}];

- Degree of hydration and normalized heat generation rate (Figure 4-15).
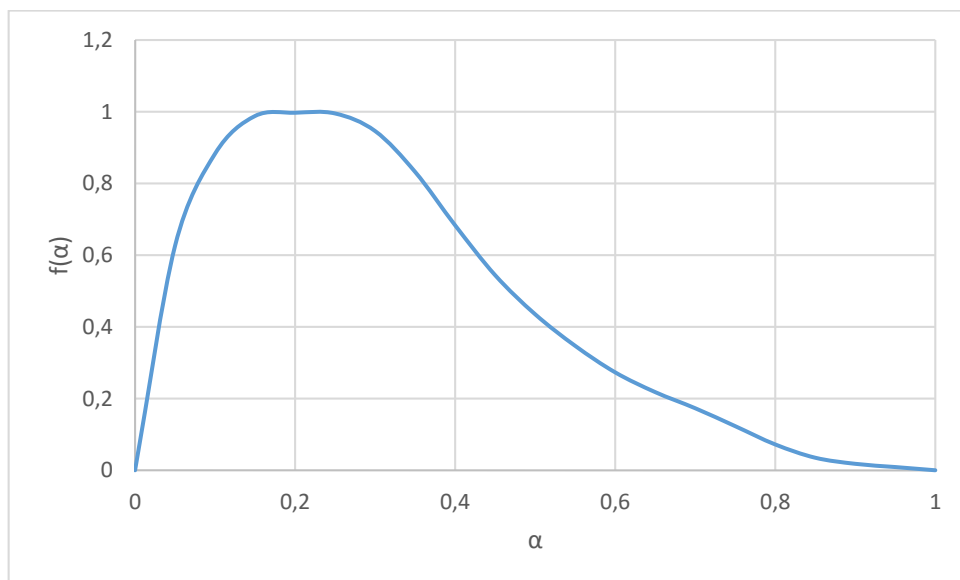
Figure 4-15 - Heat generation parameters

First validation – All boundaries adiabatic

This validation was conducted for the element presented in Figure 4-14 with all adiabatic boundaries, the above mentioned material parameters and a temperature of 20ºC. The used time step was 864 seconds and the time in study was 259000 seconds.

The temperatures were studied at the midpoint of the element (Figure 4-16).
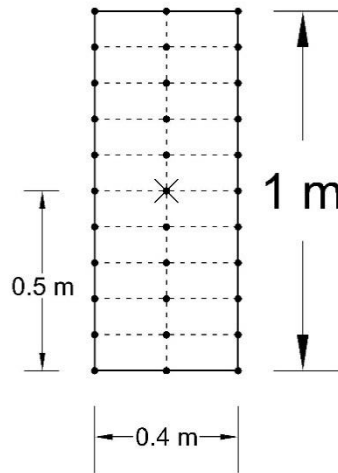
Figure 4-16 - Point of the element were the temperature were studied (crossed dot).

The resulting temperatures of the MATLAB and the DIANA models can be compared through the analysis of Figure 4-17. The maximum difference between the two curves was lower than 0.47ºC.
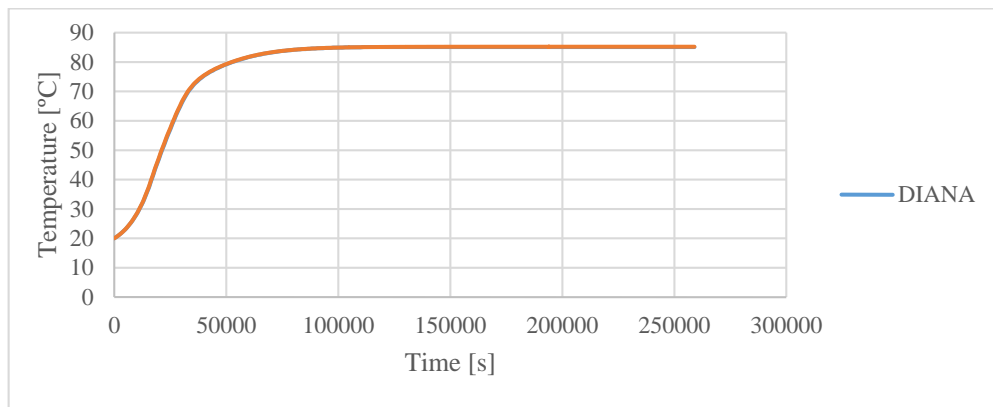
Figure 4-17 - Evolution of the temperature along time – Validation 1.

Additionally, the evolution of the degree of hydration along the time was compared between the developed tool and the DIANA simulation (Figure 4-18). The maximum registered difference was lower than 0,023.
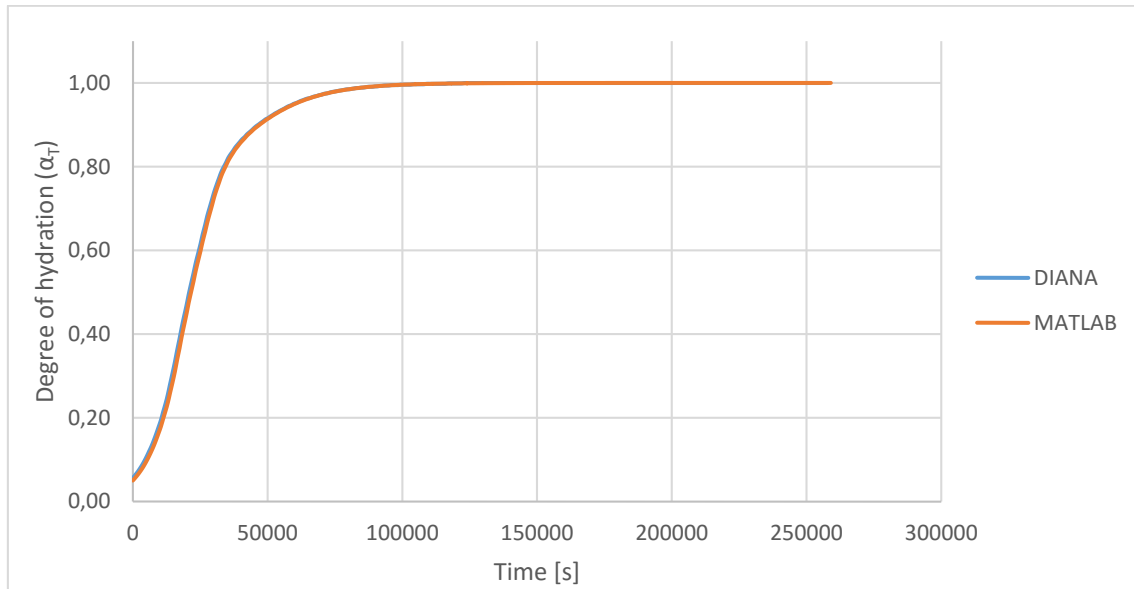
Figure 4-18 - Evolution of the degree of hydration along time – Validation 1.

Second validation – Lateral and bottom boundaries adiabatic, the above boundary with heat transfer with the environment and $T_0=T_{ext}=20^oC$

This validation was conducted for the element presented in Figure 4-19 with the lateral and bottom adiabatic boundaries, the top boundary with a heat transfer coefficient of 5.208, the above validation material parameters and an initial and environment temperature of 20ºC. The used time step was 864 seconds and the time in study was 259000 seconds.

The temperatures were studied at the points distanced 0, 0.4 and 1 meter from the bottom of the element (Figure 4-19).
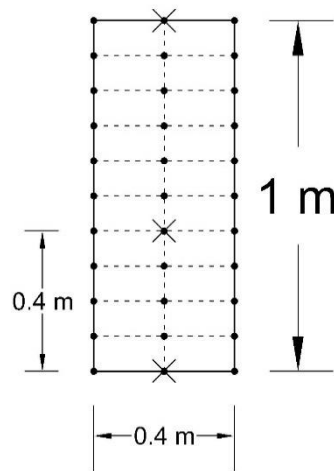
Figure 4-19 - Points of the model were the temperature were studied (crossed).

The resulting temperatures along time of the computational developed tool were compared with DIANA (Figure 4-20). Additionally, were tested the influence of the time step in the developed computational tool calculations.
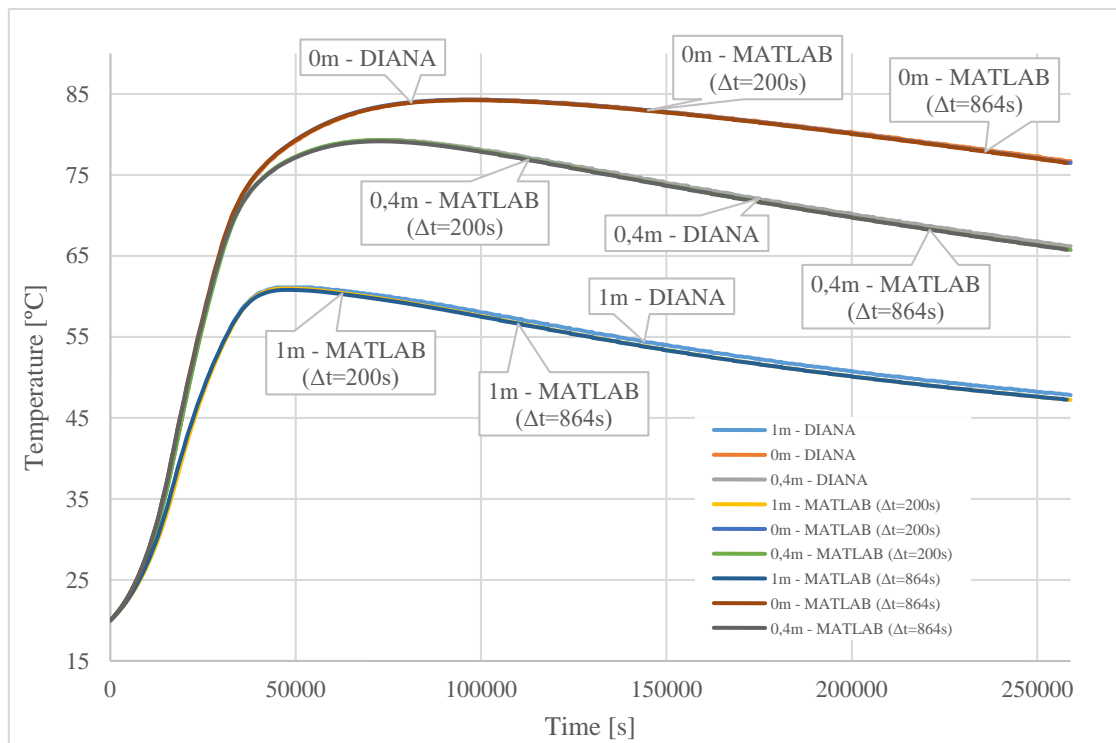
Figure 4-20 - Evolution of the temperature along time – Validation 2.

Through the analysis of the above graphic (Figure 4-20) it can be seen that the temperature differences between DIANA and the developed computational tool are minimal, below 0.68 ℃.

The accuracy of the numerical model wasn't affected by the time step, because the results with 864 seconds of time step led to practically the same results as with 200 seconds time step.

In conclusion, and taking into account the three previous validations, it's verified that the developed computational tool preforms valid thermal analysis, with a low associated error.

4.5.2 Demonstration

To demonstrate the capabilities of the developed computation program a thermal study of the generic arch dam modeled in the chapter 3 were conducted.

Taking into account the above described needed inputs to introduce by the user in the developed computational tool, the parameters used in this simulation are:

- Initial environmental temperature: 15 ºC;
- Initial temperature of the elements: 20 ºC;
- Time step: 1 hour;
- Waiting time between consecutive concreting layers: 7 days;
- Time between concreting and the formwork withdrawal: 2 days;
- Concrete: 100 Kg/m^3 of CB CEM I 42.5R and 100 Kg/m^3 of fly ashes that correspond to 120 Kg/m^3 consistent with experience or orders of magnitude reported by (Ballim & Graham, 2009) that suggest that each 100 Kg/m^3 of fly ashes are equivalent to 20 Kg/m^3 of concrete from the heat generation point of view;
- Concrete layers height: 2 meters;
- Number of concrete layers: 50;
- Dam's vertical profile width: 15 meters.

The main objective of the present chapter is to demonstrate the potentialities of the developed tool rather than the scientific discussion of the obtained results.

The control parameters adopted for discussion of cracking risks are the temporal and spatial temperature gradients.

The temporal temperature gradient (ΔT_T) corresponds to temperature variations at any point observed over time. In the context of this study temporal gradient will be systematically evaluated at the top center point, the bottom center point, the middle center point and the center point in a lateral boundary of the concrete layers, because according to the consulted

bibliography these are the important points to evaluate this parameter. The temporal temperature gradient is associated to the stage at which the risk of cracking is relevant that corresponds to the cooling stage, since it is at this stage that tensile stresses are observed in the nucleus of the elements.

The spatial temperature gradient (ΔTs) correspond to the biggest temperature difference between two points within the same concreting phase for the same instant. The spatial temperature gradient is generally associated with risk of surface cracking which is particularly important in the concrete heating stage, in which the inner areas have a greater tendency to expand than the surface zones.

Temporal gradients

The temporal gradients for the case study calculated through the computational developed tool are presented in Figure 4-21 for the middle center points, in Figure 4-22 for the middle lateral points and in Figure 4-23 for the boundary between layers points.
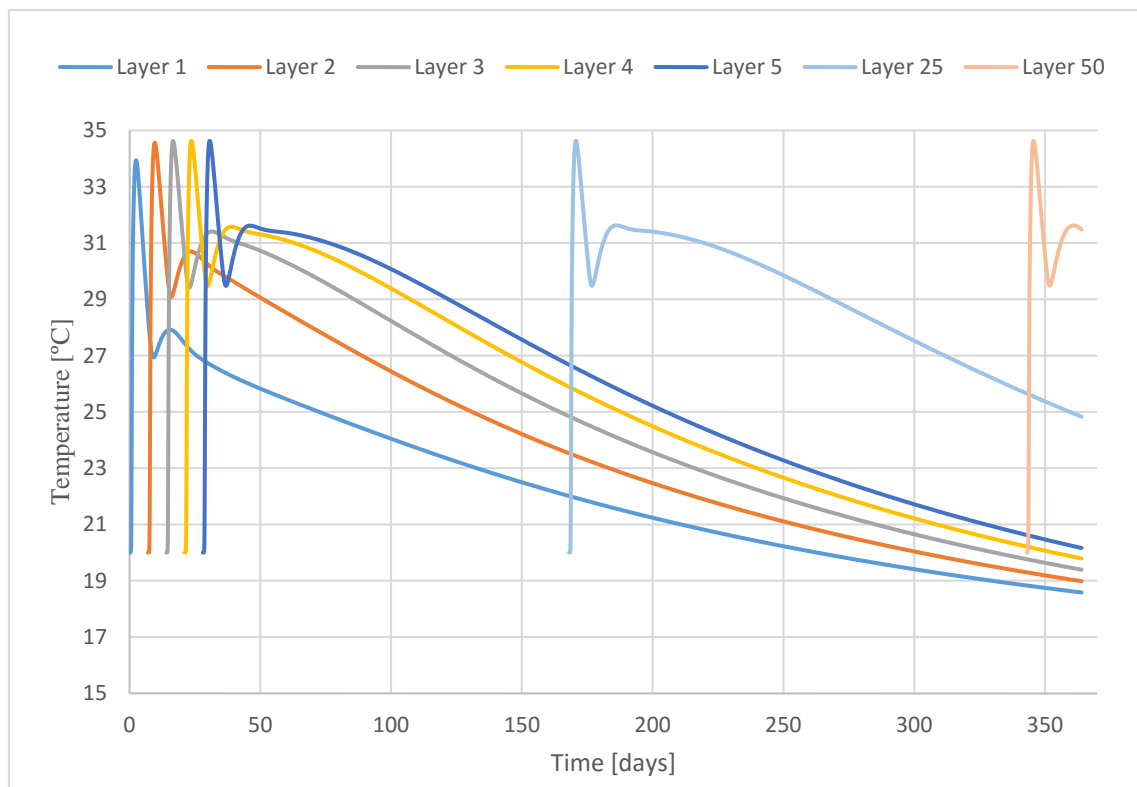
Figure 4-21 - Temporal gradient for the middle center points of the concrete layers.
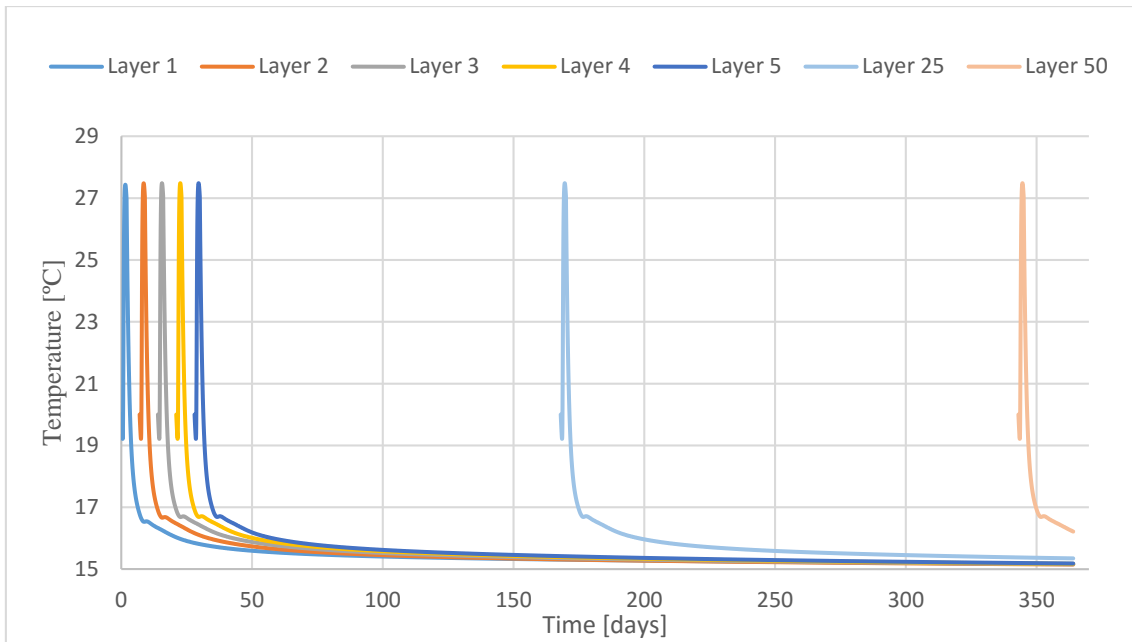
Figure 4-22 - Temporal gradient for the middle lateral points of the concrete layers.
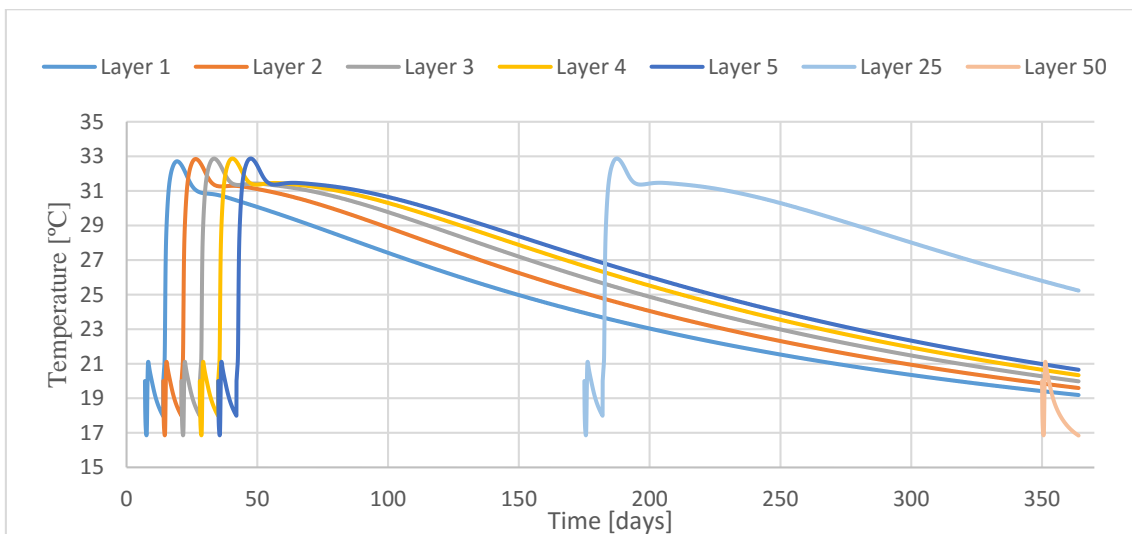
Figure 4-23 - Temporal gradient of the boundaries between concrete layers.

The temperature evolution along time for the middle center points is presented in Figure 4-21. At first the temperature rises up to a maximum of 34.63ºC, followed by a decay until the concreting of the following concrete layer, when the temperature has a slight rise and finally tends to attain the thermal equilibrium with the surrounding environment (15ºC).

In Figure 4-22 is presented the temperature evolution along time for the middle lateral points. At first temperature has a slight drop, due to the delay in the start of the cement heat hydration reaction, followed by a rise up to a maximum of 27.48°C. After that the temperature tends to attain the thermal equilibrium with the surrounding environment.

The points on the boundaries between layers has the temperature evolution over time presented in Figure 4-23. Until the concreting time of the upper concrete layer the temperature of a certain layer has an initial slight drop, due to the delay in the start of the cement heat hydration reaction, followed by a rise and a drop of the temperature. At the time of concreting the upper concrete layer this point is no longer a boundary point, it's an interior point rising again to higher temperatures than before, due the fact that at this time it's interior and finally the temperature tends to attain the thermal equilibrium with the surrounding environment.

Spatial gradient – Boundary points

The spatial gradient for the case study calculated through the computational developed tool is presented in Figure 4-24.
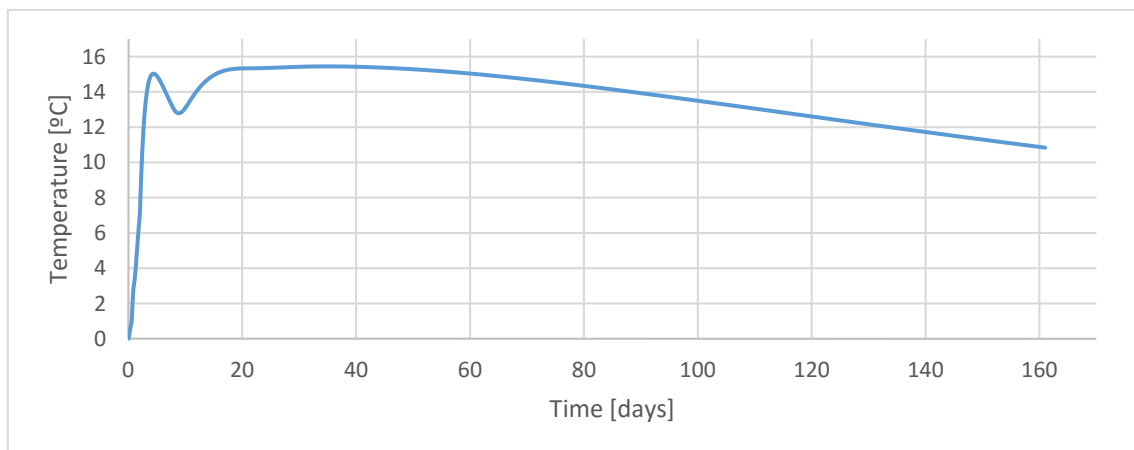
Figure 4-24 - Spatial gradient for a representative layer.

Through the observation of the spatial gradient presented in Figure 4-24 it can be concluded that the maximum spatial gradient is 15.45°C, this value is lower than the 20° C that is a commonly used value as acceptable for the spatial temperature gradient for cracking risk.

Temperature Maps

The created computational tool also allows the creation of temperature maps. As example, in Figure 4-25, are presented the temperature maps for three time instants.
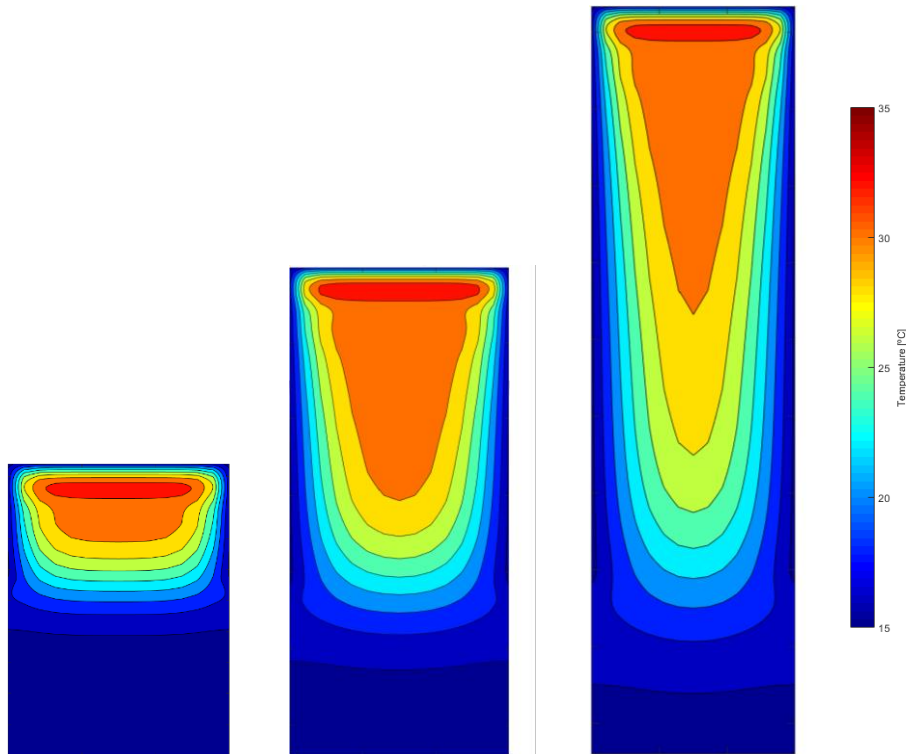
Figure 4-25 - Temperature maps for three different time instants.

4.6 Final considerations

This sub-chapter intend to answer the requirements and objectives defined for the development of the computational tool in the introduction of the present chapter.

Hence, the requirement of interoperability was accomplished through the creation of CSV (comma separated values) files in Dynamo that are posteriorly read by MATLAB.

The objective of simulating the heat conduction inside the concrete and the heat convection with the surrounding environment was accomplished through the derivation and computational

implementation of the finite difference method applied to the heat conduction. The consideration of the effect of formwork was made through the assignment of different convection coefficients to the lateral boundaries of each concrete layer at the time of withdrawal of the formwork.

The requirement of simulating the constructive phasing was accomplished considering the waiting time between concreting successive layers.

The objective of simulating the non-linear heat generation of concrete containing with the basis on a preloaded database, was accomplished through the implementation in the computational developed tool of the non-linear heat generation algorithm box and the characterization of the most common cements in the Portuguese market made by (Azenha, 2009).

The automatic generation of temperature maps and temperature plots for the selected relevant instants was embedded in the developed computation tool.

Therefore, all the proposed objectives at the beginning of the development of the computational tool were achieved.

CHAPTER 5

5   PROPOSAL OF METHOD TO GENERATE CONSTRUCTION DAM SCHEDULES

5.1   Introduction

The construction of dams is a complex process with a large execution times and associated costs. In fact, the construction schedule of the dam plays a central role in its actual cost with significant savings associated to reductions in construction duration. Thereby, it is important to have adequate tools that support optimization procedures for construction scheduling, particularly through the systematic study of alternative scenarios.

In this chapter, a method for automatic generation of construction schedules based on cellular automation algorithms is proposed, and its use is demonstrated through an illustrative example. Cellular automata are artificial intelligence algorithms that are based in simple sets of rules and allow solving complex problems.

This chapter is initially focused in the explanation of the rules that will be used to base the automation algorithm (Section 5.2) and then focuses on a brief explanation of the underlying principles behind cellular automation algorithms (Section 5.3). Then, Section 5.4 focuses in the details of implementation of the algorithm itself, which is tested and demonstrated. Ultimately, some final considerations are given in Section 5.5.

5.2   Definition of the hierarchy of dam's construction planning rules

In the definition of the schedules of dam construction are some simple rules that should be commonly used, as demonstrated at subchapter 2.3, that are related with the concreting sequence and limit the choose of which layer are concreted at each time.

One of the rules are the minimum time between concreting successive layer that is conditioned by the generated heat in the concreted layers, that require the wait time between casting two successive layers in order to let the bottom layer to cool down until the concreting of the new layer. This rule is presented in Figure 5-1.

t ≥ 7 days
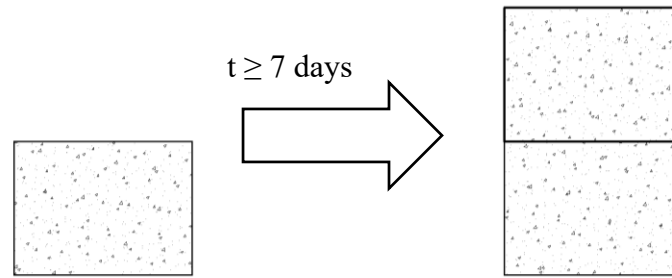
Figure 5-1 - Minimum time between concreting successive layers.

Another important rule is the difference of heights between adjacent blocks that are related with the fact that the downstream face could come out of the plumb, working as an independent cantilevers and becoming unstable, and to maintain dam temperature relatively uniform between adjacent blocks. This rule is schematically explained in Figure 5-2.

4 layers difference

3 layers difference
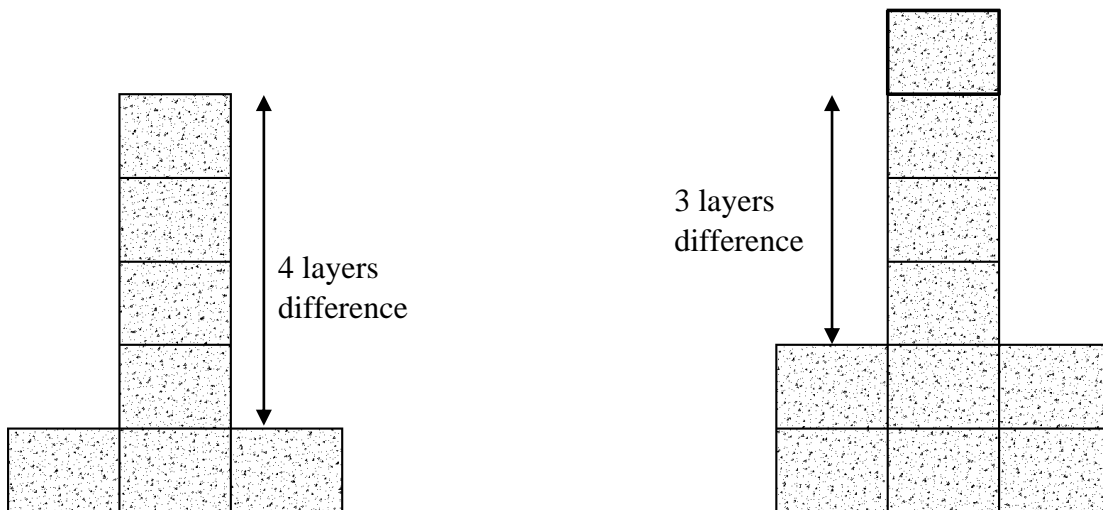
Figure 5-2 - Maximum difference of heights between adjacent layers.

The last important rule is related of the maximum time lapsing between concreting successive layers, in order to avoid detachment or cracking of the previously placed layer at an advanced stage of hardening and completely contracted, this time lapsing between concrete layers is commonly called cold joint. This rule is explained in Figure 5-3.

t ≤ 14 days
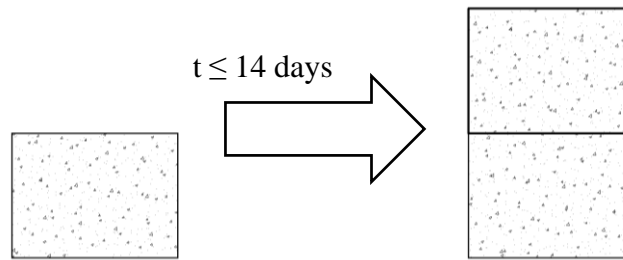
Figure 5-3 - Maximum time between concreting successive layers.

Thereby, the rules above described have a hierarchy that defines the priority of application of them in the constructive phasing of dams. The hierarchy of priorities of verification and application of the above rules is:

1. The cold joints – maximum time between concreting successive layer;
2. Concrete waiting times – minimum time between concreting successive layer;
3. Difference of height between neighbor dam vertical profiles – difference of heights between adjacent layers.

The rules above are those described in the literature as used traditionally, (Spanish Commitee on Large Dams, 1990) although the user may want to add other small rules. For this purpose, would have to change the programming behind the developed computational tool.

5.3   Cellular automata: from concept to implementation

The development of cellular automata systems is typically attributed to Stanisław Ulam and John von Neumann, who were both researchers at the Los Alamos National Laboratory in New Mexico in the 1940s. (Shiffman, 2004) Cellular automata are decision-taking algorithms that have the capability to resolve complex decision-taking problems with a few simple rules. Cellular automata is based in three basic principles that are presented next. The first important principle of a cellular automaton is his spatial structure, that consists on a grid where the calculation cells are distributed. The second principle is that each cell has a state. The simplest example has the two possibilities of 1 and 0 (otherwise referred to as "on" and "off" or "alive" and "dead"). Finally, the third principle is that each cell has a neighborhood that can be defined in any number of ways but it is typically correlated to the adjacent cells.

Figure 5-4 presented a cellular automata grid with one "alive" cell, whereas all the others are "dead".
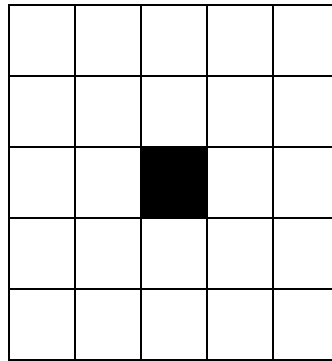
Figure 5-4 - Cellular automata spatial structure and agent.

The cellular automata algorithms also need as initial condition a pattern of "populated" cells, so at the beginning of the calculation process all the cells must be in the state "dead" or "alive".

Another important aspect about the cellular automata algorithms is the fact that the states of the cells change thought the interaction with his neighborhood cells. The neighborhood is defined by the adjacent cells to a determined cell. Thus, in every time step the pre-established set of rules are applied to all the cells, making them to change.

In order to better understand the cellular automata working process, will be detailed below the operation of a 1D cellular automata, inspired in (Shiffman, 2004). Thereby, the three basic cellular automata principles for this example are:

- The grid will be one dimensional, thus corresponding to a line of cells with ten cells for example - see
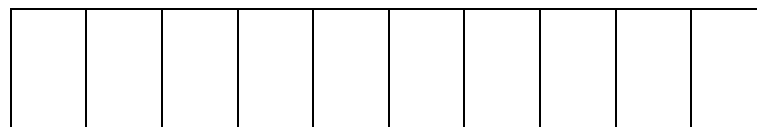
- Figure 5-5.
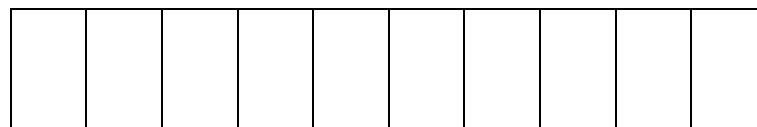
Figure 5-5 - One dimensional cellular automata grid.

- The states will be defined as two states represented as 0 or 1 disposed randomly, as shown in Figure 5-6.

1	0	1	0	1	1	1	0	0	1
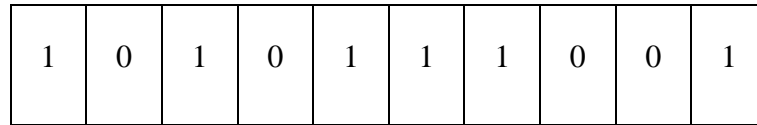
Figure 5-6 - One dimensional cellular automata states.

- The neighborhood is this one dimensional case will be constituted by the cell itself and its adjacent cells. In Figures 5-7 and 5-8 are shown a central and corner cell, respectively with a green squares and its neighbors with a red squares.

1	0	1	0	1	1	1	0	0	1
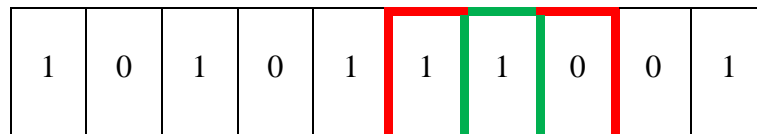
Figure 5-7 – Neighborhood for the central cells.

1	0	1	0	1	1	1	0	0	1
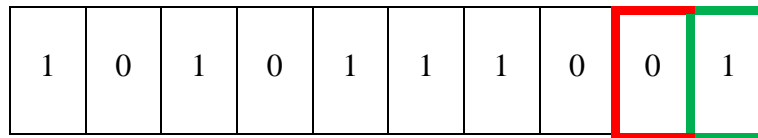
Figure 5-8 - Neighborhood for the corner cells.

Another important thing to define is the interactions of a cell with their neighbors, so at first it's important to define all the possible neighborhoods. For the central cells, this 3-bit binary neighbors have 8 possible outcomes, as presented in Figure 5-9. In Figure 5-10 are presented the corner nodes possible neighborhood configurations.

000   001   010   011   100   101   110   111

Figure 5-9 – Possible central cells neighborhood configurations – cell itself in green and the neighbors in red.

00   01   10   11

Figure 5-10 – Possible corner cells neighborhood configurations – cell itself in green and the neighbor in red.

Once we have defined all the possible neighborhoods, is necessary define an outcome state for each neighborhood configuration, based on a pre-established set of rules. The adopted rules for this particular example were:

1. ***Death.*** If a cell is "alive" it will "die" under the following circumstances.

   - ***Overpopulation:*** If the cell has two "alive" neighbors.

   - ***Loneliness:*** If the cell has no "alive" neighbors.

2. ***Birth.*** If a cell is "dead" it will come to "life" if it has exactly one "alive" neighbor.

3. ***Stasis.*** Otherwise, the cell state does not change:

   - ***Staying "Alive":*** If a cell is "alive" and has exactly one "live" neighbor, it stays "alive".

   - ***Staying "Dead":*** If a cell is "dead" and has two "live" neighbors, it stays "dead".

Thereby, all the possible outcomes based on the above rules are shown in Figure 5-11 and 5-12, for the central and corner nodes respectively.

000	001	010	011	100	101	110	111
↓	↓	↓	↓	↓	↓	↓	↓
0	1	0	1	1	0	1	0

Figure 5-11 - Neighborhood possible outcomes for the central cells – cell itself in green and the neighbors in red.

00	01	10	11
↓	↓	↓	↓
0	1	0	1
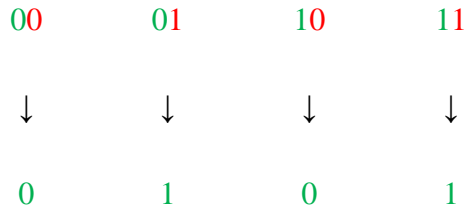
Figure 5-12 - Neighborhood possible outcomes for the corner cells – cell itself in green and the neighbors in red.

Taking into account the above explained rules and outcomes in Figure 5-13 is presented the cellular automata evolution in the first ten steps.

Initial Conditions	1	0	1	0	1	1	1	0	0	1

Step 1	0	0	0	0	1	0	1	1	1	0
Step 2	0	0	0	1	0	0	1	0	1	1
Step 3	0	0	1	0	1	1	0	0	1	1
Step 4	0	1	0	0	1	1	1	1	1	1
Step 5	1	0	1	1	1	0	0	0	0	1
Step 6	0	0	1	0	1	1	0	0	1	0
Step 7	0	1	0	0	1	1	1	1	0	1
Step 8	1	0	1	1	1	0	0	1	0	0
Step 9	0	0	1	0	1	1	1	0	1	0
Step 10	0	1	0	0	1	0	1	0	0	1

Figure 5-13 - One dimensional cellular automata for the first ten time steps.

The cellular automata calculation proceeds to the subsequent steps following the logic above presented. The cellular automata algorithms only ends by two possible ways: (Berto & Tagliabue, 2012)

- Fading away completely from overcrowding or from becoming too sparse;
- Settling into a stable configuration that remains unchanged thereafter, or entering an oscillating phase in which they repeat an endless cycle of two or more periods.

The amount of iterations needed to an end of this type of cellular automata algorithm is almost impossible to predict, because it depends on the rules and on the initial conditions.

The "Game of Life" is probably the most well-known and disseminated cellular automation algorithm. It was initially revealed to the public in 1970 when Martin Gardner wrote an article in Scientific American that documented mathematician John Conway's new "Game of Life," describing it as "recreational" mathematics. (Adamatzky, 2010)

The universe of the Game of Life is an infinite two-dimensional grid of square *cells*, each of which may be in one of two states: "alive" or "dead". Every cell interacts with its eight neighbors as shown in Figure 5-1, which are the cells that are horizontally, vertically, or diagonally adjacent. At each time step the following rules are applied:

4. ***Death.*** If a cell is "alive" it will "die" under the following circumstances.

    - ***Overpopulation:*** If the cell has four or more "alive" neighbors.

    - ***Loneliness:*** If the cell has one or fewer "alive" neighbors.

5. ***Birth.*** If a cell is "dead" it will come to "life" if it has exactly three "alive" neighbors.

6. ***Stasis.*** In all other cases, the cell state does not change. To be thorough, let's describe those scenarios:

    - ***Staying "Alive":*** If a cell is "alive" and has exactly two or three "live" neighbors, it stays "alive".

    - ***Staying "Dead":*** If a cell is "dead" and has anything other than three "live" neighbors, it stays "dead".

The system also needs a start pattern, as an initial condition and it follows applying the above rules simultaneously to every cell in the grid to create further generations, as shown in Figure 5-14.
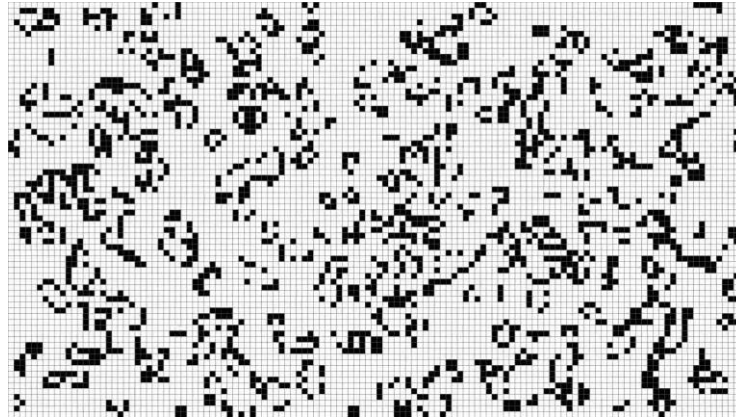
Figure 5-14 - Example of a game of life pattern.

Figure 5-15 presents a cellular automata evolution of an initial pattern along time.
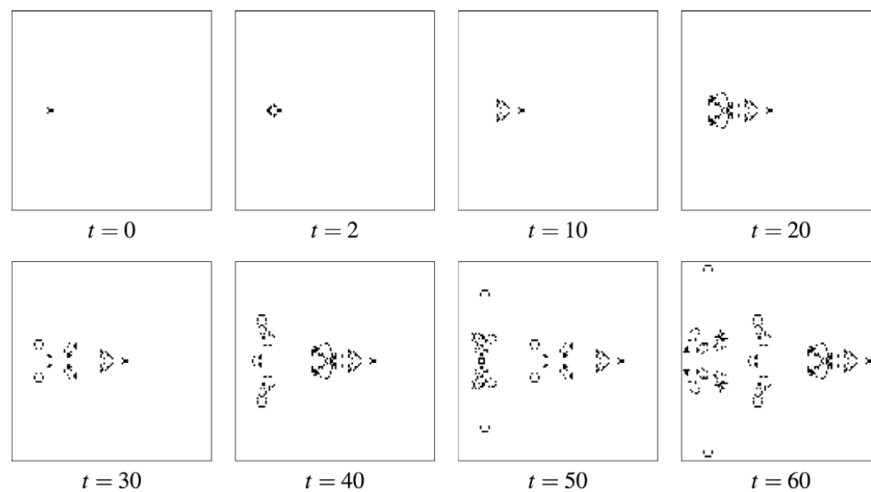
Figure 5-15 - Cellular automata propagation over time. (Adamatzky, 2010)

The cellular automata applications are vast, among them stand out the simulation of car traffic and the optimization of structural design. The cellular automata algorithms adapt very well to the form that car traffic flows, allowing traffic simulation studies to better understanding the measures to make the traffic flow better. (Rickert & Nagel, 1996)

Another interesting application of the cellular automata algorithms is the structural design and optimization of trusses, were the cellular automata is used to achieve the minimum weight of the structure under stress, nodal displacement, cross-sectional area and kinematic stability constraints. (Faramarzi & Afshar, 2012)

5.3.1 Explanation of the produced algorithm

The easiest way to explain the way in which a cellular automation algorithm was implemented for dam construction scheduling is probably by showing an example. Therefore, a set of steps of the rules shown in Chapter 5.2 will be applied to the dam and the respective constructive phasing described in Chapter 3 with nineteen vertical profiles and two meters of concrete layers' height. Thus, the grid used for the cellular automata calculations was the presented in Figure 5-16.
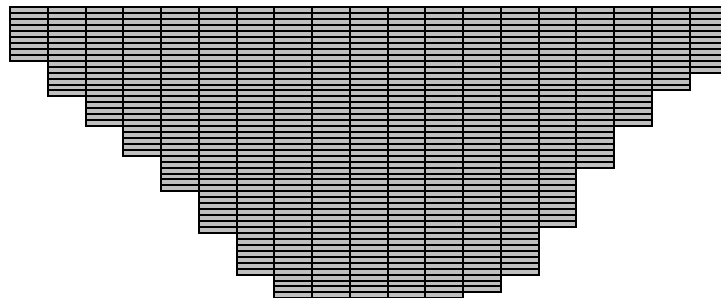
Figure 5-16 - Used grid for the cellular automata algorithm.

The adopted rules to this example of demonstration produced algorithm were:

- Number of simultaneous work fronts: 3 fronts;
- Start of the works: 19th of November of 2015;
- Minimum waiting time between concreting successive layers: 7 days;
- Maximum waiting time between concreting successive layers (cold joint): 14 days.
- Maximum acceptable difference of adjacent casting layers: 4 layers.

In order to not sparse the casting of the concrete layers, and this way, maintain the work fronts relatively close, making the dam construction from the middle to the sides, the algorithm was an internal rule that all the empty the columns on the grid which the first concrete layer is higher than the highest concreted layer are unavailable for casting.

The first step, at 19 of November of 2015, is the concreting of the 3 first concrete layers.

At first the algorithm divides in half the number of vertical profiles of the dam, represented as columns in Figure 5-16. Rounding that value and finding the lower position for that vertical profile the algorithm places the first concrete layer. The other two concrete layers are placed in the lower position of the adjacent vertical profiles. The first day of the work is shown in Figure 5-17.
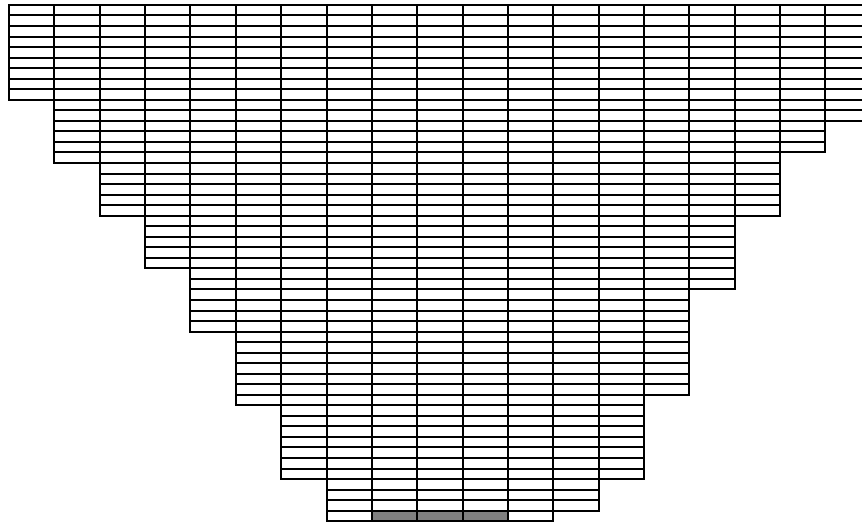
Figure 5-17 - First concreting steps.

At this point, according to the above enunciated laws, the available concreting layers are presented in Figure 5-18. Hereinafter the cells presented green correspond the eligible positions according to the pre-established set of rules, the cells presented blue represent the non-eligible cells according to the heights difference criteria and the cells presented red correspond the non-eligible cells according to the concrete waiting times.
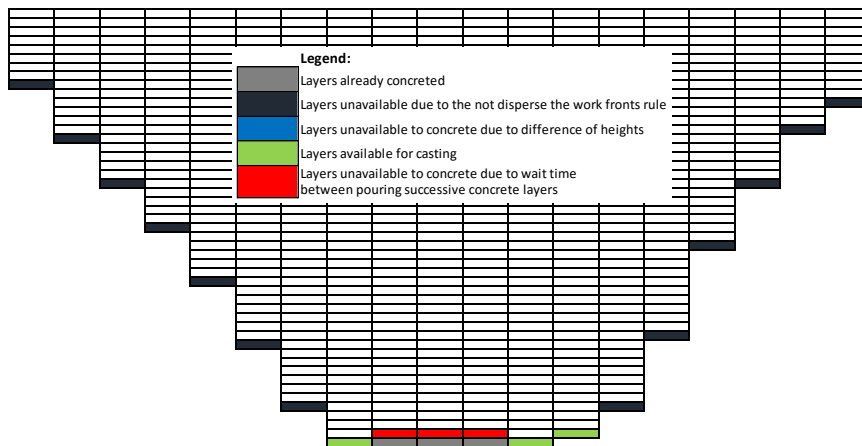
Figure 5-18 – Available concreting positions for step 2.

Taking into account the available concreting positions presented in Figure 5-18, in second step, at 20 of November of 2015, the layers were concrete in the most central available positions (green positions in Figure 5-18), as shown in Figure 5-19.
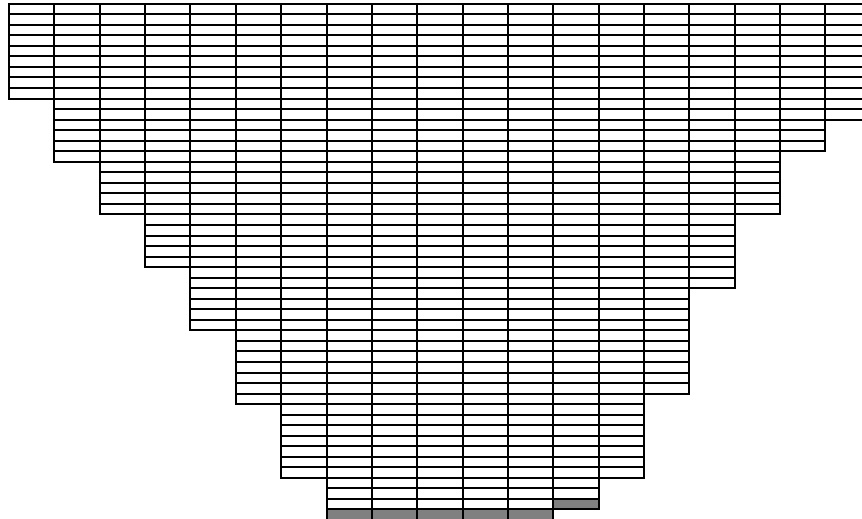
Figure 5-19 – Concreted layers after the second step.

After the second step and according to the above described rules, there aren't any available concreting layers until the seventh step, as presented in Figure 5-20.
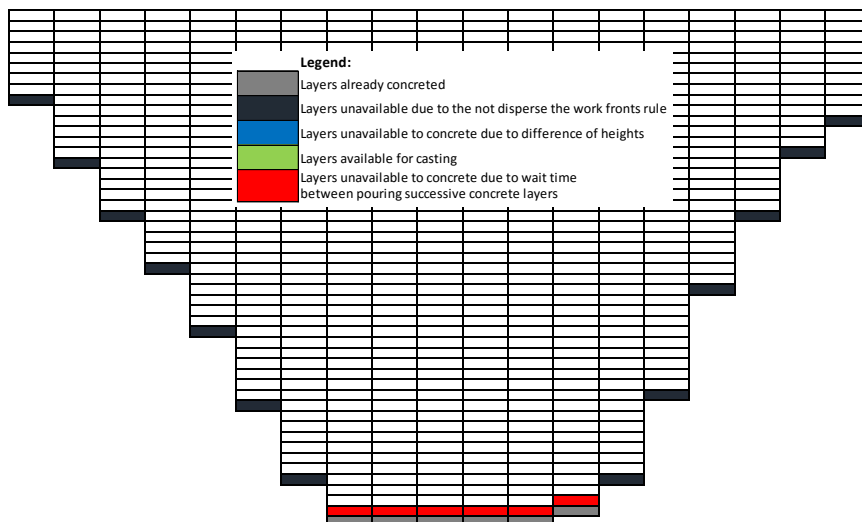
Figure 5-20 - Available concreting positions until the step 6.

In the seventh step the layers above the ones casted in the first step are available to cast because the minimum waiting time between concreting successive layer has already passed. The available positions to cast in seventh step are presented in Figure 5-21.
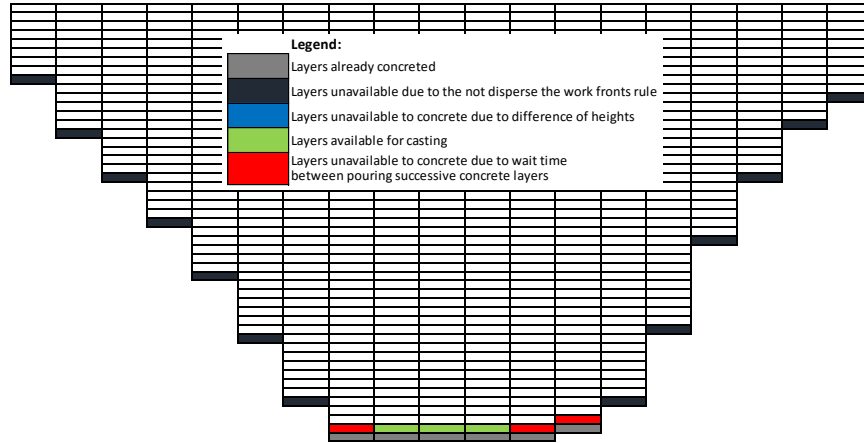
Figure 5-21 - Concreted layers after the seventh step.

The available positions to cast in seventh step are presented in Figure 5-21.
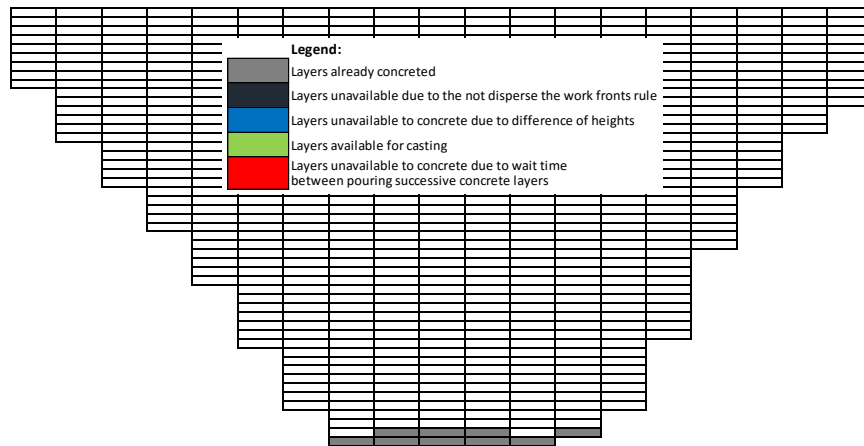
Figure 5-22 - Concreted layers after the third step.

By this way, the computational developed tool proceeds with the calculations until the grid is fully filled and the result times as well as the waiting times between layers and the trimestral construction evolution are the presented in Appendix II.

The developed algorithm avoids to the maximum cold joints occurrence so in this particular example there was no place the existence of cold joints.

The dam's construction according to the simulation of the developed computational tool ends at the 20th of October of 2016, eleven months after the work start. Although this type of works has a typical construction time of two years, this simulation takes into account only the rules above mentioned in chapter 5.2, so the simulation times may be quite different from the real construction times.

5.4 Implementation of the computational tool

The developed computational tool was implemented the cellular automation principles and the rules above explained in order to generate automatic construction dam schedules.

The support grid to implement the developed algorithm using the above described cellular automata methodology was created through the import of the number of concrete layers in each of the dam's vertical profiles through a CSV file created in Dynamo and read by MATLAB. In Figure 5-23 are presented the dam modeled in chapter 3 and in Figure 5-24 are presented the grid created by the developed computational tool based in the interoperable information read from dynamo.

The developed computational tool corresponds each cell to a concrete layer, with the layers' height established in the Chapter 3 adopted constructive phasing. giving that cells the value 0 or to the terrain beneath the dam's body giving that cells the designation NaN (not a number).
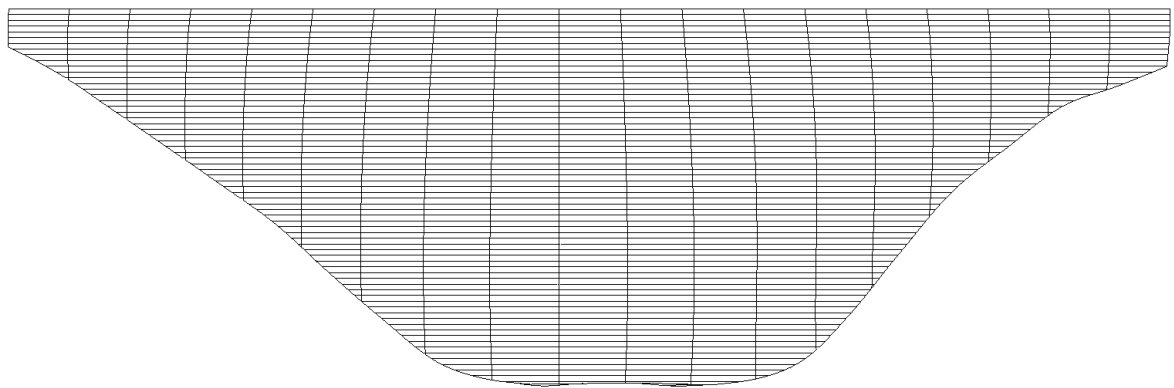
Figure 5-23 – Elevation of the dam modeled in chapter 3.
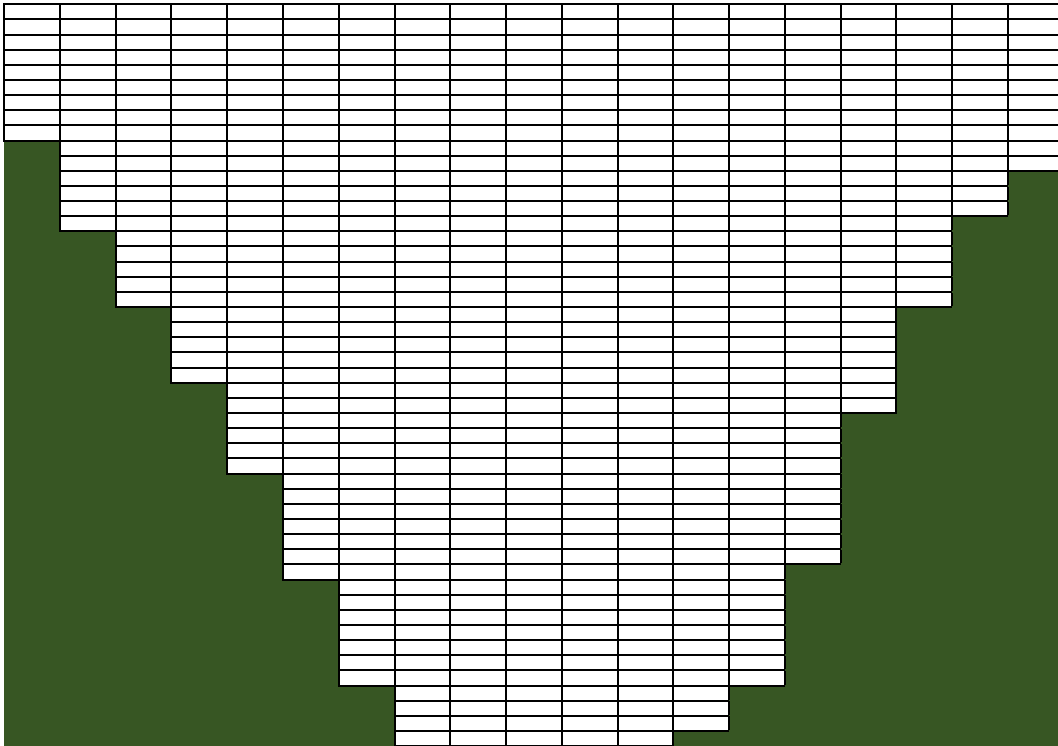
Figure 5-24 - Used grid in the cellular automata algorithm.

Additionally to the above mentioned matrix, the user only has to introduce five parameters in the developed computational tool:

- The minimum waiting time between concreting successive layers, as an integer;
- The maximum waiting time between concreting successive layers (cold joints), as an integer;
- The maximum acceptable difference between adjacent layers height, as an integer;
- The number of work fronts, as an integer;
- The works start date, as the day, the month and the year integers.

A brief outline of the overall procedure of the cellular automata algorithm will be presented next.

Box 5-1 - Outline of the developed cellular automata algorithm.

Until there are empty cells in the grid:
1. Update time;
2. Search in the highest concrete layers (highest lines with a non-zero value) of each vertical profile (matrix columns) by a layer with a waiting time higher than the minimum waiting time between concreting successive layers:
    a. If it finds one available location, place a new concrete layer there (write the time in that position);
    if it finds multiple available locations, place the new concrete layer (write the time in that position) in the location that have longer wait times since the casting of the concrete layer below;
    b. If it does not find any available location to concrete a layer go to step 3;
3. Search in the highest concrete layers (highest lines with a non-zero value) of each vertical profile (matrix columns), taking into account the waiting time between layers and the height differences between adjacent layers:
    a. If it finds available(s) location(s), place the new layer (write the time in that position) in the most central available position;
    b. If it doesn't find any eligible location go to step 1.

Every time there are multiple possible choices after the application of all the pre-established criterions the developed computational tool breaks the tie through a random selection of a casting position from the eligible ones.

5.5 Final considerations

In order to demonstrate how quick is to simulate different construction scenarios another simulation with 3 meters' concrete layers were conducted. The 3 meters' layer thick has a construction time of approximately seven and a half months, two and a half months faster than the 2 meters' layer's thick scenario above presented.

Another's construction scenarios can be tested with the developed computational tool, changing the initial introduced inputs. Thereby, can be equated different construction scenarios, like more thin layers, with more fixed associated costs but a lower waiting time between concreting successive layers or more thick layers with less fixed associated costs but a higher waiting time between concreting successive layers due to the higher heat generated by the cement hydration reaction.

It also can be run multiple simulations to test if there is a faster dam's construction schedule due to the fact of the application of a random selection to tie break when there are more than one possible layer to concrete.

The initial objective of develop a computational tool that allows the automatically generation of different construction scenarios was accomplished.

CHAPTER 6

6 PROPOSED FRAMEWORK FOR INTEROPERABILITY AND IMPLEMENTATION

6.1 Proposed framework

In the previous three chapters were developed three different tools important to the early stages of development of a dam. Although the interoperability created between the three developed tools, they aren't integrated in a common process that could increase the efficiency of the utilization of these three tools, turning their use even more interesting in the early stages of the project.

The proposed framework is, according to an integrated project delivery approaches advocated by BIM philosophies. It integrates several valences in an automated way supported in software tools combining various capacities both in terms of modelling BIM models, but also of thermal calculations and the definition of the construction phasing. Integrated Project Delivery (IPD) is a project delivery approach that integrates practices into a collaborative process to optimize project results and maximize efficiency through all phases of design and construction.

The IPD based framework intends to anticipate the design efforts and by this way, making the design decisions earlier when opportunity to influence positive outcomes is maximized and the cost of changes minimized. (Aia, 2007)

The proposed framework will be described in detail and presented using the Business Process Model and Notation (BPMN) graphical presentation. BPMN is a graphical notation that depicts the flow of steps in a business process, specifically created to coordinate the sequence of processes between different participants in a related set of activities (Object Management Group, 2015).

The developed framework process map is presented in the Figure 6-1 and will be carefully explained next.

All the ER (Exchange Requirements) represent the exchanges of information between two entities in the framework. This Exchange Requirements are all listed in the Appendix III with all the variables, their unities, their symbols, their type and their file format.
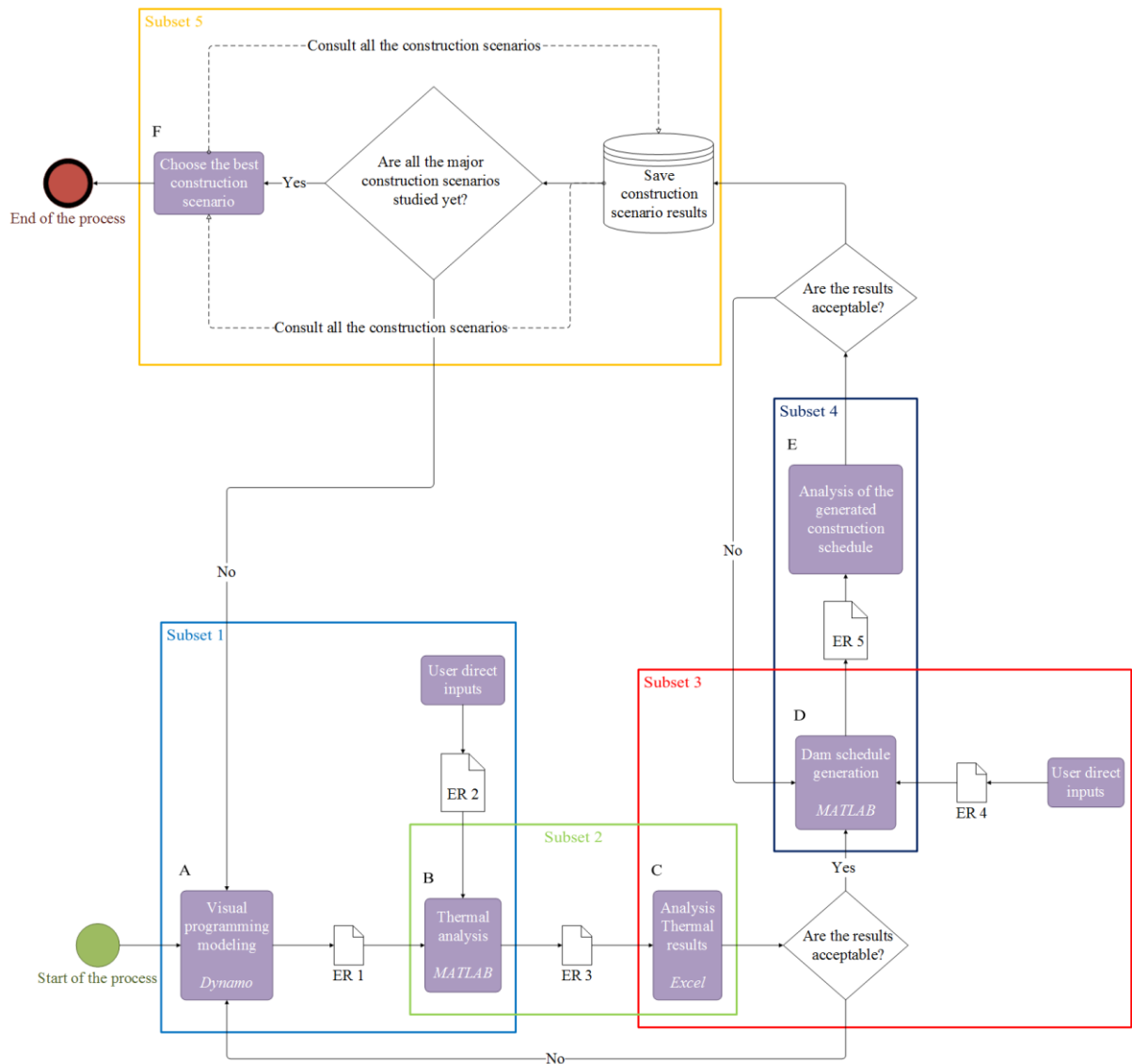
Figure 6-1 - Proposed framework.

In order to better understand the whole process described above in the proposed framework, all the subsets defined in Figure 6-1 will be detailed next.

The process described in this framework starts when a demand of a thermal and constructive study about a dam arises. In subset 1, presented in Figures 6-1 and 6-2 are described the first steps of the proposed framework.
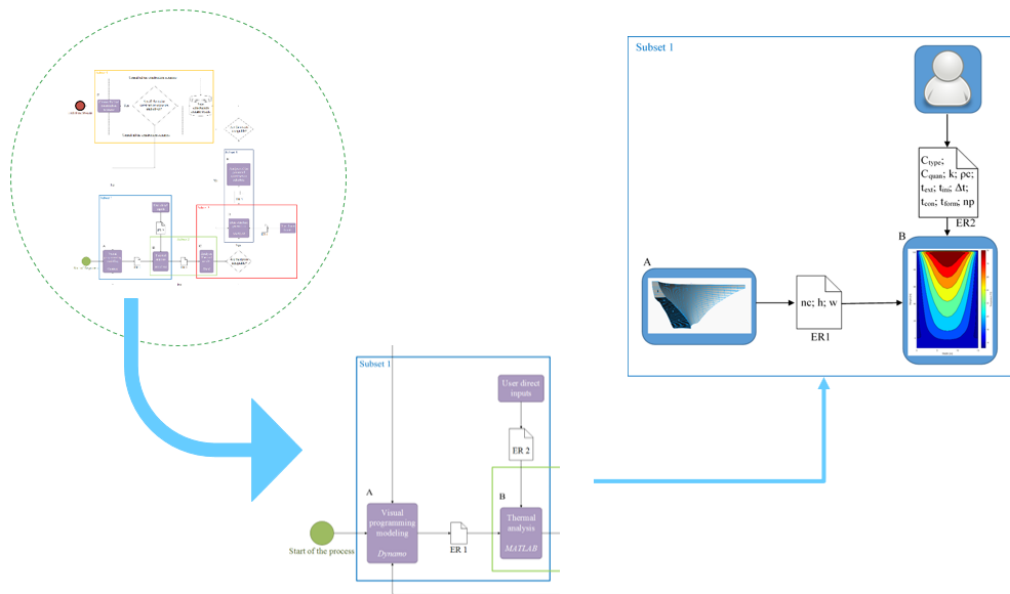
Figure 6-2 - Proposed framework subset 1 – see Figure 6-1.

The first task is modeling of dam's body, in Dynamo, following the same logic explained along chapter 3 (box A in Figures 6-1 and 6-2). After the dam is modelled is time to proceed to the thermal calculations, as explained in detail in chapter 4 (box B in Figures 6-1 and 6-2). The developed computational tool to perform the thermal calculations rely on the interoperable information with the modelling tool. This information in related to the adopted constructive phasing and is created automatically when the modeling was made (ER1 in Figures 6-1 and 6-2). The developed computational tool also need some inputs from the user that are introduced directly in MATLAB (ER2 in Figures 6-1 and 6-2). The information introduced directly by the user is related to the material properties of the concrete, to the environmental and initial temperatures, to the waiting times between concreting successive layers and the number of nodes of the finite difference mesh to use in the simulation.

After performing the thermal calculations (box B in Figures 6-1 and 6-3), a thermal analysis of the temporal and spatial gradients is made, as shown in Subset 2 presented in Figures 6-1 and 6-3.
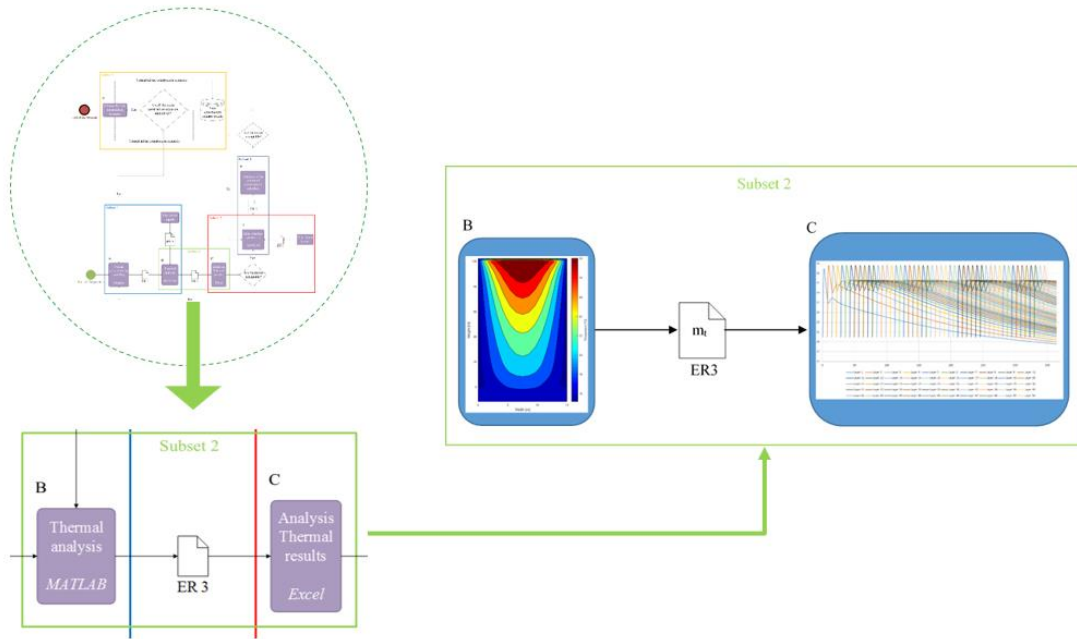
Figure 6-3 - Proposed framework subset 2 – see Figure 6-1.

The developed computational tool (box B in Figures 6-1 and 6-3) makes the temperature maps itself and writes an Excel file (ER3 in Figures 6-1 and 6-3) with the matrix of temperatures, that include the temperatures in all points in all the time steps in study. Then, is necessary to make an evaluation of the temporal and spatial gradients (box C in Figures 6-1 and 6-3). If the temperature gradients are not according to the project requirements all the framework process must be restarted, starting again with a different adopted constructive phasing in Dynamo (box A in Figures 6-1 and 6-2). When the temperature gradients meet the project demands it's time to proceed to the constructive phasing studies, as shown in Subset 3, presented in Figure 6-1 and 6-4.
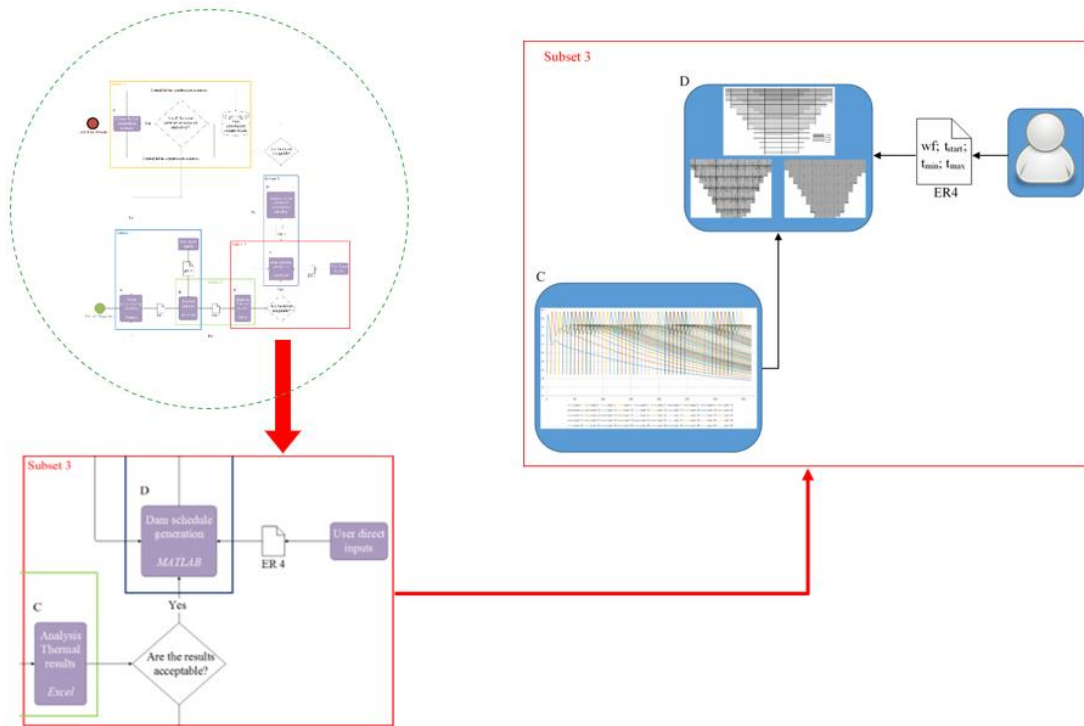
Figure 6-4 - Proposed framework – see Figure 6-1.

The computational tool developed for conducting constructive phasing studies (box D in Figure 6-1 and 6-4) needs as inputs from the user the number of work fronts, the time of start of the works, the maximum and minimum waiting times between concreting successive layer and the maximum acceptable difference of heights between adjacent concrete layers (ER 4 in Figure 6-1 and 6-4).

By changing the pre-established set of rules parameters the user can obtain different construction schedules for the same concrete layers' height, as shown in Subset 4, presented in 6-5.
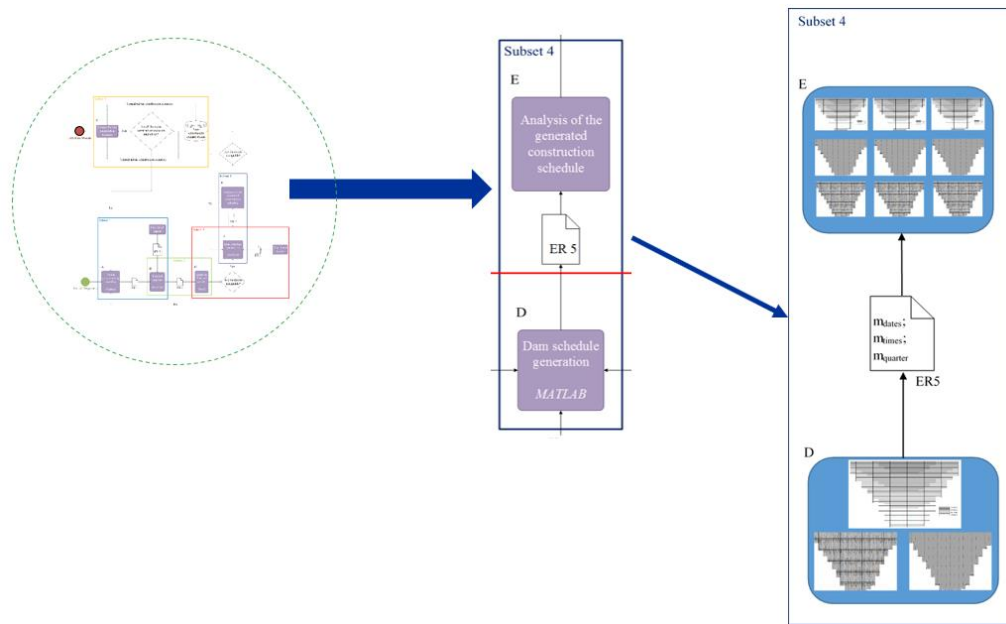
Figure 6-5 - Proposed framework – see Figure 6-1.

The constructive phasing has as outputs the constructive phasing schedule with the days of cast of each concrete layer, the constructive schedule with the waiting times between concreting of successive concrete layers and the trimestral of cast of each concrete layer (ER5 in Figures 6-1 and 6-5).

As the constructive schedule doesn't meet the project requirements the user keeps running simulations until obtain the best solution that meets the project requirements for that adopted concrete layers' height (goes back from box E to box D in Figures 6-1 and 6-5).

All that modelling, thermal and constructive phasing data for an adopted concrete layers' height are posteriorly saved in a repository allowing the user to choose the best constructive scenario, as shown in Figures 6-1 and 6-6.
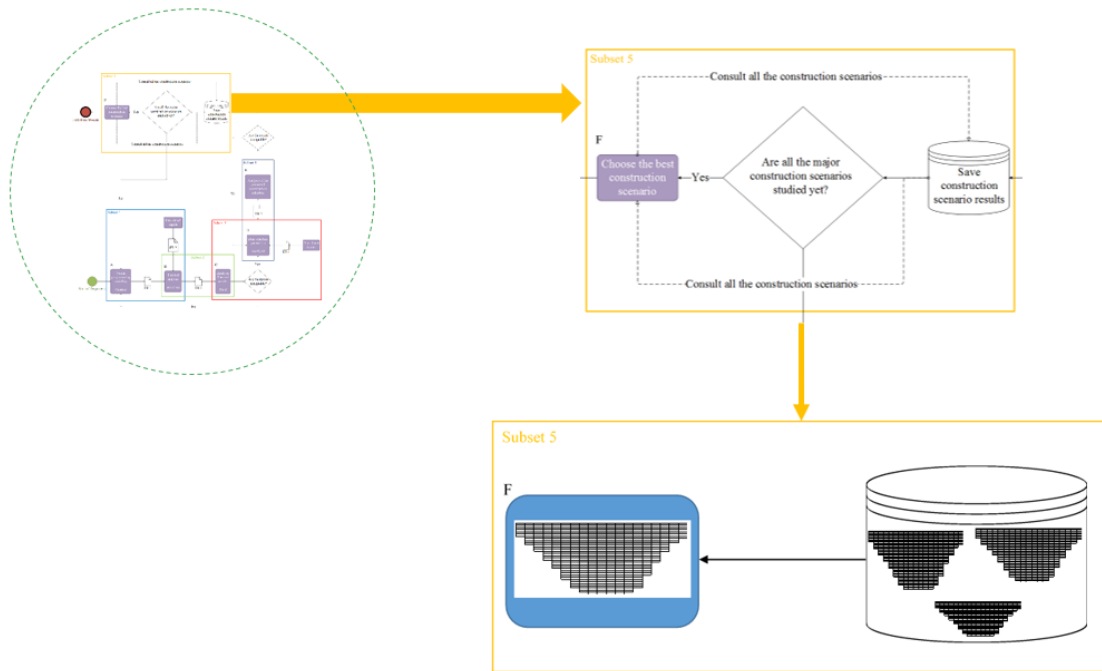
Figure 6-6 - Proposed framework – see Figure 6-1.

6.2 Examples of above framework related to the case study

In order to validate the proposed framework some studies will be conducted. It will be tested a few examples in order to exemplify the above proposed framework for a few different construction scenarios. To reduce the thermic model calculation time by the developed computational tool were simulated only five concrete layers of the dam modelled in chapter 3, because the fifth layer is already representative of the dam's concrete layers, due to the fact of all the concrete layers have the same height and the same boundaries. Thereby, from the fifth layer the heat distribution on the concrete layers is practically the same.

The generated dam schedules are according to the rules and criterions defined in chapter 5.

6.2.1 Reference scenario – Concrete layers of 2 meters height

In this example, as a reference scenario, will be tested a dam with all the simulation parameters of the simulation conducted in chapter 4.

In figures 6-7, 6-8, 6-9 and 6-10 are presented the temporal and spatial gradients to the scenario in study.
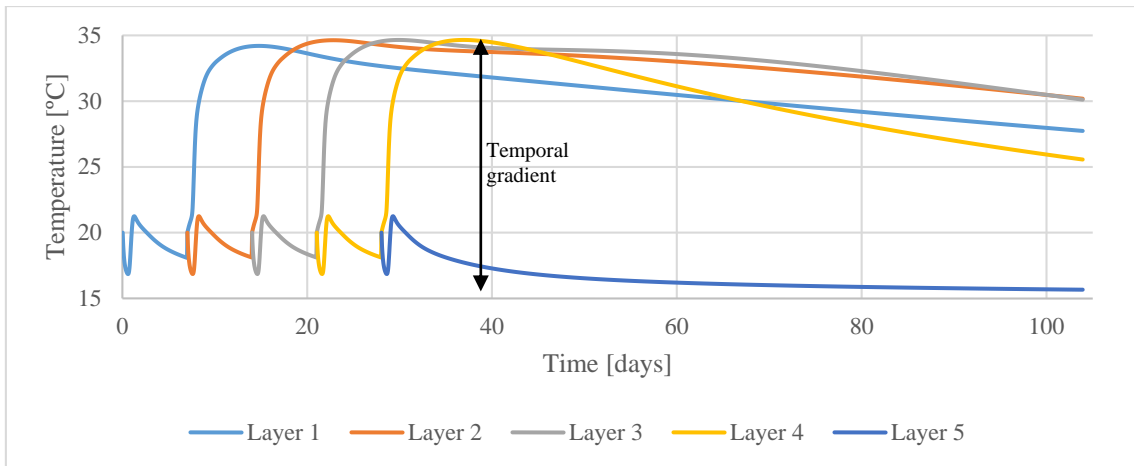
Figure 6-7 – Temperature evolution over time in the boundaries between layers for the example 1 simulation.
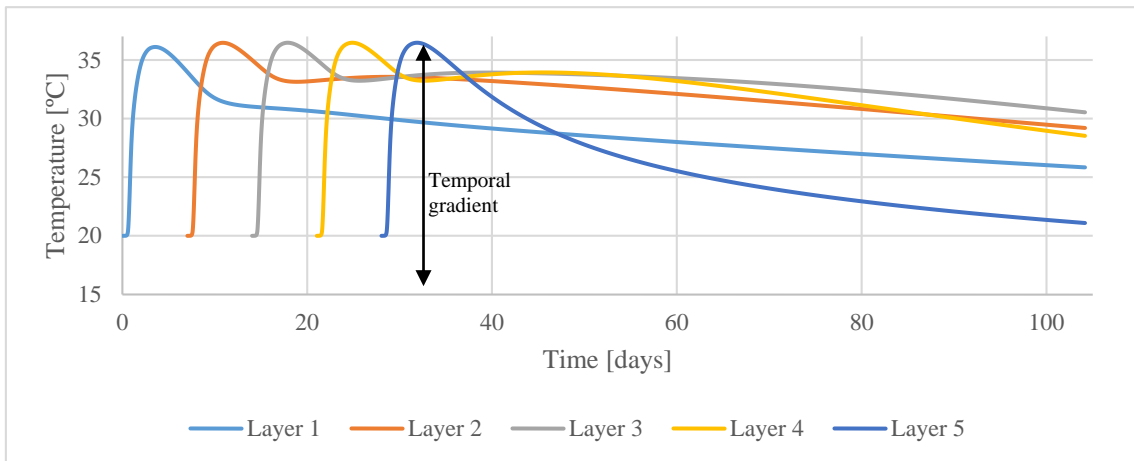
Figure 6-8 - Temperature evolution over time in the middle center points of the concrete layers for the example 1 simulation.
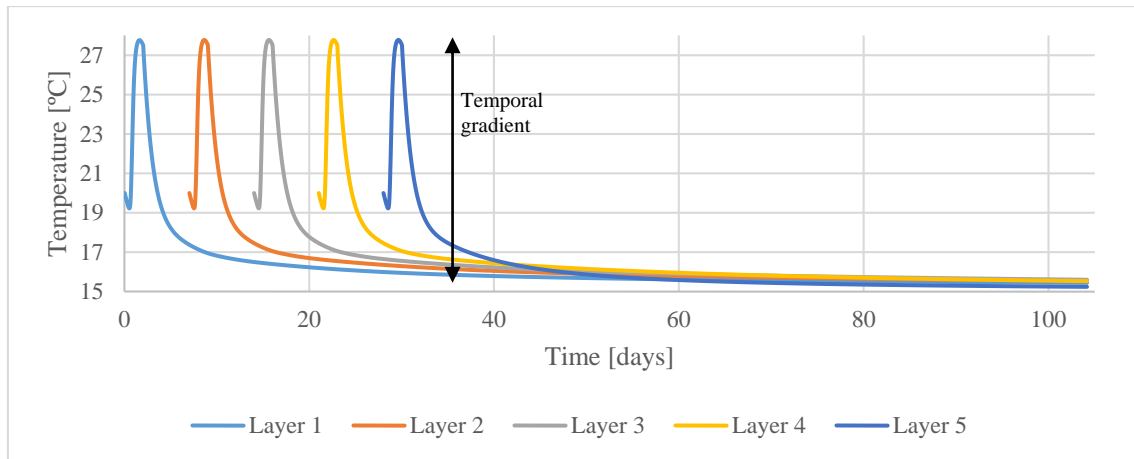
Figure 6-9 - Temperature evolution over time in the middle lateral points for the example 1 simulation.
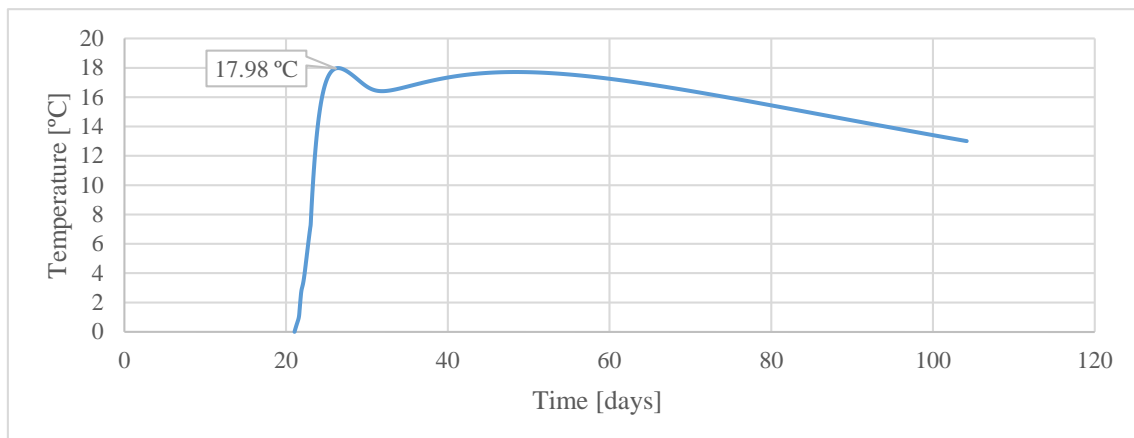
Figure 6-10 – Spatial gradient for the example 1 simulation.

Through the analysis of the above graphic it can be concluded that the reference temporal gradient for the boundary points is 18ºC, for the middle center points is 19.65ºC, for the middle lateral points is 12.96ºC and the reference spatial gradient is 17.98ºC.

The dam scheduled construction time by the use of two meters' height concrete layers, which will serve as a reference, are ten months as presented Chapter 5 and Appendix II.

6.1.1. Different concrete layers' height with the use of pre-cooling

In this sub-chapter will be tested the influence of pre-cooling of the concrete with variable concrete layers' height. The layers' height will be increased and the concrete casting temperature will be decreased using pre-cooling methods. The results for all the tested scenarios are presented in Table 6-1.

	Reference scenario	Scenario 1	Scenario 2
Layer height [m]	2	2.5	2.6
T$_{ext}$ [ºC]	15	15	15
T$_{int}$ [ºC]	20	15	12
Boundary temporal gradient [ºC]	18	15.38	16.36
Middle center point temporal gradient [ºC]	19.65	15.92	16.53
Middle lateral point temporal gradient [ºC]	12.96	9.66	10.07
Spatial gradient [ºC]	17.98	13.19	11.32
Execution time [month]	10	9.5	8.5

Table 6-1 - Studied parameters for the studied scenarios.

Through the analysis of Table 6-1 it can be concluded that the pre-cooling is very advantageous in this type of study. All the studied scenarios present lower cracking risk than the reference scenario. So, the increasing of the concrete layers' height is feasible using pre-cooling methods.

So, the above examples intended to prove that by the correct utilization of the created framework, different construction scenarios can be studied allowing the choice for the better construction schedule from the costs and construction point of views. The cost could in a general view be assessed by the construction times. In general, higher construction times result in higher construction costs.

6.3 Discussion about the practical feasibility of this framework:

The main encountered problem in the above framework is the calculation time of some tasks. All of the calculations were performed in a computer with an Intel i7-4700HQ CPU and 32Gb of 1600MHz RAM. The medium calculation times for the above framework are:

- Forty-five minutes for running code developed in Dynamo for the dam's modelling;
- Nine and a half hours for the thermal calculation of the entire dam with a fifty elements square mesh by the thermal analysis developed computational tool;
- Thirty minutes for the thermal calculation of the five representative layers of the dam with a fifty elements square mesh by the thermal analysis developed computational tool;
- The developed computational tool for the automatic generation of dam's construction scenarios it is almost instantaneous, it takes only a couple of seconds to generate the construction schedule.

All the calculations in the thermal developed computational tool were made with a tolerance of the non-linear process of heat generation of 0.001. A higher tolerance could result in faster calculation times.

As a future development, the visual programming code in Dynamo and the code behind the developed computational tool to perform the thermic calculations should be reviewed to make it more efficient and so optimize the calculation times.

CHAPTER 7

7 CONCLUSIONS

7.1 General conclusions

In the present dissertation are presented an integrated framework compounding parametric modelling, thermal calculations and constructive phasing.

Regarding fully parametric modeling of dams by visual programming contemplating the phases of the construction phasing in full solid and exportable to BIM platforms, as REVIT, it was concluded that in fact there is a high feasibility, ease of use and it is possible to create parametric objects. These objects due to this parametric nature any decision amending the dam geometry (upstream and downstream faces, concrete layers height, among others) are automatically reflected in the design and so this tool for any arch dam can make alternative geometry studies with instant information about important consequences as volumes, centers of gravity, among other very important variables in the design phase of alternative solutions. It allows the creation a repository of parametric objects for future applications so that a nearby modelling dam is made by simply number alterations on the visual programming code. Additionally, the dam body modeling is interesting to note the ease with which it is made the intersection with the underlying terrain and the galleries modelling. The interoperability between BIM platforms of this created models is also very important, so, although at this point in is impracticable, it is predictable that with new REVIT releases that impossibility is solved. Nevertheless, the used methodology has a lot of potential and presents as an extremely good solution to adopt in the dam's modelling.

Concerning to thermal calculation it was deduced the complete algorithm implementation of two dimensional finite differences with phasing, with the formwork placement and withdrawal and thermal non-linearity based on a database for Portuguese cements which was conveniently validated with DIANA software and demonstrated capacity through imported information on a list in a CSV file and minimal user inputs to performs the thermal calculations. That minimal quantity of user inputs greatly facilitates the study of alternative scenarios, as for example, studying different temperature and concrete different concrete layers height.

The implementation of the thermal analysis developed computational tool was made on MATLAB with a simplification of the finite difference method boundaries, considering that the dam has a constant thickness corresponding to the medium dam thickness, what it is considered as a minor simplification, because for pre-dimensioning proposes it is sufficiently good, much better than the one dimensional formulation. The developed computational tool beyond validation it was tested in multiple situations along the development of the dissertation have shown a good performance, without errors and with the automatic results extraction for the user for temporal gradients, spatial gradients and maps of temperatures, what allows a quick evaluation of the thermal cracking risk. This ease of use and quickness of the process is not normal in the commercial software's that are very complicated to use. The capacities of the developed computational tool were demonstrated by the performance of the thermal calculations of the case study dam. The main limitation of the developed computational tool is their calculation time, that is very time consuming the complete dam calculation, taking nine and a half hours to run, but for pre-dimensioning purposes only a fewer layers need to be calculated, reducing the calculation times for a couple of hours.

In the context of the construction phasing it has been proposed and implement a new way to study the constructive phasing dams taking into account the rules of good practice that are already commonly applied. These rules include criteria as varied as the waiting time between concreting, the differences in height between the layers and attempt to avoid the occurrence of cold joints. These rules were implemented in a cellular automata algorithm that has proved effective and flexible to changing the rules while maintaining its good performance. The algorithm was tested on a possible solution for the complete dam having performed the calculations quickly and very consistent with what would be done manually. The algorithm in situations in which there is ambiguity, more than one possible path, makes a random choice, but after several runs of the same dam phasing the construction times conducted always to a similar construction time. The developed computational tool has performed the thermal calculation very well in all the simulation run during the dissertation and has a promising role in the use as a quick tool for the engineer instead of the manual typically used process, that is very time consuming in the study of different construction scenarios with different layers' height or any alteration in another rule. This innovative for each there is no parallel in the literature, as proven to be advantageous and very capable in the automatic generation of dam's construction schedules.

All the tools developed here were integrated into a common framework. This is a real IPD viewpoint of setting of the construction phasing, which through three-dimensional modeling of the dam incorporates its automatic division of blocks in accordance with the construction joints and no graphic information associated with this model can be exported directly or for thermal calculation of what information quickly on the feasibility of the construction phasing previously defined but also about the calculation of their impact.

The framework proposed in BPMN format and carefully explained in Figure 6-1. This framework was tested in for multiple possible scenarios related to different layers by the reduction of temperature of placing of concrete. The cost of this temperature reduction could be minimized by the reduction of the construction time and thereby allows the engineer quickly compare costs of concrete cooling with the associated gains to a faster conclusion of the dam construction.

As final conclusion highlights the success compared to initial proposed objectives of implementation of the framework together in a true spirit of early project decision-making allowing the integration of skills not usually available in the very preliminary stages of dam studies.

7.2 Future challenges

Taking into account the work started with this thesis and being conscious that by no means can any of the considered subject be considered solved or finished by the creation of this framework, a list of the most relevant acknowledged limitations (and future developments) are presented in this section:

- The dam's spillways were not modelled in Dynamo. That could be hereafter modeled in order to obtain an 3D model that entirely reproduces the real dam shape;
- Improvement of the interoperability between dynamo and REVIT, that allows the introduction of non-geometrical information (project parameters) in a more practical way into BIM model, what nowadays is conditioned by an impossibility in the REVIT Family Editor that disallow the simultaneous explosion of more than one object at a time. As a future development, when a new release of REVIT corrects that problem, all the objects should be exploded an all the non-geometrical information should be included in the BIM model.

- The finite difference derivation used for the thermic calculations is not capable of consider the curved boundaries. As a future development the derivation could be made to consider the curved boundaries and implemented in the thermal analysis developed computational tool;

- The developed computational tool calculation time is quite large, so, as future development, the created computational code must be reviewed in order turn more efficient;

- The implemented rules in the automatic dam construction schedules generation developed computational tool could be revised, proceeding to the introduction and removal of the implemented ones.

- In developed computational tool in the scope of the dam construction phasing could be implemented the days can't be any concreting (weekends and holydays).

REFERENCES

Adamatzky, A. (2010). *Game of Life Cellular Automata. Journal of Chemical Information and Modeling*. Springer- Verlag Wien GmbH. http://doi.org/10.1007/978-1-84996-217-9

Aia. (2007). Integrated Project Delivery: A Guide. *American Institute of Architects*, 1–62. Retrieved from http://www.aia.org/groups/aia/documents/pdf/aiab083423.pdf

Azenha, M. (2004). *Comportamento do betão nas primeiras idades. Fenomenologia e análise termo-mecânica*. Universidade do Porto.

Azenha, M. (2009). *NUMERICAL SIMULATION OF THE STRUCTURAL BEHAVIOUR OF CONCRETE SINCE ITS EARLY AGES*. University of Porto.

Azenha, M., Lino, J. C., & Caires, B. (2015). Curso BIM: Building Information Modeling. In *Ordem dos Engenheiros*.

Ballim, Y., & Graham, P. C. (2009). The effects of supplementary cementing materials in modifying the heat of hydration of concrete. *Materials and Structures*, *42*, 803–811. http://doi.org/10.1617/s11527-008-9425-3

Batista, A. (1998). *Análise do comportamento ao longo do tempo de barragens abóbada.* Instituto Superior Técnico, Tese de Doutoramento.

Berto, F., & Tagliabue, J. (2012). Cellular Automata. Retrieved August 20, 2015, from http://plato.stanford.edu/entries/cellular-automata/

Bofang, Z. (2014). *Temperature Control of Concrete Dam in Cold Region. Thermal Stresses and Temperature Control of Mass Concrete*. http://doi.org/10.1016/B978-0-12-407723-2.00021-X

Dynamo Primer. (2015).

Faramarzi, a., & Afshar, M. H. (2012). Application of cellular automata to size and topology optimization of truss structures. *Scientia Iranica*, *19*(3), 373–380.

http://doi.org/10.1016/j.scient.2012.04.009

Farinha, M. (2003). *Extensões e tensões observadas em barragens de betão. Laboratório Nacional de Engenharia Civil (LNEC)*.

Iberdrola. (2014). Presa de Almendra. Retrieved August 5, 2015, from https://www.flickr.com/photos/iberdrola/14509687004

IFC Exporter 2016. (n.d.). Retrieved November 19, 2015, from https://apps.autodesk.com/RVT/pt/Detail/Index?id=appstore.exchange.autodesk.com%3a ifc2016_windows32and64%3aen

Incropera, F. P., & DeWitt, D. P. (2001). *Introduction to heat transfer*. New York: John Wiley & Sons, Inc.

Kim, S. G. (2010). *Effect oh heat generation from cement hydration on mass concrete placement*. Iowa State University. Retrieved from http://citeseerx.ist.psu.edu/viewdoc/summary?doi=10.1.1.146.4675

Li, S., Ren, J., Wu, Z., & Zhao, L. (2008). Simulation of Temperature Field – RCC arch dam. Retrieved from http://www.waterpowermagazine.com/features/featuresimulation-of-temperature-field-rcc-arch-dam/

Object Management Group. (2015). BPMN. Retrieved August 1, 2015, from http://www.omg.org/bpmn/Documents/FAQ.htm

Ozisik, M. N. (1985). *Heat transfer: a basic approach*. New York: McGraw-Hill.

Ozisik, N. (1994). *Finite difference methods in heat transfer*. Boca Raton: CRC Press.

Pedro, J. O. (1999). *Arch Dams. Designing and Monitoring For Safety. CISM Courses and lectures* (Vol. 367). Springer- Verlag Wien GmbH. http://doi.org/10.1017/CBO9781107415324.004

Rickert, M., & Nagel, K. (1996). Two lane traffic simulations using cellular automata. *Physica A: Statistical Mechanics and Its Applications*, *231*, 534–550. http://doi.org/10.1016/0378-4371(95)00442-4

Shiffman, D. (2004). Cellular automata. Retrieved September 16, 2015, from

http://natureofcode.com/book/chapter-7-cellular-automata/

Spanish Commitee on Large Dams. (1990). *Conventional Methods in Dam Construction*. CIGB ICOLD.

Teles, M. (1985). *Comportamento térmico de barragens de betão.* Tese de Doutoramento.

Teresko, J. (1993). Parametric Technology Corp.: Changing the way products are designed. *Industry Week*. Industry Week.

Townsend, C. L. (1965). Control of Cracking in Mass Concrete Structures. Bureau of Reclamation.

U.S. Army Corps of Engineers. (1994). *Engineering and Design: Arch dam design.* Washingtom DC: Department of the Army.

USDI. (1977). *(United States Department Of The Interior). Design of arch dams. Design Manual For Concrete Arch Dams*. Denver: United States Government Printing Office.

APPENDIX I – PRODUCED CODE IN DYNAMO
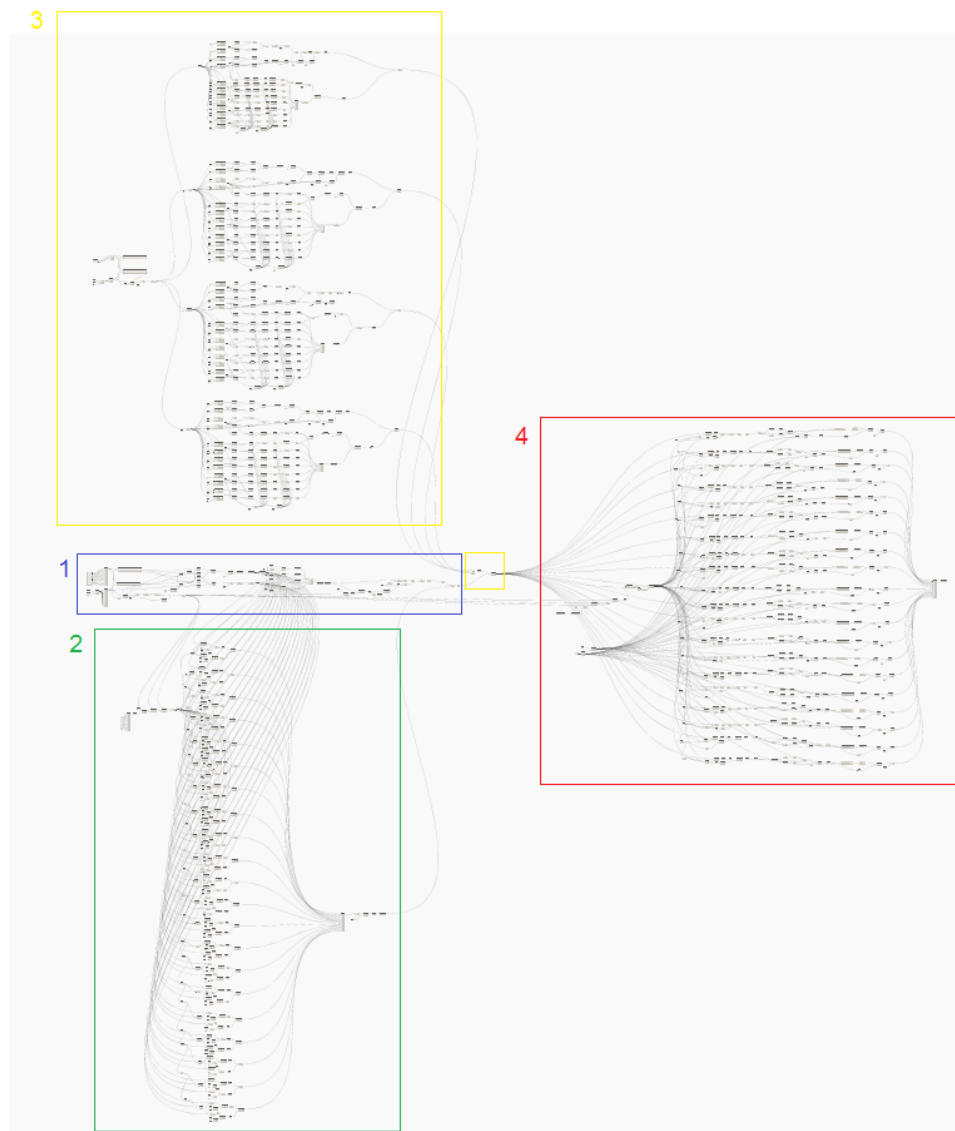
Figure I-1 - Overview of the produced dynamo code.
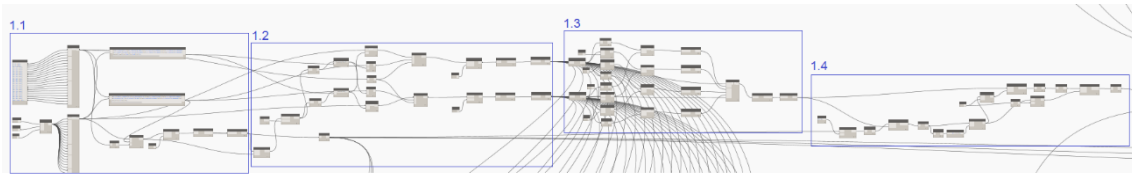
Figure I-2 - Overview of the code in section 1 (see Figure I-1).
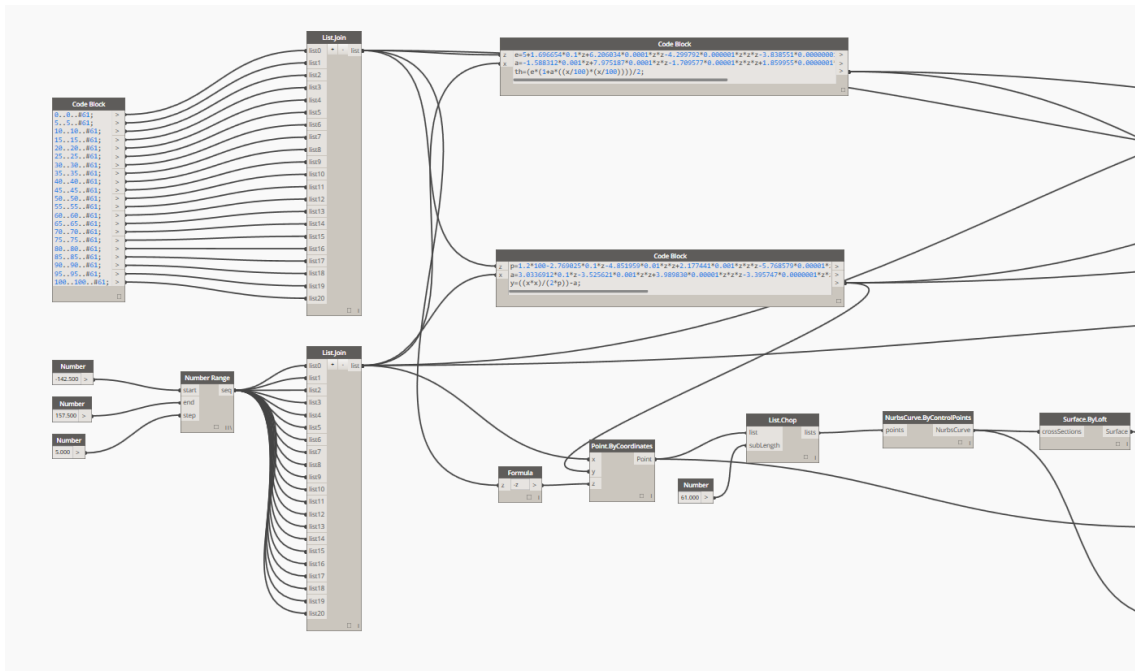
Figure I-3 - Code used to model the dam's medium sheet (section 1.1 - see Figure I-2).
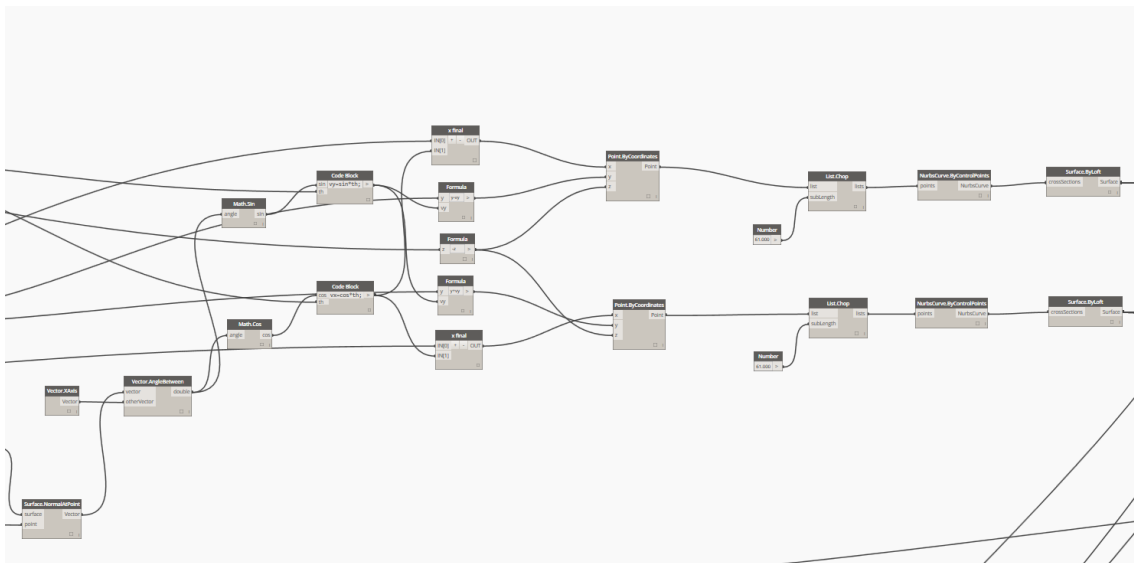
Figure I-4 - Code used to give thickness to dam's medium sheet (section 1.2 - see Figure I-2).
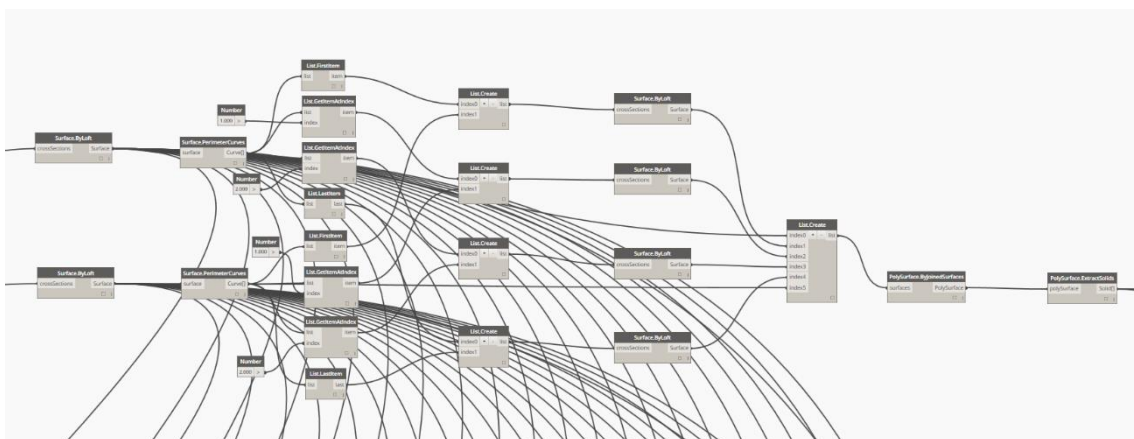
Figure I-5 - Generation of dam's body solid (section 1.3 - see Figure I-2).
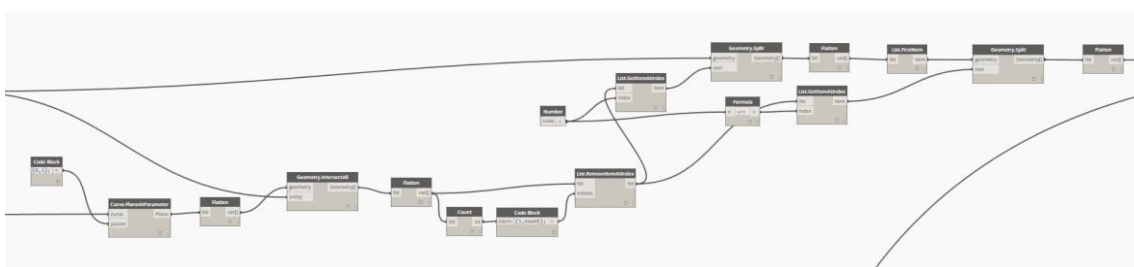
Figure I-6 - Cut of the dam's solid by the left and right banks (section 1.4 - see Figure I-2).

Figure I-7 - Overview of the code in section 2 (see Figure I-1).
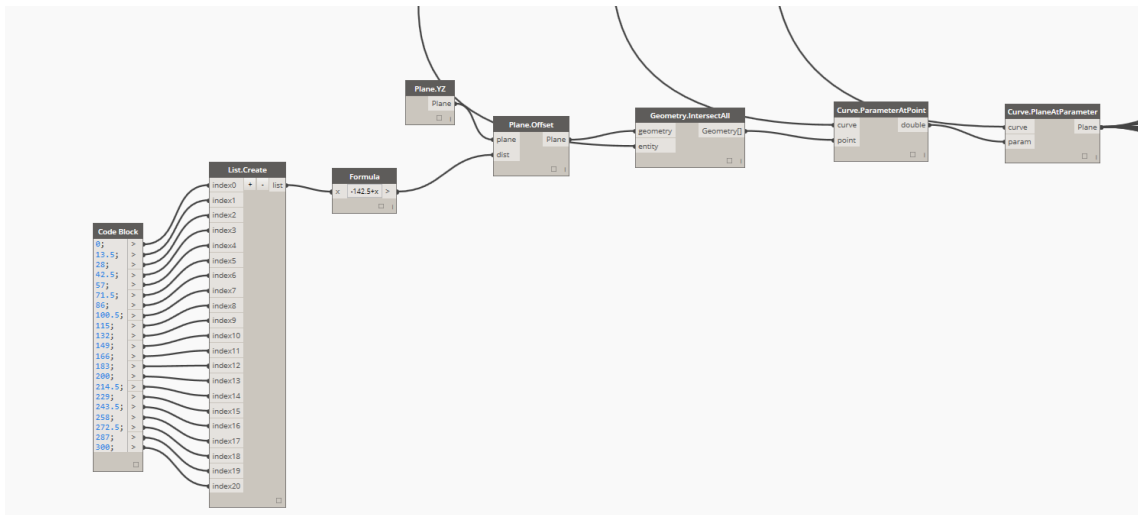
Figure I-8 - Definition of the vertical planes that represent the vertical construction joints (section 2.1 - see Figure I-7).
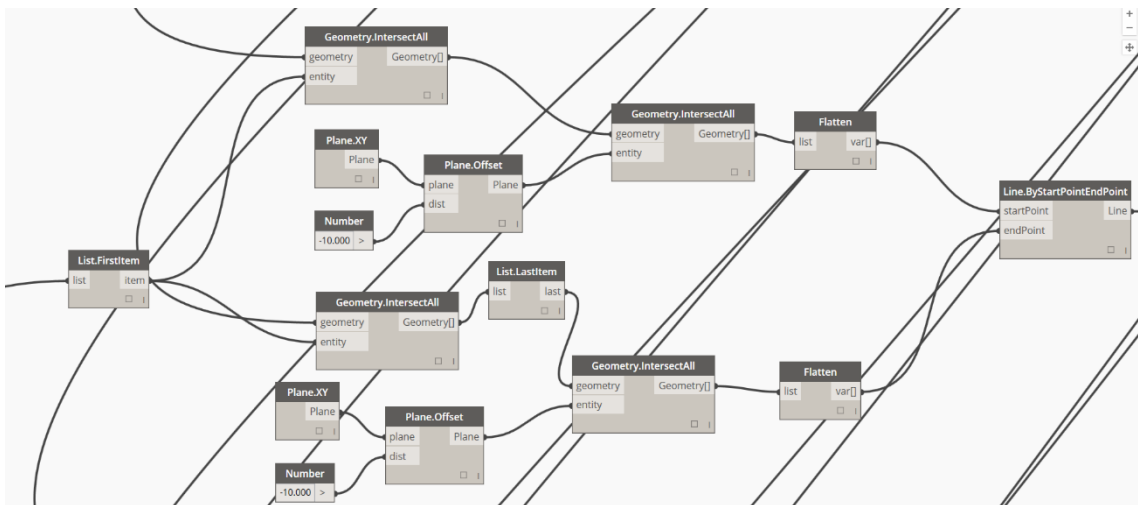
Figure I-9 - Definition of one of the lines that will be used to create the surface on intersection of the dam with the ground (section 2.2 - see Figure I-7).
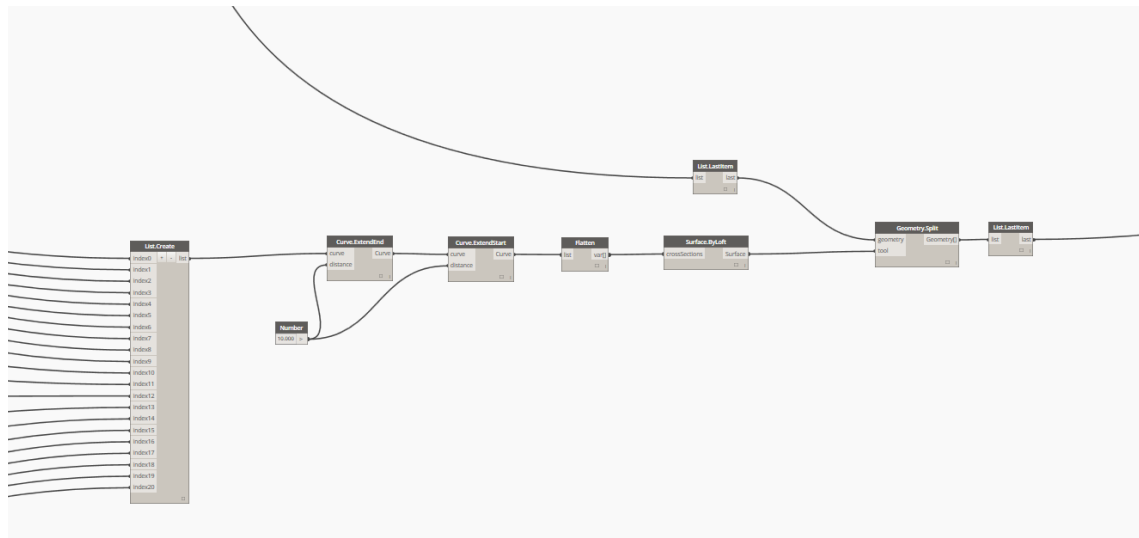
Figure I-10 - Creation of the surface on intersection of the dam with the ground and split the dam's body by the created surface (section 2.4 - see Figure I-7).
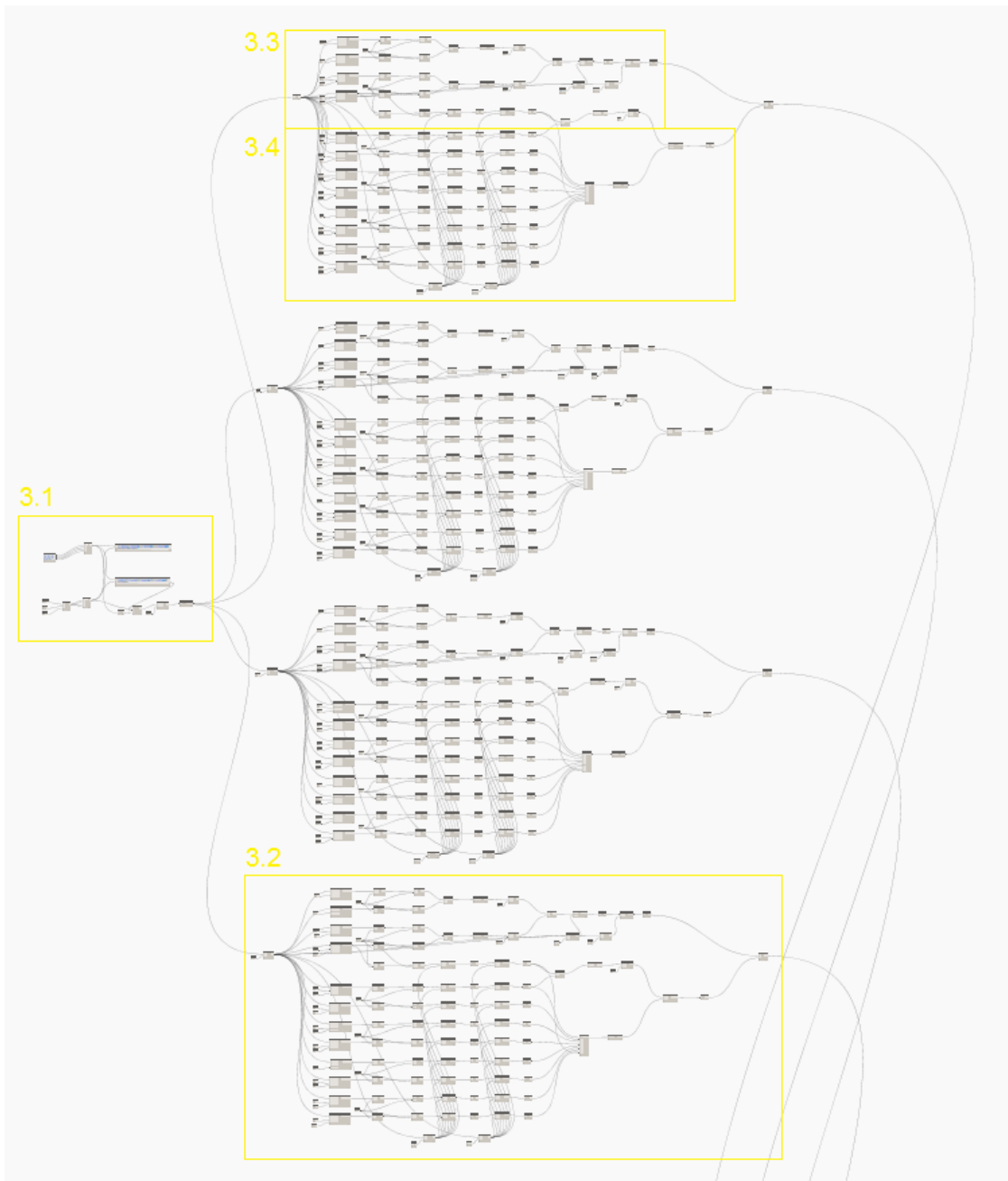
Figure I-11 - Overview of the code in section 3 (see Figure I-1).
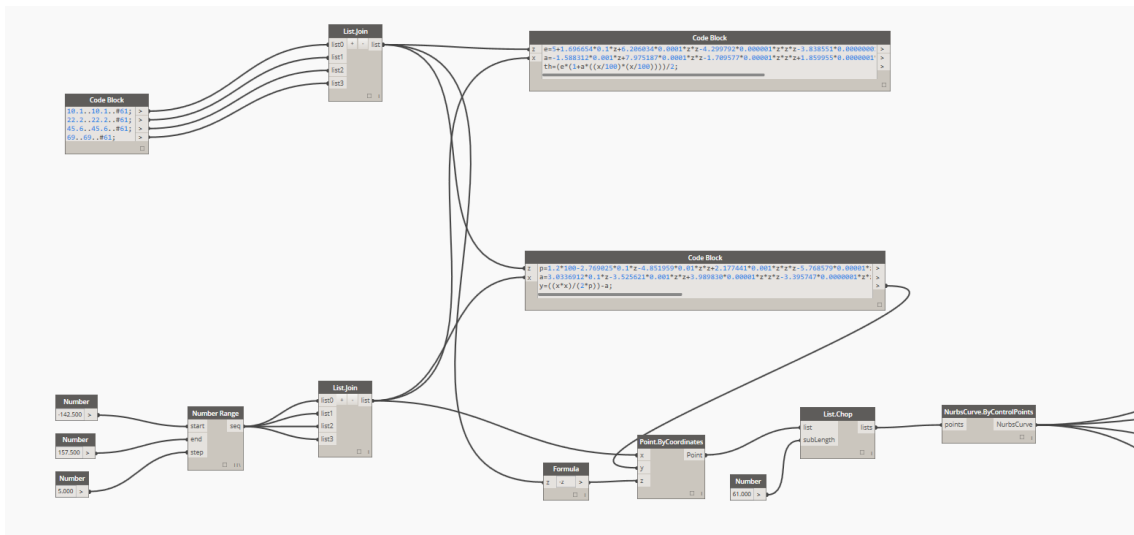
Figure I-12 - Creation of the NURBS curve parallel of the medium sheet in all the dam's galleries (section 3.1 - see Figure I-11).
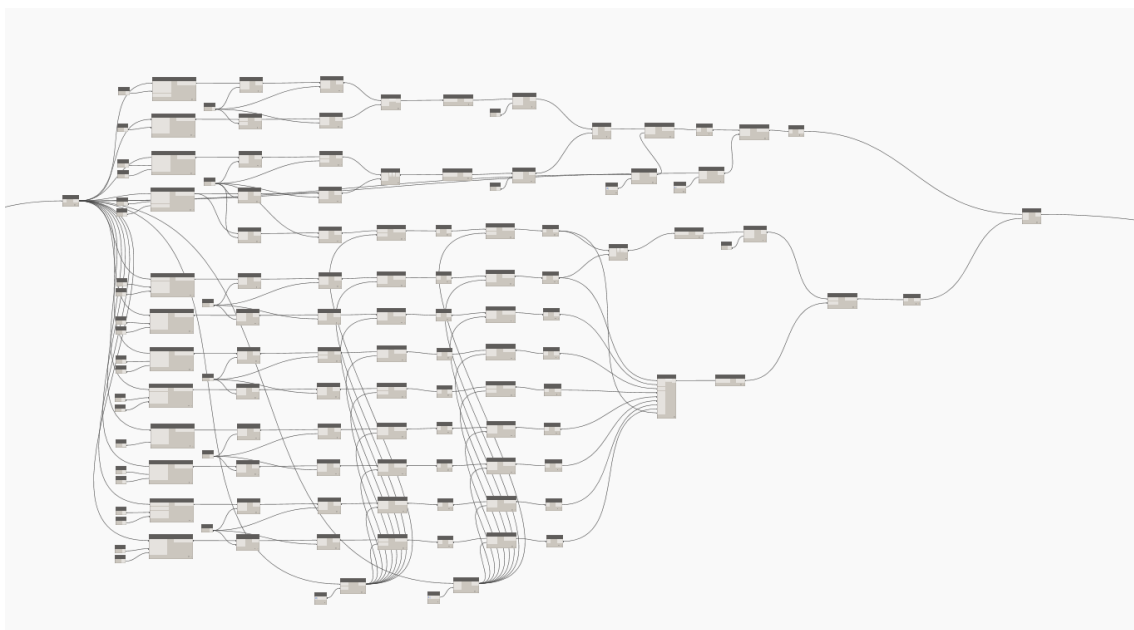
Figure I-13 - Overview of the code used to model one dam gallery (section 3.2 - see Figure I-11).
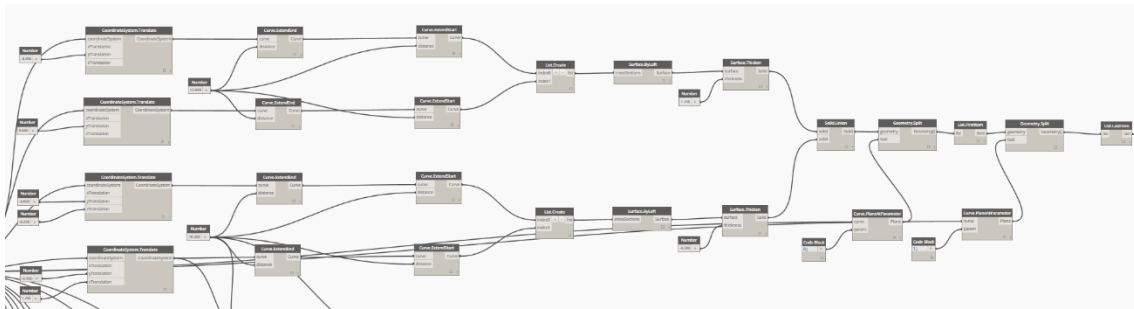
Figure I-14 - Creation of the solid with an exaggerated height that will be used to model the dam's galleries (section 3.3- see Figure I-11).
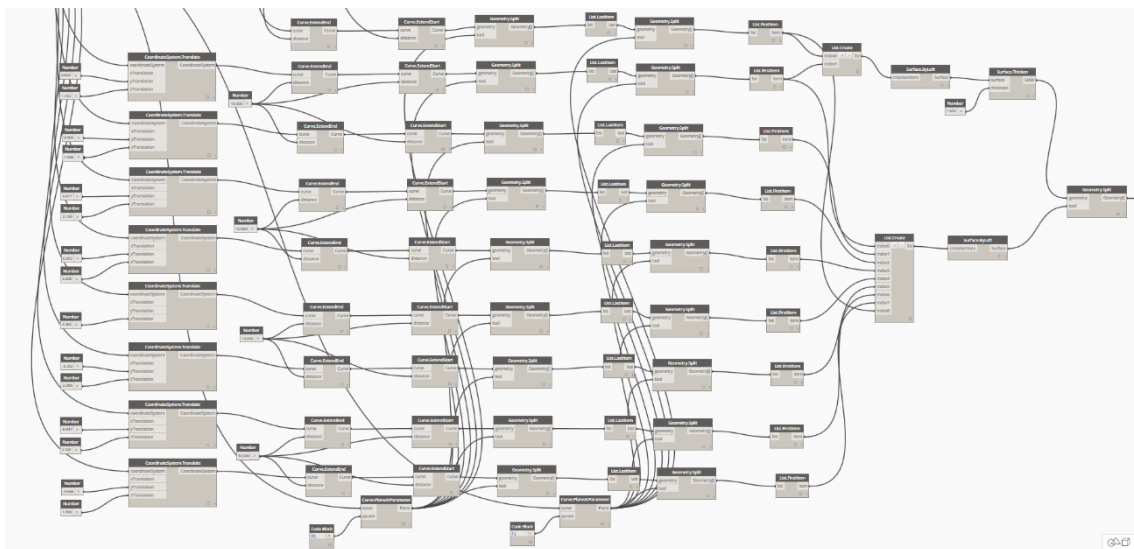
Figure I-15 - Creation of the surface of the top of the dam's gallery and cut of the previously created solid (section 3.4 - see Figure I-11).
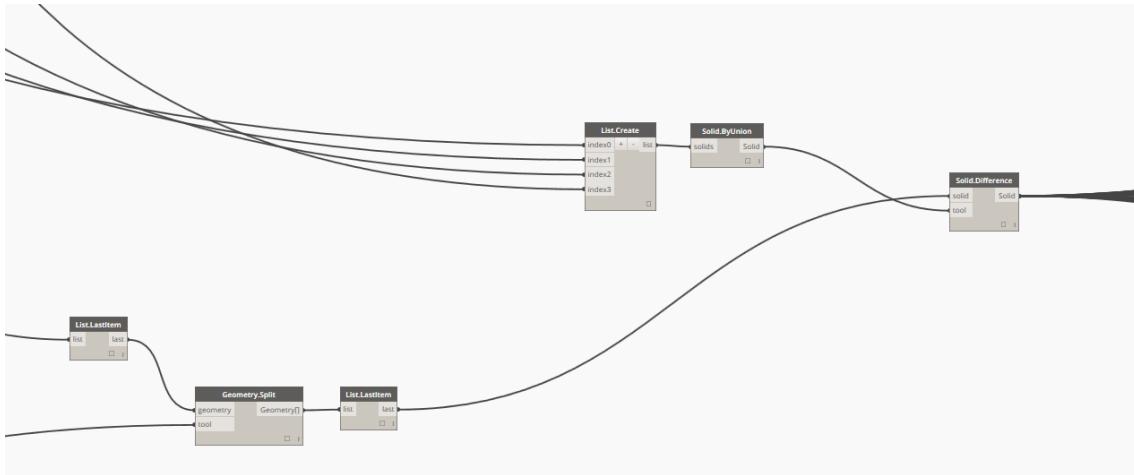
Figure I-16 - Union of the four dam's galleries and subtraction of these to the dam's body solid (section 3.5 - see Figure I-11).

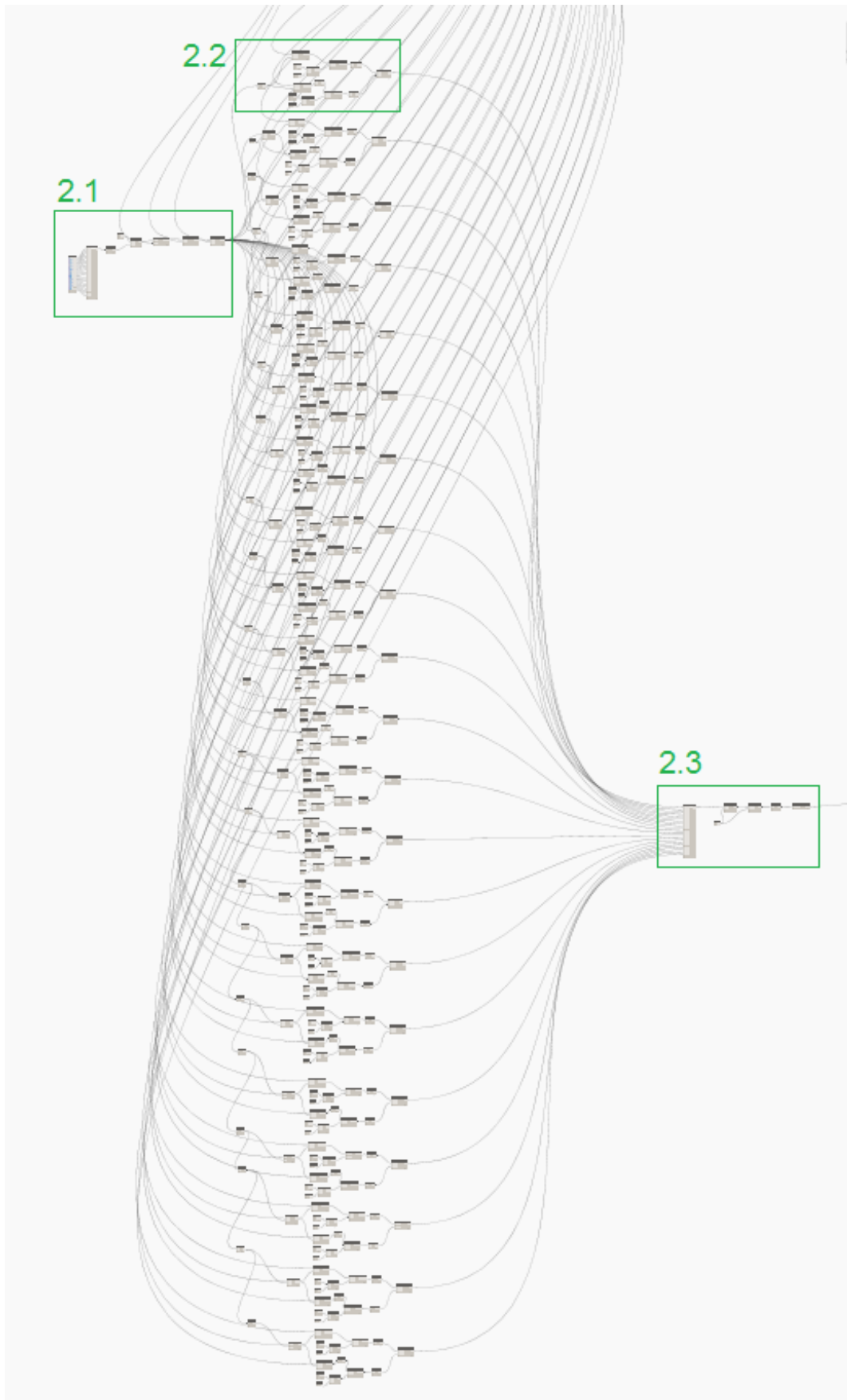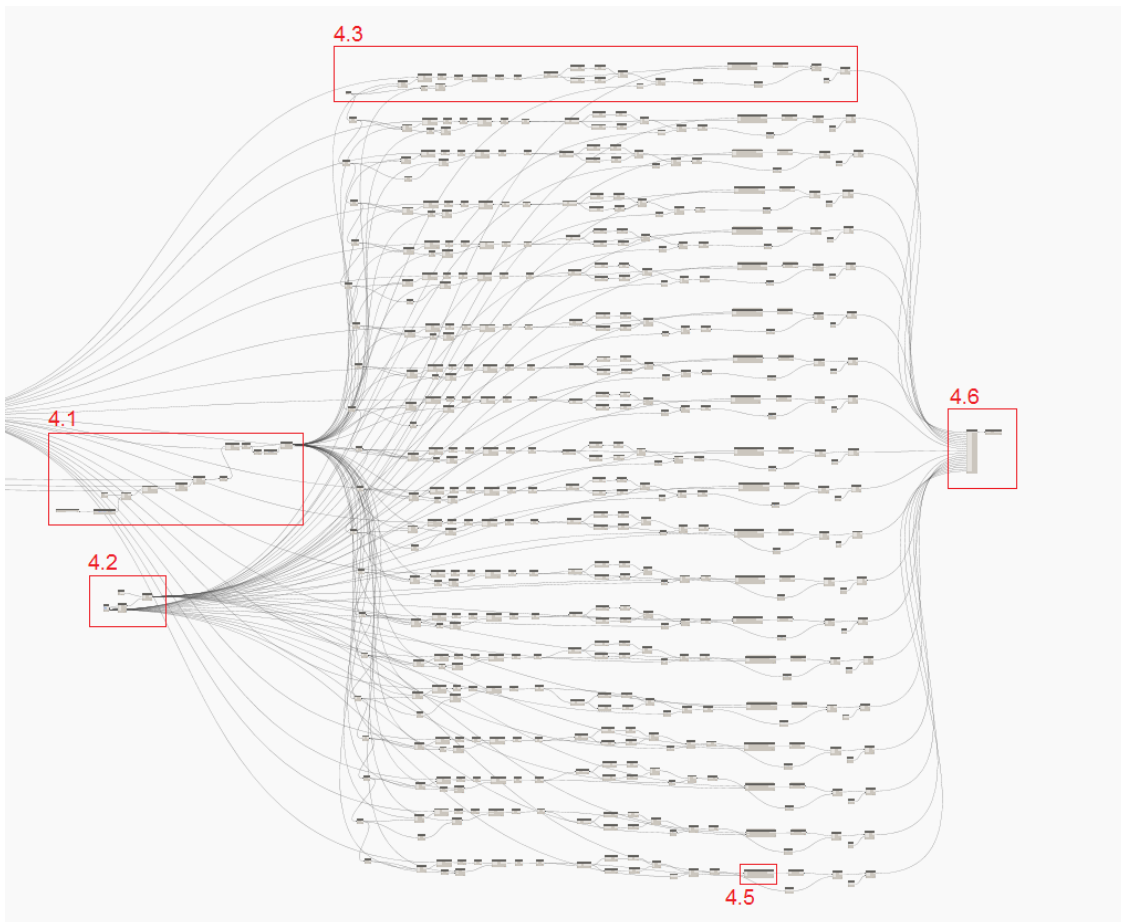Figure I-17 - Overview of the code in section 4 (see Figure I-1).
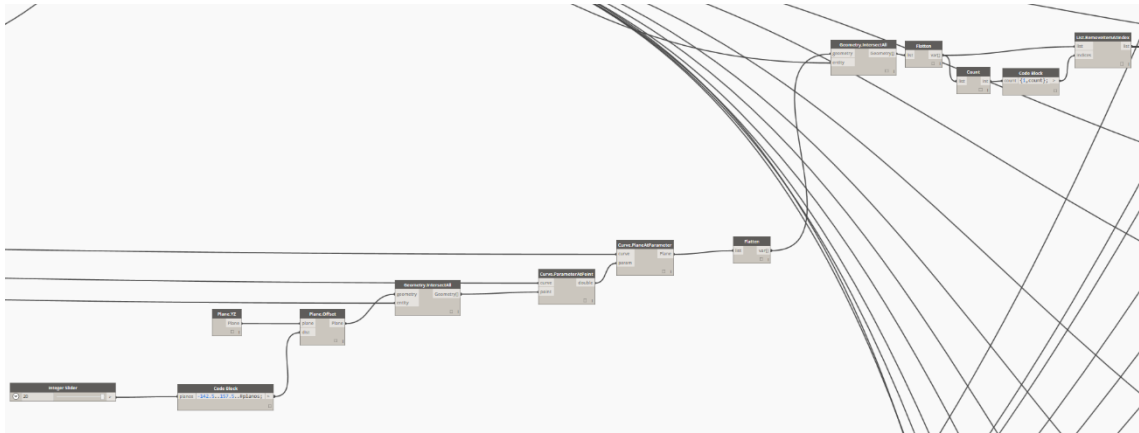
Figure I-18 - Definition of the number of vertical planes that represent the dam's construction joints and will vertically slice the dam's body (section 4.1 - see Figure I-17).
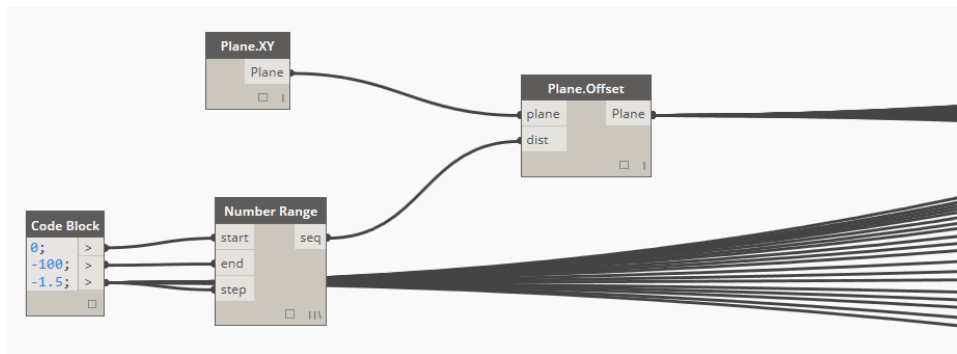
Figure I-19 - Definition of the horizontal planes that will slice the dam's body according with a given concreting layer height (section 4.2 - see Figure I-17).

Figure I-20 - Code used to slice the dam's body by the previously defined horizontal planes (section 4.3 - see Figure I-17).
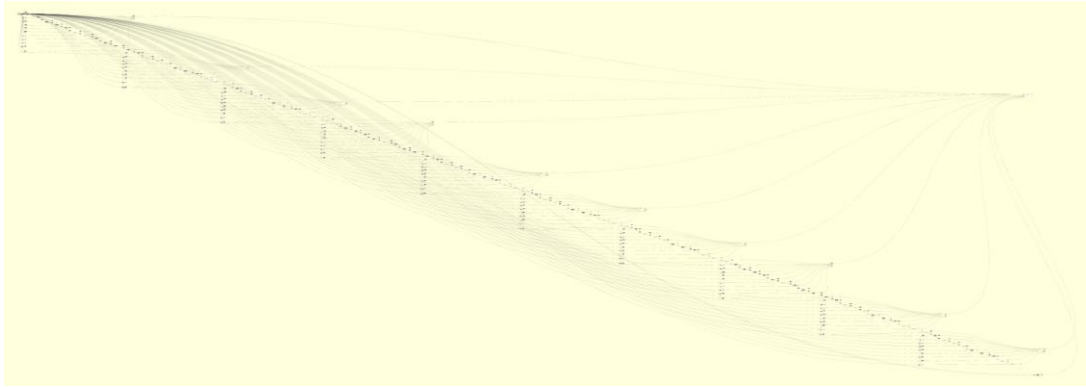
Figure I-21 – Overview of the custom node created to cut the dam's body by any number of horizontal planes (Section 4.4 - see Figure I-17).
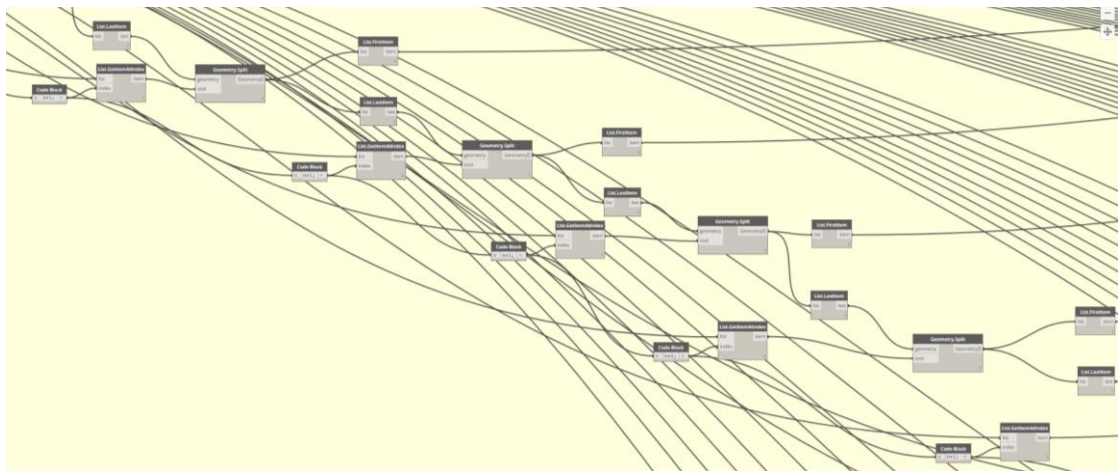
Figure I-22 - Zoom at the created algorithm to create to cut the dam's body by horizontal planes (see Figure I-21 and Figure I-17).

Figure I-23 - Import of all the construction blocks to Autodesk REVIT (section 4.6 - see Figure I-17).

Figure I-24 - Developed code in Dynamo for the introduction of the non-geometrical information in the model.

APPENDIX II – GENERATED SCHEDULE FOR THE CASE STUDY

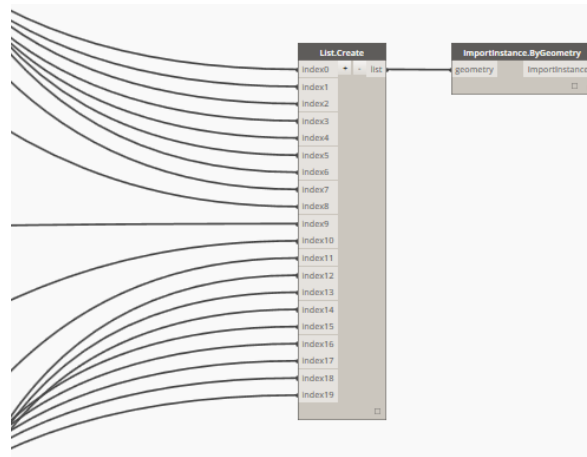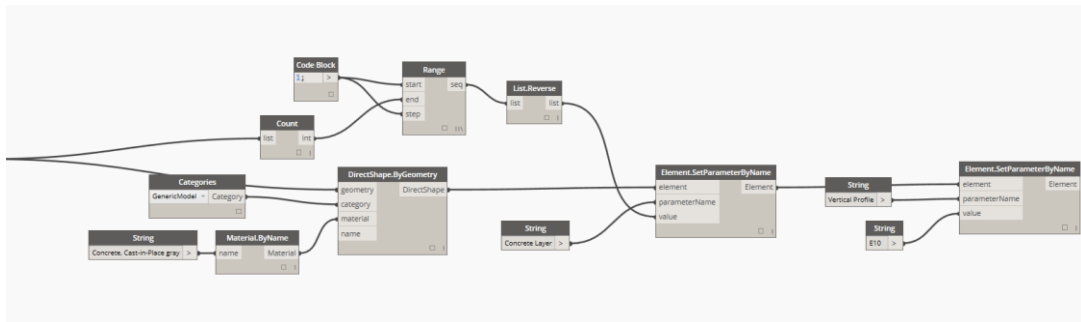| 14-Jun-16	11-Jul-16	24-Jul-16	6-Aug-16	30-Aug-16	18-Sep-16	1-Oct-16	21-Oct-16	20-Oct-16	20-Oct-16	20-Oct-16	21-Oct-16	14-Oct-16	1-Oct-16	12-Sep-16	17-Aug-16	24-Jul-16	5-Jul-16	22-Jun-16
7-Jun-16	4-Jul-16	17-Jul-16	30-Jul-16	23-Aug-16	11-Sep-16	24-Sep-16	14-Oct-16	13-Oct-16	13-Oct-16	13-Oct-16	14-Oct-16	7-Oct-16	24-Sep-16	5-Sep-16	10-Aug-16	17-Jul-16	28-Jun-16	15-Jun-16
31-May-16	27-Jun-16	10-Jul-16	23-Jul-16	16-Aug-16	4-Sep-16	17-Sep-16	7-Oct-16	6-Oct-16	6-Oct-16	6-Oct-16	7-Oct-16	30-Sep-16	17-Sep-16	29-Aug-16	3-Aug-16	10-Jul-16	21-Jun-16	8-Jun-16
24-May-16	20-Jun-16	3-Jul-16	16-Jul-16	9-Aug-16	28-Aug-16	10-Sep-16	30-Sep-16	29-Sep-16	29-Sep-16	29-Sep-16	30-Sep-16	23-Sep-16	10-Sep-16	22-Aug-16	27-Jul-16	3-Jul-16	14-Jun-16	1-Jun-16
17-May-16	13-Jun-16	26-Jun-16	9-Jul-16	2-Aug-16	21-Aug-16	3-Sep-16	23-Sep-16	22-Sep-16	22-Sep-16	22-Sep-16	23-Sep-16	16-Sep-16	3-Sep-16	15-Aug-16	20-Jul-16	26-Jun-16	7-Jun-16	25-May-16
10-May-16	6-Jun-16	19-Jun-16	2-Jul-16	26-Jul-16	14-Aug-16	27-Aug-16	16-Sep-16	15-Sep-16	15-Sep-16	15-Sep-16	16-Sep-16	9-Sep-16	27-Aug-16	8-Aug-16	13-Jul-16	19-Jun-16	31-May-16	18-May-16
3-May-16	30-May-16	12-Jun-16	25-Jun-16	19-Jul-16	7-Aug-16	20-Aug-16	9-Sep-16	8-Sep-16	8-Sep-16	8-Sep-16	9-Sep-16	2-Sep-16	20-Aug-16	1-Aug-16	6-Jul-16	12-Jun-16	24-May-16	11-May-16
26-Apr-16	23-May-16	5-Jun-16	18-Jun-16	12-Jul-16	31-Jul-16	13-Aug-16	2-Sep-16	1-Sep-16	1-Sep-16	1-Sep-16	2-Sep-16	26-Aug-16	13-Aug-16	25-Jul-16	29-Jun-16	5-Jun-16	17-May-16	4-May-16
18-Apr-16	16-May-16	29-May-16	11-Jun-16	5-Jul-16	24-Jul-16	6-Aug-16	26-Aug-16	25-Aug-16	25-Aug-16	25-Aug-16	26-Aug-16	19-Aug-16	6-Aug-16	18-Jul-16	22-Jun-16	29-May-16	10-May-16	27-Apr-16
	9-May-16	22-May-16	4-Jun-16	28-Jun-16	17-Jul-16	30-Jul-16	19-Aug-16	18-Aug-16	18-Aug-16	18-Aug-16	19-Aug-16	12-Aug-16	30-Jul-16	11-Jul-16	15-Jun-16	22-May-16	3-May-16	20-Apr-16
	2-May-16	15-May-16	28-May-16	21-Jun-16	10-Jul-16	23-Jul-16	12-Aug-16	11-Aug-16	11-Aug-16	11-Aug-16	12-Aug-16	5-Aug-16	23-Jul-16	4-Jul-16	8-Jun-16	15-May-16	26-Apr-16	13-Apr-16
	25-Apr-16	8-May-16	21-May-16	14-Jun-16	3-Jul-16	16-Jul-16	5-Aug-16	4-Aug-16	4-Aug-16	4-Aug-16	5-Aug-16	29-Jul-16	16-Jul-16	27-Jun-16	1-Jun-16	8-May-16	19-Apr-16	
	18-Apr-16	1-May-16	14-May-16	7-Jun-16	26-Jun-16	9-Jul-16	29-Jul-16	28-Jul-16	28-Jul-16	28-Jul-16	29-Jul-16	22-Jul-16	9-Jul-16	20-Jun-16	25-May-16	1-May-16	12-Apr-16	
	11-Apr-16	24-Apr-16	7-May-16	31-May-16	19-Jun-16	2-Jul-16	22-Jul-16	21-Jul-16	21-Jul-16	21-Jul-16	22-Jul-16	15-Jul-16	2-Jul-16	13-Jun-16	18-May-16	24-Apr-16	5-Apr-16	
	4-Apr-16	17-Apr-16	30-Apr-16	24-May-16	12-Jun-16	25-Jun-16	15-Jul-16	14-Jul-16	14-Jul-16	14-Jul-16	15-Jul-16	8-Jul-16	25-Jun-16	6-Jun-16	11-May-16	17-Apr-16		
		10-Apr-16	23-Apr-16	17-May-16	5-Jun-16	18-Jun-16	8-Jul-16	7-Jul-16	7-Jul-16	7-Jul-16	8-Jul-16	1-Jul-16	18-Jun-16	30-May-16	4-May-16	10-Apr-16		
		3-Apr-16	16-Apr-16	10-May-16	29-May-16	11-Jun-16	1-Jul-16	30-Jun-16	30-Jun-16	30-Jun-16	1-Jul-16	24-Jun-16	11-Jun-16	23-May-16	27-Apr-16	3-Apr-16		
		27-Mar-16	9-Apr-16	3-May-16	22-May-16	4-Jun-16	24-Jun-16	23-Jun-16	23-Jun-16	23-Jun-16	24-Jun-16	17-Jun-16	4-Jun-16	16-May-16	20-Apr-16	27-Mar-16		
		20-Mar-16	2-Apr-16	26-Apr-16	15-May-16	28-May-16	17-Jun-16	16-Jun-16	16-Jun-16	16-Jun-16	17-Jun-16	10-Jun-16	28-May-16	9-May-16	13-Apr-16	20-Mar-16		
		13-Mar-16	26-Mar-16	19-Apr-16	8-May-16	21-May-16	10-Jun-16	9-Jun-16	9-Jun-16	9-Jun-16	10-Jun-16	3-Jun-16	21-May-16	2-May-16	6-Apr-16	13-Mar-16		
			19-Mar-16	12-Apr-16	1-May-16	14-May-16	3-Jun-16	2-Jun-16	2-Jun-16	2-Jun-16	3-Jun-16	27-May-16	14-May-16	25-Apr-16	30-Mar-16			
			12-Mar-16	5-Apr-16	24-Apr-16	7-May-16	27-May-16	26-May-16	26-May-16	26-May-16	27-May-16	20-May-16	7-May-16	18-Apr-16	23-Mar-16			
			5-Mar-16	29-Mar-16	17-Apr-16	30-Apr-16	20-May-16	19-May-16	19-May-16	19-May-16	20-May-16	13-May-16	30-Apr-16	11-Apr-16	16-Mar-16			
			27-Feb-16	22-Mar-16	10-Apr-16	23-Apr-16	13-May-16	12-May-16	12-May-16	12-May-16	13-May-16	6-May-16	23-Apr-16	4-Apr-16	9-Mar-16			
			20-Feb-16	15-Mar-16	3-Apr-16	16-Apr-16	6-May-16	5-May-16	5-May-16	5-May-16	6-May-16	29-Apr-16	16-Apr-16	28-Mar-16	2-Mar-16			
				8-Mar-16	27-Mar-16	9-Apr-16	29-Apr-16	28-Apr-16	28-Apr-16	28-Apr-16	29-Apr-16	22-Apr-16	9-Apr-16	21-Mar-16	24-Feb-16			
				1-Mar-16	20-Mar-16	2-Apr-16	22-Apr-16	21-Apr-16	21-Apr-16	21-Apr-16	22-Apr-16	15-Apr-16	2-Apr-16	14-Mar-16	17-Feb-16			
				23-Feb-16	13-Mar-16	26-Mar-16	15-Apr-16	14-Apr-16	14-Apr-16	14-Apr-16	15-Apr-16	8-Apr-16	26-Mar-16	7-Mar-16				
				16-Feb-16	6-Mar-16	19-Mar-16	8-Apr-16	7-Apr-16	7-Apr-16	7-Apr-16	8-Apr-16	1-Apr-16	19-Mar-16	29-Feb-16				
				9-Feb-16	28-Feb-16	12-Mar-16	1-Apr-16	31-Mar-16	31-Mar-16	31-Mar-16	1-Apr-16	25-Mar-16	12-Mar-16	22-Feb-16				
				2-Feb-16	21-Feb-16	5-Mar-16	25-Mar-16	24-Mar-16	24-Mar-16	24-Mar-16	25-Mar-16	18-Mar-16	5-Mar-16	15-Feb-16				
					14-Feb-16	27-Feb-16	18-Mar-16	17-Mar-16	17-Mar-16	17-Mar-16	18-Mar-16	11-Mar-16	27-Feb-16	8-Feb-16				
					7-Feb-16	20-Feb-16	11-Mar-16	10-Mar-16	10-Mar-16	10-Mar-16	11-Mar-16	4-Mar-16	20-Feb-16	1-Feb-16				
					31-Jan-16	13-Feb-16	4-Mar-16	3-Mar-16	3-Mar-16	3-Mar-16	4-Mar-16	26-Feb-16	13-Feb-16	25-Jan-16				
					24-Jan-16	6-Feb-16	26-Feb-16	25-Feb-16	25-Feb-16	25-Feb-16	26-Feb-16	19-Feb-16	6-Feb-16	18-Jan-16				
					17-Jan-16	30-Jan-16	19-Feb-16	18-Feb-16	18-Feb-16	18-Feb-16	19-Feb-16	12-Feb-16	30-Jan-16	11-Jan-16				
					10-Jan-16	23-Jan-16	12-Feb-16	11-Feb-16	11-Feb-16	11-Feb-16	12-Feb-16	5-Feb-16	23-Jan-16	4-Jan-16				
					3-Jan-16	16-Jan-16	5-Feb-16	4-Feb-16	4-Feb-16	4-Feb-16	5-Feb-16	29-Jan-16	16-Jan-16					
						9-Jan-16	29-Jan-16	28-Jan-16	28-Jan-16	28-Jan-16	29-Jan-16	22-Jan-16	9-Jan-16					
						2-Jan-16	22-Jan-16	21-Jan-16	21-Jan-16	21-Jan-16	22-Jan-16	15-Jan-16	2-Jan-16					
						26-Dec-15	15-Jan-16	14-Jan-16	14-Jan-16	14-Jan-16	15-Jan-16	8-Jan-16	26-Dec-15					
						19-Dec-15	8-Jan-16	7-Jan-16	7-Jan-16	7-Jan-16	8-Jan-16	1-Jan-16	19-Dec-15					
						12-Dec-15	1-Jan-16	31-Dec-15	31-Dec-15	31-Dec-15	1-Jan-16	25-Dec-15	12-Dec-15					
						5-Dec-15	25-Dec-15	24-Dec-15	24-Dec-15	24-Dec-15	25-Dec-15	18-Dec-15	5-Dec-15					
						28-Nov-15	18-Dec-15	17-Dec-15	17-Dec-15	17-Dec-15	18-Dec-15	11-Dec-15	28-Nov-15					
							11-Dec-15	10-Dec-15	10-Dec-15	10-Dec-15	11-Dec-15	4-Dec-15						
							4-Dec-15	3-Dec-15	3-Dec-15	3-Dec-15	4-Dec-15	27-Nov-15						
							27-Nov-15	26-Nov-15	26-Nov-15	26-Nov-15	27-Nov-15	20-Nov-15						
							20-Nov-15	19-Nov-15	19-Nov-15	19-Nov-15	20-Nov-15							

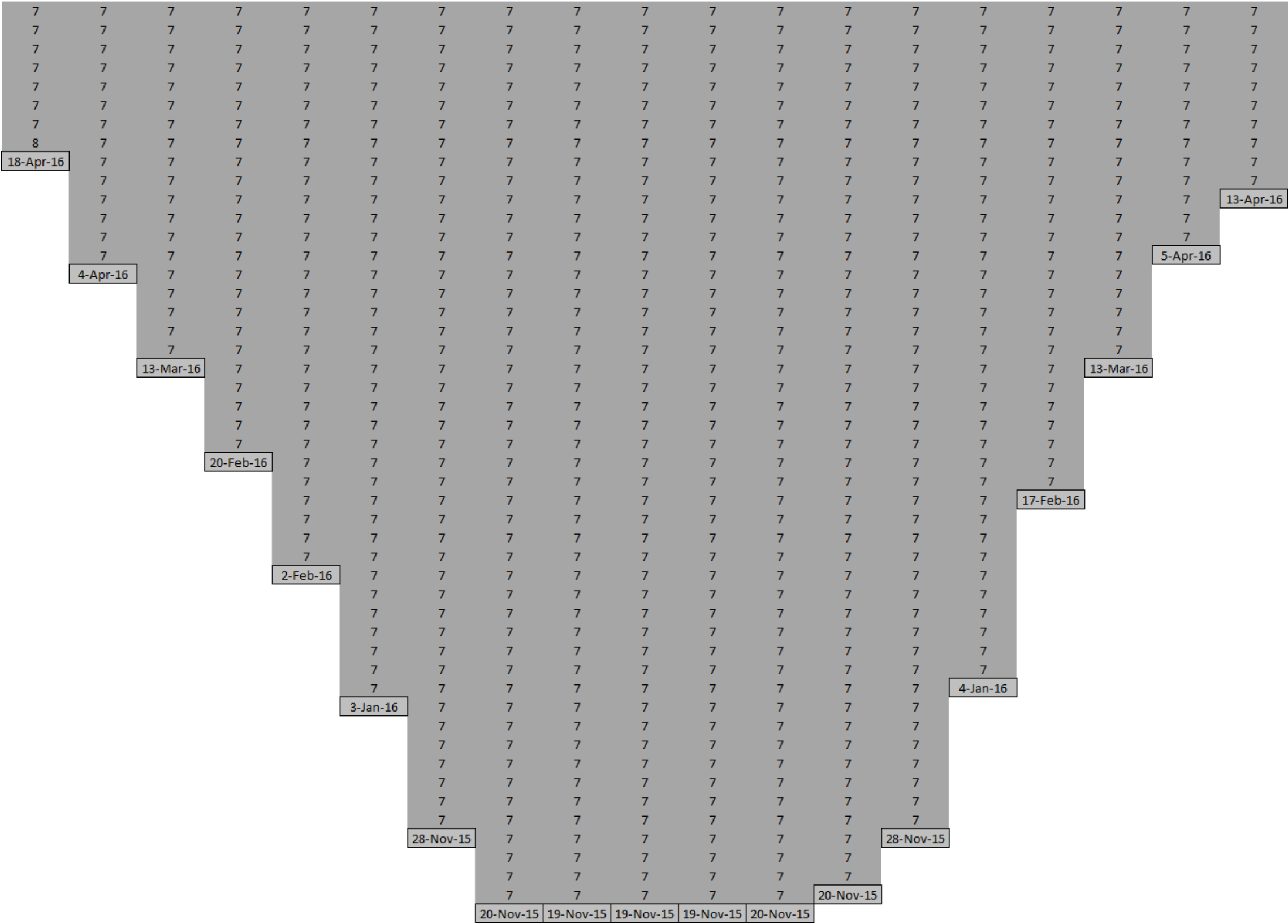Figure II-1 - Dam construction schedule for the case study dam.

Figure II-2 - Waiting times between concreting successive layers.
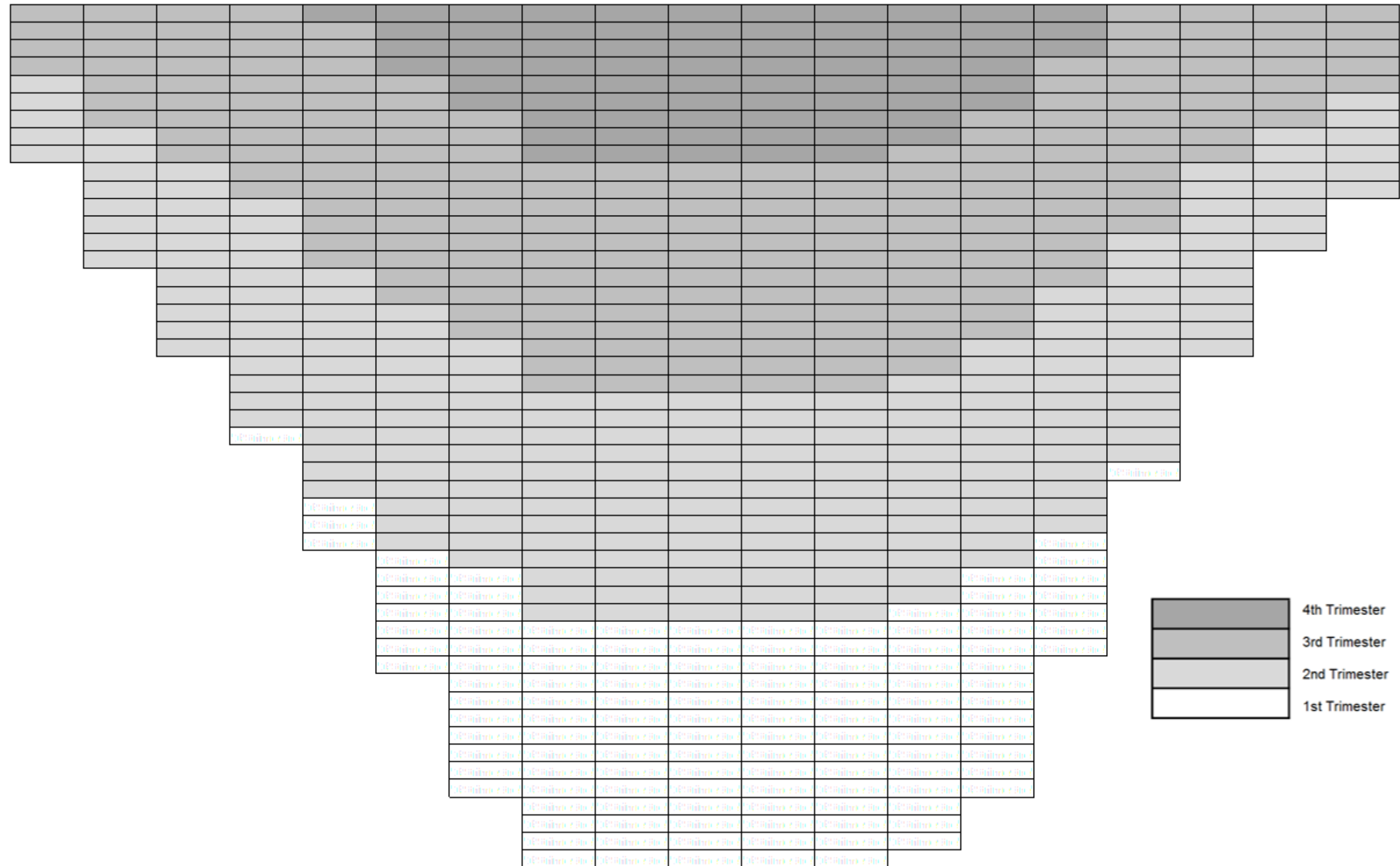
Figure II-3 - Trimestral evolution of the dam's construction schedule.

APPENDIX III – EXCHANGE REQUIREMENTS MODELS

- ER1:

Variables:	Variable units:	Variable symbol:	Variable type:	File type
Number of concrete layers		nc	integer	
Concrete layers height	meters	h	real	.csv
Medium width of the center vertical profile	meters	w	real	

Table III-1 - Exchange Requirement 1.

- ER2:

Variables:	Variable units:	Variable symbol:	Variable type:	File type
Kind of cement		C_{type}	integer	
Amount of cement in concrete mix	Kg/m^3	C_{quan}	integer	
Thermal conductivity of concrete		k	real	
Volumetric specific heat	J/ m^3.K	ρc	real	
Ambient temperature	ºC	t_{ext}	real	
Initial temperature of elements	ºC	t_{ini}	real	Direct input by the user on MATLAB
Time step	seconds	Δt	integer	
Waiting time between consecutive concreting layers	seconds	t_{con}	integer	
Time between placing and withdrawal of the formwork	seconds	t_{form}	integer	
Number of elements by concrete layer in the finite difference mesh		np	integer	

Table III-2 - Exchange Requirement 2.

- ER3:

Variables:	Variable units:	Variable symbol:	Variable type:	File type
Temperature vs time	ºC	m_t	Matrix of numbers	.csv .png .avi

Table III-3 - Exchange Requirement 3.

- ER4:

Variables:	Variable units:	Variable symbol:	Variable type:	File type
Number of work fronts	°C	wf	number	
Date of start of work		t_{start}	Date	
Minimum time between concreting successive layer	days	t_{min}	integer	Direct input by the user on MATLAB
Maximum time between concreting successive layer	days	t_{max}	integer	
Maximum acceptable difference between adjacent concrete layers		h_{dif}	integer	

Table III-4 - Exchange Requirement 4.

- ER5:

Variables:	Variable units:	Variable symbol:	Variable type:	File type
Dam's construction schedule by dates		m_{dates}	Matrix of dates	
Wanting times between layers		m_{times}	Matrix of dates	.xls
Concrete trimesters		$m_{quarter}$	Matrix of dates	

Table III-5 - Exchange Requirement 5.